UNIVERSITY OF LATVIA

FACULTY OF MEDICINE

Vladimirs Piļipenko

STUDIES OF GABAERGIC SYSTEM-TARGETED SUBSTANCES IN A RAT MODEL OF SPORADIC ALZHEIMER'S DISEASE

DOCTORAL THESIS

Submitted for the degree of Doctor of Medicine

Subfield of Pharmacology

Riga, 2019

The doctoral thesis study was carried out at the Department of Pharmacology, Faculty of Medicine, University of Latvia, from 2014 to 2019.

The thesis contains the introduction, 5 chapters, reference list, and the list of scientific publications.
Form of the thesis: dissertation in Medicine, Pharmacology
Supervisor: Dr. habil. med., Professor **Vija Zaiga Kluša**

Reviewers:

1) Dr. habil. Biol., Professor **Ruta Muceniece**, Faculty of Medicine, University of Latvia
2) Dr. med., Senior Researcher **Līga Zvejniece**, Latvian Institute of Organic Synthesis
3) Dr. med., Professor **Anti Kalda**, Faculty of Medicine, University of Tartu

The thesis will be defended at the public session of the Doctoral Committee of Medicine, Pharmacy and Biology Sciences, University of Latvia, at 12:00 on October 11th, 2019 at the University of Latvia House of Science, 3 Jelgavas Street, room 202.

The thesis is available at the Library of the University of Latvia, 19 Raina blvd.

This thesis is accepted for the commencement of the degree of Doctor of Medicine on ___ 20___ by the Doctoral Committee of Medicine, Pharmacy and Biology Sciences, University of Latvia.

Chairman of the Doctoral Committee _____/

Dr. med., Professor **Valdis Pīrāgs**

Secretary of the Doctoral Committee _____/

Dr. biol., Associated Professor **Līga Plakane**

ANNOTATION

Incidence of neurodegenerative diseases is rapidly increasing, thus creating an economic, financial and social burden for the patients, their families and the government. The most common neurodegenerative disease is the sporadic Alzheimer's disease (sAD), for which no effective preventive or halting treatments have been discovered yet.

Neuroinflammation, imbalance in neurotransmitter systems, oxidative stress and mitochondrial impairments play a crucial role in the progression of sAD. Since these pathological processes start several decades before clinical symptoms manifest, in the 21st century a new imperative has been put forward: "let us stop this disease before it starts!". Consequently, approaches that would halt the impairments in cognitive functions in pre-dementia stages are being searched for.

Our hypothesis is that the maintenance of brain cell functioning and memory stimulation does not solely depend on the regulation of the activatory neurotransmitter (acetylcholine, glutamate) system, but the most important is the balance between it and the inhibitory gamma-aminobutyric acid (GABA) system. In accordance to our hypothesis, in this doctoral thesis we investigated the agonists of GABA-A and GABA-B receptors (muscimol/diazepam and baclofen, respectively), as well as GABA elements-containing compound gammapyrone. We anticipated that at very low or low doses these compounds would possess neuroprotective and memory-enhancing effects, as opposed to the memory-impairing action at high doses.

We have studied these compounds in a sAD type rat model obtained by intracerebroventricular (icv) injection of neurotoxin streptozocin (STZ). We have discovered, for the first time, that the studied compounds improved spatial learning/memory processes and normalized STZ-induced pathological changes in the expression of cortical and hippocampal brain proteins which are involved in neuroinflammation, acetylcholine cleavage, GABA synthesis and synaptic plasticity. Although gammapyrone did not demonstrate binding affinity towards GABA receptors, it acted similarly to GABA receptor agonists *in vivo* and *ex vivo*, as well as showed the ability to regulate mitochondrial functions *in vitro*.

The obtained data indicate allosteric regulatory mechanisms of all studied compounds and indicate the rationale of GABA receptor agonists use for the treatment of the early symptoms of sAD to halt its developments and progression. These compounds, as well as gammapyrone, could serve as candidate molecules for the design of novel anti-dementia drugs.

Keywords: GABA, streptozocin, muscimol, baclofen, diazepam, gammapyrone

ANOTĀCIJA

Neirodeģeneratīvo slimību izplatība strauji pieaug, radot ekonomisko, finansiālo un sociālo slogu gan slimniekiem, gan viņu tuviniekiem un valstij. Visbiežāk sastopamā neirodeģeneratīvā saslimšana ir sporādiskā Alcheimera slimība (sAD), kuras apturēšanai un izārstēšanai joprojām nav atrasti efektīvi līdzekļi.

Būtisku lomu sAD progresēšanā spēlē neiroiekaisums, neirotransmiteru sistēmu disbalanss, oksidatīvais stress un mitohondriālie traucējumi. Ņemot vērā, ka šie patoloģiskie procesi sākas vairākas dekādes pirms klīnisko simptomu manifestācijas, 21. gadsimtā ir izskanējis jauns imperatīvs: "apstādināsim šo slimību pirms tā ir sākusies!". Līdz ar to tiek meklētas iespējas, kā apstādināt kognitīvo funkciju pasliktināšanos jau pre-demences stadijā.

Saskaņā ar mūsu koncepciju, ka smadzeņu šūnu funkcionēšanas uzturēšanai un atmiņas stimulēšanai nepieciešama ne tikai aktivējošo neirotransmiteru (acetilholīna, glutamāta) sistēmu regulācija, bet svarīgāk ir nodrošināt balansu starp tās un inhibējošās gamma-aminosviestskābes (GABA) sistēmas aktivitāti, promocijas darbā esam pētījuši GABA-A un GABA-B receptoru agonistus (muscimolu/diazepāmu un baklofēnu, attiecīgi), kā arī GABA molekulu un tās elementus saturošu savienojumu gammapironu. Šis vielas ievadītas ļoti zemās vai zemās devās, sagaidot neiroprotektīvos un atmiņu uzlabojošos efektus, atšķirībā no lielo devu atmiņu depresējošās darbības.

Esam pētījuši šīs vielas sAD tipa žurku modelī, kas iegūts, intracerebroventrikulāri (icv) ievadot neirotoksīnu streptozocīnu (STZ). Pirmo reizi esam atklājuši, ka pētāmie savienojumi uzlaboja telpiskās atmiņas procesus, kā arī normalizēja STZ izraisītās patoloģiskās izmaiņas smadzeņu garozas un hipokampa audu proteīnu ekspresijā, kas atbild par neiroiekaisumu, acetilholīna šķelšanu un GABA sintēzi, sinaptisko plasticitāti. Gammapirons, kaut arī neuzrāda saistīšanās afinitāti pret GABA receptoriem, darbojās līdzīgi GABA receptoru agonistiem *in vivo* un *ex vivo* eksperimentos, bez tam *in vitro* uzrādot arī mitohondriju funkciju regulējošās īpašības.

Iegūtie dati liecina par pētāmo vielu alostēriskās regulācijas mehānismiem un norāda uz GABA receptoru agonistu lietošanas perspektivitāti, lai novērstu sAD agrīnos simptomus, aizkavējot slimības attīstību un progresēšanu. Šīs vielas un arī gammapirons var kalpot kā kandidātmolekulas jaunu pretdemences preparātu dizainā.

Atslēgvārdi: GABA, streptozocīns, muscimols, baklofēns, diazepāms, gammapirons

CONTENTS

ABBREVIATIONS

*OH – hydroxyl radical

Aß42 – amyloid beta peptide 1-42

AChE – acetylcholine esterase

aCSF – artificial cerebrospinal fluid

AD – Alzheimer's disease

ADP – adenosine diphosphate

AICD – APP intracellular domain

ANOVA – analysis of variance

APP – amyloid precursor protein

ATP – adenosine triphosphate

Bax – Bcl2 associated X protein

BCL – baclofen

Bcl2 – B-cell lymphoma 2 protein

BZD – benzodiazepine

C83 – C-terminal fragment 83

C99 – C-terminal fragment 99

CA – *cornu ammonis*

CASP 3 – caspase 3

CAT – catalase

CMR – cerebral metabolic rate

CO_2 – carbon dioxide

CoQ – coenzyme Q

CNS – central nervous system

DCF – 2,7-dichlorofluorescein

DEHP – di-2-ethylhexyl phthalate

DG – dentate gyrus

DHP – 1,4-dihydropyridine

DMEM – Dulbecco's modified Eagle medium

DNA – deoxyribonucleic acid

DZP – diazepam

ETC – electron transport chain

fAD – familial Alzheimer's disease

FAD – flavin adenine dinucleotide

Fe^{2+} – ferrous ion

G6P-DH – glucose 6-phosphate dehydrogenase

GABA – gamma-aminobutyric acid

GAD67 – glutamic acid decarboxylase 67

GFAP – glial fibrillary acidic protein

GLUT – glucose transporter

GMP – gammapyrone

GPX – glutathione peroxidase

GSH – glutathione

GSK-3β – glycogen synthase kinase-3β

GSSG – glutathione disulfide

GWAS – genome wide association studies

H^+ – hydrogen ion

H_2O_2 – hydrogen peroxide

HEPES – 4-(2-hydroxyethyl)-1-piperazine ethanesulfonic acid

Iba-1 – ionized calcium-binding adapter molecule-1

icv – intracerebroventricularly

ip – intraperitoneally

KH – Krebs-Henseleit

M – muscimol

MCI – mild cognitive impairment

miRNA – micro RNA

mTOR – mechanistic target of rapamycin

MTT – (3-(4,5-dimethylthiazol-2-yl)-2,5-diphenyltetrazolium bromide)

N_2O – nitrous oxide

NAD^+ – nicotinamide adenine dinucleotide

NADH – reduced nicotinamide adenine dinucleotide

$NADP^+$ – nicotinamide adenine dinucleotide phosphate

NMDA – N-methyl-D-aspartate

O_2 – oxygen

$ONOO^-$ – peroxynitrite

p3 – 3-kDa peptide

p53 – tumor protein 53

PBS – phosphate buffered saline

Pi – phosphate ion

PI3K – phosphatidylinositide 3-kinase

PN – principal neurons

PSEN – presenilin gene

RNA – ribonucleic acid

ROS – reactive oxygen species

sAD – sporadic Alzheimer's disease

sAPP – soluble APP

siRNA – small interfering RNA

SNPs – single nucleotide polymorphisms

SOD – superoxide dismutase

STZ – streptozocin

SYP1 – synaptophysin1

TCA – tricarboxylic acid cycle

TREM-2 – triggering receptor expressed on myeloid cells-2

tRNA – transfer RNA

INTRODUCTION

The actuality of the study

Incidence of neurodegenerative diseases is rapidly increasing, thus creating an economic, financial and social burden for the patients, their families and the government. Among the common neurodegenerative diseases – Parkinson's disease, Huntington's disease, multiple sclerosis and others – the most widespread is the Alzheimer's disease (AD). Currently, it affects approximately 50 million people worldwide, but this number is expected to triple by 2050. In contrast to the inherited or familial AD (about 1-5% of all AD cases) that starts at 40-45 years of age and is characterized by the generation and brain accumulation of misfolded amyloid beta peptide 1-42 (Aß42), sporadic (sAD) type constitutes 95-99% of all cases and is characterized by late onset (60-65 years of age) of cognitive impairments. Unfortunately, effective therapeutic compounds that would halt the progression of the disease have not yet been developed.

The aim of the study

The aim of the current thesis was to study the effects of GABA-A, GABA-B receptor agonists, as well as GABA elements-containing compound on cognitive functions and the expression intensity of proteins that are involved in neuroinflammation, synthesis of neurotransmitters, synaptic plasticity and mitochondrial functioning using a rat model of sAD (obtained by intracerebroventricular streptozocin injection).

Tasks of the study

1. To assess the effects of GABA-A receptor agonists muscimol and diazepam, GABA-B receptor agonist baclofen and GABA elements-containing compound gammapyrone on rat spatial learning/memory.
2. *Ex vivo*: to detect the effects of the studied compounds on the changes in the density of brain proteins involved in: astroglial (GFAP) and microglial (Iba-1) activation, synaptic plasticity (SYP1), acetylcholine cleavage (AChE) and GABA synthesis (GAD67).
3. *In vitro*: to assess the binding of gammapyrone to GABA-A and GABA-B receptors, as well as the effects of gammapyrone on PC12 cell viability, changes in mitochondrial membrane potential, activity of mitochondrial complexes and on apoptosis (Bcl2, Bax, CASP 3 and p53).
4. To identify the main pathological processes that are targeted by the studied compounds.

Concept of the study

Opposite to the classical sedative/tranquilizing or memory-impairing effects of GABA receptor agonists that occur after these compounds bind to their receptor sites, our concept is that at very low and low (10-100 times lower) subsedative doses, GABA-A and GABA-B receptor agonists might act by allosterically modulating either GABA receptors or other non-specific receptor proteins, thereby resulting in memory-stimulating activity. Similar activity might be caused by GABA and its elements-containing compound gammapyrone.

Theoretical basis of our concept is the information on the complexity of GABA receptors: they have a large number of subunit combinations, as well as different localization sites (synaptic, extrasynaptic and perisynaptic in glial cells). Allosteric modulation is provided by molecules that do not bind to the neurotransmitter receptor orthosteric binding sites, but bind to the topographically distinct sites (Urwyler et al., 2005). Allosteric modulators do not possess the intrinsic affinity of agonists, however, after binding they can induce conformational changes in the proteins, thereby inducing cell responses that are different from the typical ones (Urwyler et al., 2005).

Thesis for the defense

1. GABA-A and GABA-B receptor agonists at very low and moderate doses may stimulate spatial learning/memory processes in a rat model of sAD.
2. This stimulatory effect might be also produced by GABA elements-containing compound gammapyrone.
3. GABA-A, GABA-B receptor agonists and gammapyrone at low doses might show regulating effects on the expression of brain proteins which are involved neuroinflammation, acetylcholine cleavage, GABA synthesis and synaptic protein expression.
4. Gammapyrone *in vitro* might protect against mitochondrial dysfunction and apoptosis.

Methods

The following methods were used in the studies:

1) *In vivo*: Morris water maze test for the assessment of spatial learning and memory, open field test for the assessment of the locomotory performance;

2) *Ex vivo*: immunohistochemical and histochemical methods for the assessment of brain protein expression;
3) *In vitro*: binding of gammapyrone to GABA-A and GABA-B receptors; in PC12 cells, the assessment of gammapyrone effects on mitochondrial processes.

Selection of compounds

1) GABA-A receptor GABA site specific agonist muscimol and benzodiazepine site regulator diazepam (Fig. 1A and 1B, respectively);
2) GABA-B receptor specific agonist baclofen (Fig. 1C);
3) Gammapyrone, compound that contains three GABA molecules: one natural (free) GABA, joined with 1,4-dihydropyridine (DHP) ring at position 4, and two "crypto" GABAs enclosed in DHP molecule. Free and "crypto" GABAs are connected by a peptide bond (-CONH-) that makes gammapyrone a peptide-mimicking structure (Fig. 1D). Gammapyrone belongs to the atypical DHPs, since it does not possess calcium channel blocking activity (Klusa, 2016).

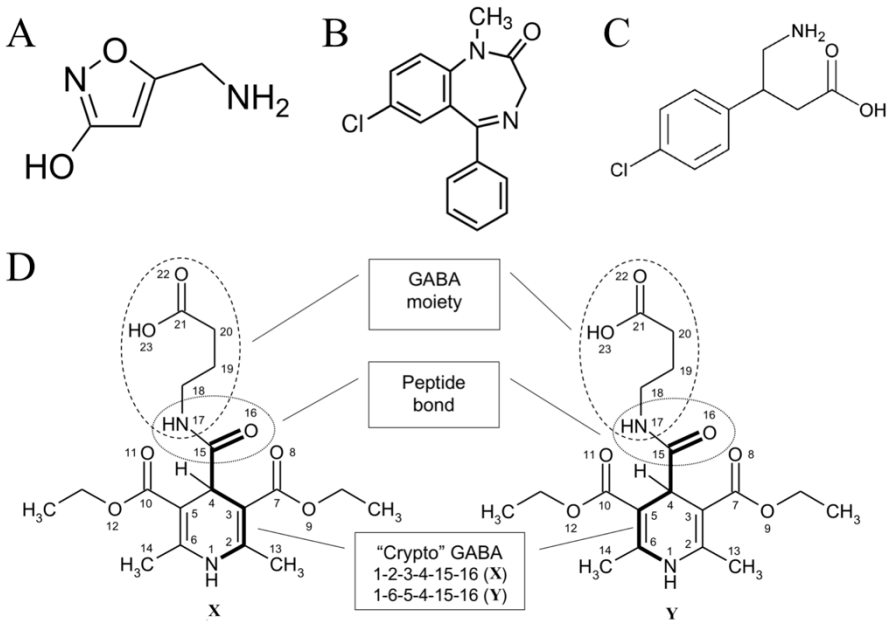

Figure 1. **Structures of the studied compounds: muscimol (A), diazepam (B), baclofen (C) and gammapyrone (D). A, B and C – internet sources, D – from (Pilipenko et al., 2019).**

1. LITERATURE OVERVIEW

1.1. Alzheimer's disease (AD)

AD is a multifaceted, age-related progressive neurodegenerative disease and the most prevalent cause and form of dementia (Scheltens et al., 2016). Currently, 50 million people worldwide are diagnosed with dementia, but it is likely that this number will triple by 2050s (Mendiola-Precoma et al., 2016). The exact mechanism of AD is still unknown. Initially, in 1908, German physician Alois Alzheimer characterized AD with profound memory loss, post-mortem brain atrophy, changes in the morphology of brain cells and abnormal protein deposits around nerve cells. Later, these pathologies were identified as microgliosis, accumulation of amyloid beta peptide 1-42 (Aß42) plaques and formation of neurofibrillary tangles. Unfortunately, more than hundred years after, the clinical diagnosis remains almost the same, although AD treatment strategies have changed in the years due to the discovery of new factors that played a crucial role in the etiopathogenesis of AD. Thus, one of the first AD hypotheses was the progressive deficits of the cholinergic system, hence, the design of drugs that would selectively target the cholinergic system, the anticholinesterases, were initiated in the 1970s. In the 1980s, glutamatergic theory was the predominant theory of AD pathology, and antagonists of glutamate receptors were put forward. Since the 1980s, AD was considered to be a proteopathy and the role of misfolded Aß and hyperphosphorylated tau protein was defined as critical for the progression of the disease.

At present, multiple detrimental mechanisms that result in neuronal death are known to be involved in the neuropathology of AD (Magalingam et al., 2018). There are distinct etiopathogenetic causes of AD that are defined by the type of the disease – familial or sporadic. Both forms and the pharmacological strategies that aim to prevent the progression of the disease are described below.

1.2. Types of AD

1.2.1. Familial AD (fAD)

The early onset type of AD, fAD generally occurs at 40 years of age and accounts for 1-5% of all AD cases. Extensive research has identified the genetic cause for only 1% of all fAD cases. It is connected to mutations in the genes that encode proteins which participate in the generation of Aß. This includes mutations in three genes: *amyloid precursor protein* (*APP*) and *presenilins* (*PSEN*)- *PSEN1* and *PSEN-2* (Sun et al., 2017). The *APP* gene encodes APP, a large protein that can range from 365 to 770 amino acid residues depending on the isoform. Both *PSEN* genes

encode γ-secretase, an enzyme that cleaves APP. Normally, 90% of APP is processed in a non-amyloidogenic way by two enzymes, α- and γ-secretase (Fig. 2). α-Secretase catalyzes the formation of neurotrophic soluble APPα and C-terminal fragment 83. The latter is then cleaved by γ-secretase to produce non-toxic APP intracellular domain (AICD) and a 3-kDa peptide.

In fAD, gene mutations, environmental factors and nutrition can create a shift towards amyloidogenic APP processing (Sun et al., 2017). In this case, ß-secretase cleaves APP, thus generating significantly less active soluble APPß and C-terminal fragment 99. When the latter is cleaved by γ-secretase, AICDs and Aß peptides are produced (Sun et al., 2017). In general, about 90% of the produced Aß are less toxic Aß40 and the remaining 10% are Aß42, which is a lot more toxic due to its ability to form soluble oligomers. Soluble Aβ42 oligomers can induce multiple neurotoxic effects, such as perturbations in the synaptic transmission, decreased synaptic density, inbhition of the hippocampal long-term potentiation and impairments in the cognitive functions (Nhan et al., 2015).

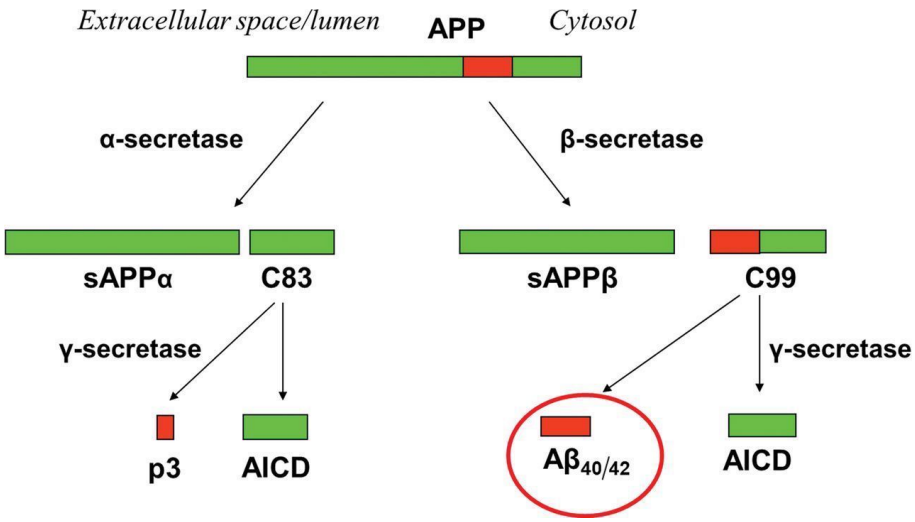

Figure 2. **Generation of Aß through proteolytic processing of APP. APP – amyloid precursor protein; sAPP – soluble APP; C83 – C-terminal fragment 83; C99 – C-terminal fragment 99; AICD – APP intracellular domain; p3 – 3-kDa peptide. Adapted from (Teich and Arancio, 2012).**

The prevailing hypothesis of AD is still the so-called "amyloid cascade hypothesis", which postulates that the excessive aggregation of Aß in the brain leads to a cascade of events that end in cognitive decline and neurodegeneration. (Fig. 3).

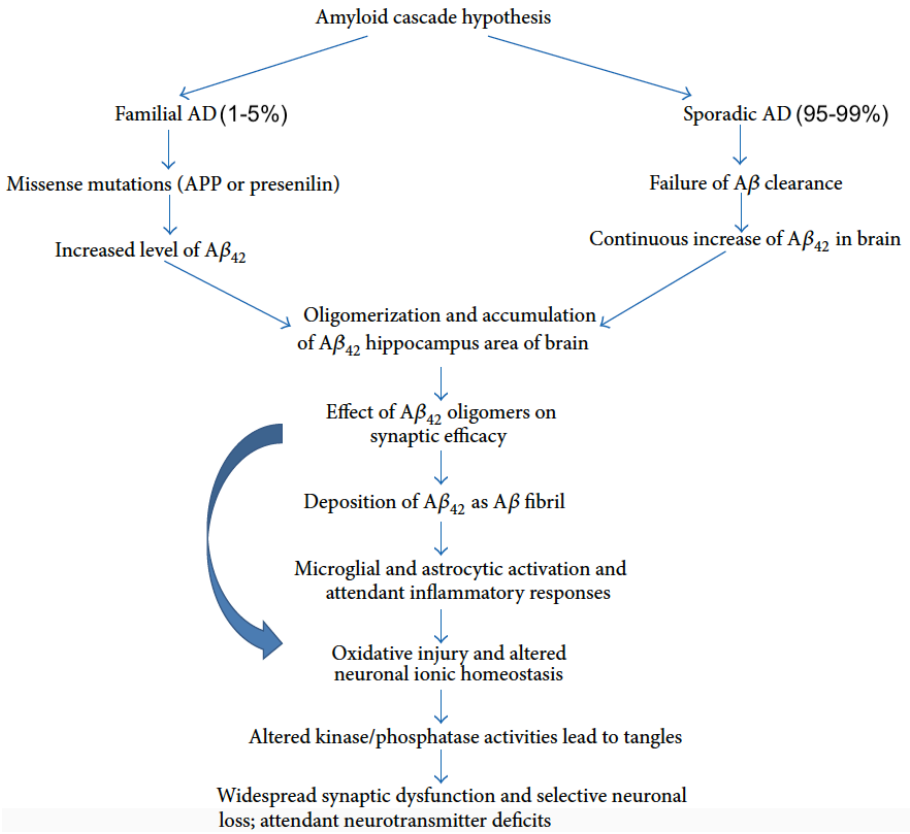

Figure 3. **The amyloid cascade hypothesis of AD. Adapted from (Singh et al., 2016).**

Multiple therapeutical approaches have been tested with the aim to prevent or decrease the formation of Aß42 oligomers. Unfortunately, secretase inhibitors and active immunization with fragments of Aß oligomers failed to prevent the AD-related neurodegeneration. Moreover, although passive immunization with monoclonal antibodies against Aß42 (the "zumabs", such as bapineuzumab, solanezumab, crenezumab) was able to dissolve the Aß plaques, but did not improve cognitive functions of the individuals. Therefore, this therapeutic approach has brought rather disappointing results (Bachmann et al., 2018).

1.2.2. Sporadic AD (sAD)

sAD constitutes 95-99% of all AD cases and is also generally characterized by protein pathologies that results from the insufficient clearance of Aß42, but its onset is later than in the fAD – at 65 years of age. According to the amyloid cascade hypothesis, oligomerization and accumulation of Aß also occurs in sAD, however, it starts decades later than in fAD. In sAD, the pathological processes start about two decades before they are clinically manifested as cognitive and neurodegenerative changes. This early stage of sAD is termed the prodromal sAD, where a significant brain pathology has been initiated, but negligent influence on the cognitive abilities of

the individual is observed. Mild cognitive impairment (MCI) is a transitional state between normal aging and dementia, characterized a certain extent of memory loss, although not all MCI patients develop AD (Markesbery, 2010). Since MCI and prodromal AD represent the early phases of sAD, new anti-dementia initiatives are designed to prevent the onset of the disease by targeting the pathogenic mechanisms that occur at these stages. Thus, the imperative "stop AD before it starts" is now considered to be the most beneficial strategy for the prevention of multiple neurodegenerative events that lead to dementia (McDade and Bateman, 2017). The disease-modifying approaches are being designed to target multiple specific mechanisms that occur decades before the excessive Aß accumulation is clinically detectable (Xiaonan Liu et al., 2018).

Multiple factors that have a role early in the disease progression have been recognized in the several years of AD research and include epigenetic mechanisms, neurotransmitter imbalance, neuroinflammation, oxidative stress, mitochondrial dysfunction, impairments in glucose metabolism and various viral species. The major pathological processes that appear to be dysregulated early in AD and need to be targeted by disease-modifying therapies are discussed below.

1.3. Etiopathogenetic mechanisms of AD

1.3.1. Epigenetic mechanisms

Epigenetic regulation plays several important roles in the modulation of neuroinflammation in AD. It includes aberrations in deoxyribonucleic acid (DNA) methylation, histone deacetylation and subsequent chromatin remodeling, as well as dysregulation of noncoding ribonucleic acids (RNAs) (X. Liu et al., 2018). Methylation of DNA results in the modification of cytosine residues via addition of methyl groups to regions of DNA that are rich in cytosine/guanine (Mehler, 2008). In AD, reduced methylation of cytosines was found in the promoter region of the *APP* gene (Tohgi et al., 1999). Chromatin is necessary to assemble genomic DNA and histone proteins; altered in chromatin can be induced by changes in the histones. The most widely reported change in the histone proteins is the deacetylation, a process that leads to the condensing of chromatin and subsequent suppression in gene transcription (Datta et al., 2018). Gene expression can also be influenced by non-coding RNAs, e.g., circular, messenger and micro RNAs that were found to be dysregulated in Aß42-induced AD rats (Wang et al., 2018). These mechanisms are summarized in Figure 4.

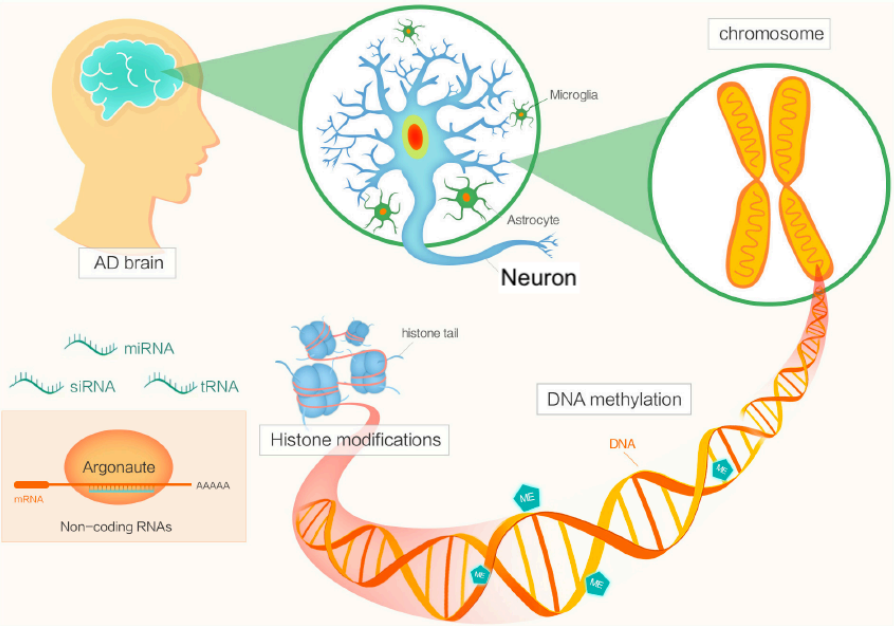

Figure 4. **Overview of the epigenetic mechanisms in AD. miRNA – micro RNA; siRNA –small interfering RNA; tRNA – transfer RNA. Adapted from (X. Liu et al., 2018).**

1.3.2. Mitochondrial dysfunction and oxidative stress

Oxidative phosphorylation is essential for the synthesis of the main energy substrate – adenosine triphosphate (ATP). The production of ATP required aerobic, enzyme-mediated synthesis through mitochondrial electron transport chain (ETC). Oxidative phosphorylation includes the involvement of five protein complexes: reduced nicotinamide adenine dinucleotide:ubiquinone oxidoreductase (complex I), succinate-cytochrome c oxidoreductase (complexes II+III), cytochrome c oxidase (complex IV) and ATP synthase (complex V) (Sousa et al., 2018). Briefly, a high energy hydrogen electron is passed along the ETC with the aid of complexes I to IV and reaches the complex V, which then synthesizes ATP from adenosine diphosphate (Sousa et al., 2018).

The depletion of mitochondrial DNA and its lesions are the mechanisms that drive to the reduced expression to the abovementioned enzymes (Krishnan et al., 2012).

Impaired cell bioenergetics, which originates from mitochondrial dysfunction, usually result in oxidative stress and the formation of reactive oxygen species (ROS), common features of the AD brain (Wang et al., 2014). Neurons are extremely susceptible to mitochondrial dysfunction, since they largely rely on oxidative phosphorylation (Cardoso et al., 2016). Impaired functioning of the ETC results in the generation of ROS, thereby contributing to the damage of DNA, proteins and lipids. The most affected brain regions in AD – frontal, parietal and temporal lobes – are the most susceptible to oxidative damage (Wang et al., 2014).

Moreover, oxidative stress induces damage to the enzymes that participate in the tricarboxylic acid cycle (TCA), ATP biosynthesis and glycolysis (Cheignon et al., 2018). Oxidative changes in the brain largely contribute to impairments in normal glucose utilization through augmenting the activity of glucose metabolism-participating enzymes. Redox proteomics is a branch of proteomics that is utilized to identify oxidized modifications and determine the localization and extent of them (Butterfield and Perluigi, 2016; Di Domenico et al., 2017). With the aid of redox proteomics methods, specific oxidative modifications of the following enzymes were discovered in human AD brains: glycolytic enzyme fructose bisphosphate aldolase, alpha-enolase, glyceraldehyde-3-phosphate dehydrogenase, triosephosphate isomerase and phosphoglycerate mutase (Butterfield and Boyd-Kimball, 2018; Di Domenico et al., 2017). Additionally, oxidative metabolism of an iron-sulfur-containing TCA cycle enzyme aconitase, creatine kinase and ATP synthase in the mitochondria point to insufficient glucose metabolism and low ATP production in both MCI and AD patients (Butterfield and Boyd-Kimball, 2018; Di Domenico et al., 2017; Sultana et al., 2009). These changes result in substantially lower ATP production and decrease the maintenance of the ionic gradients in the neurons, diminishing the production and propagation of neuronal action potential and, hence, impairing neurotransmission. Loss of neuronal ion gradients can result in further synaptic dysfunction through the increase in free intracellular Ca^{2+} levels. Higher intracellular Ca^{2+} increases the activities of Ca^{2+}-dependent enzymes, endonucleases, proteinases and phospholipases, leading to the breakdown of DNA, proteins and lipids, respectively (Bhatti et al., 2017). Mitochondrial dysfunction in AD is summarized in Figure 5.

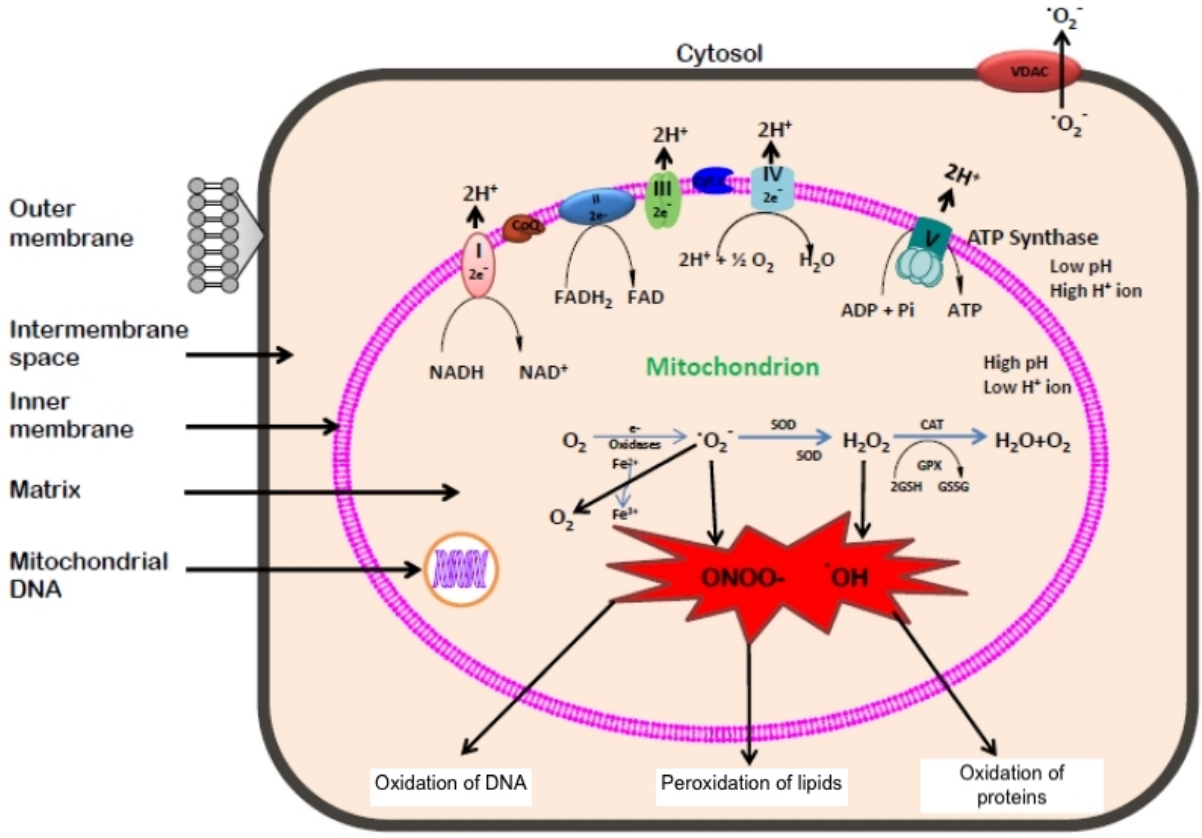

Figure 5. **Mitochondrial dysfunction in AD. *OH – hydroxyl radical; ADP – adenosine diphosphate; ATP – adenosine triphosphate; CAT – catalase; CoQ – coenzyme Q; FAD – flavin adenine dinucleotide; Fe^{2+} – ferrous ion; GPX – glutathione peroxidase; GSH – glutathione; GSSG – glutathione disulfide; H^{+} – hydrogen ion; H_2O_2 – hydrogen peroxide; O_2 – oxygen; $ONOO^{-}$ – peroxynitrite; NAD^{+} – nicotinamide adenine dinucleotide; NADH – reduced nicotinamide adenine dinucleotide; Pi – phosphate ion; SOD – superoxide dismutase. Adapted from (Bhatti et al., 2017).**

1.3.3. Neuroinflammation

Neuroinflammation is an excessive inflammatory response of the central nervous system (CNS) and a fundamental neuropathological process that is observed in multiple diseases, e.g., amyotrophic lateral sclerosis (McCombe and Henderson, 2011), Parkinson's disease (Wang et al., 2015), multiple sclerosis (Chen et al., 2016) and AD (Kinney et al., 2018). A close spatio-temporal relationship between activated microglia and Aß plaques has been well described, indicating the role of microglia in the clearance of Aß, and it was considered that the plaques activate microglia (Wisniewski et al., 1981). However, it has now been proven that microgliosis actually precedes the accumulation of Aß in sAD and fAD, and may further contribute to the seeding of amyloid plaques (Sosna et al., 2018). Inflammation in the brain, however, has a dual role: it is neuroprotective in the early AD phases, but shifts towards hazardous when the response is chronic

(Kim and Joh, 2006). When microglial cells become chronically activated, numerous toxic and proinflammatory molecules are released, namely cytokines, ROS and nitric oxide (McQuade and Blurton-Jones, 2019). Early in AD, acute response to the inflammatory stimuli produces neuroprotective effects through the cleavage of Aß. Nevertheless, chronic immune response is detrimental, since chronically activated microglial cells become involved in a vicious feedback loop, otherwise termed reactive microgliosis. Due to the sustained release of proinflammatory cytokines, microglial cells become unable to effectively cleave the Aß, which leads to the accumulation of Aß plaques (McQuade and Blurton-Jones., 2019). The release of cytokines and accumulation of Aß eventually damages the neurons. Neuroinflammatory microglia might also impair the ability of reactive astrocytes to promote neuronal survival, synaptogenesis and phagocytosis (Liddelow et al., 2017). A simplified schematic of neuroinflammation in AD is shown in Figure 6.

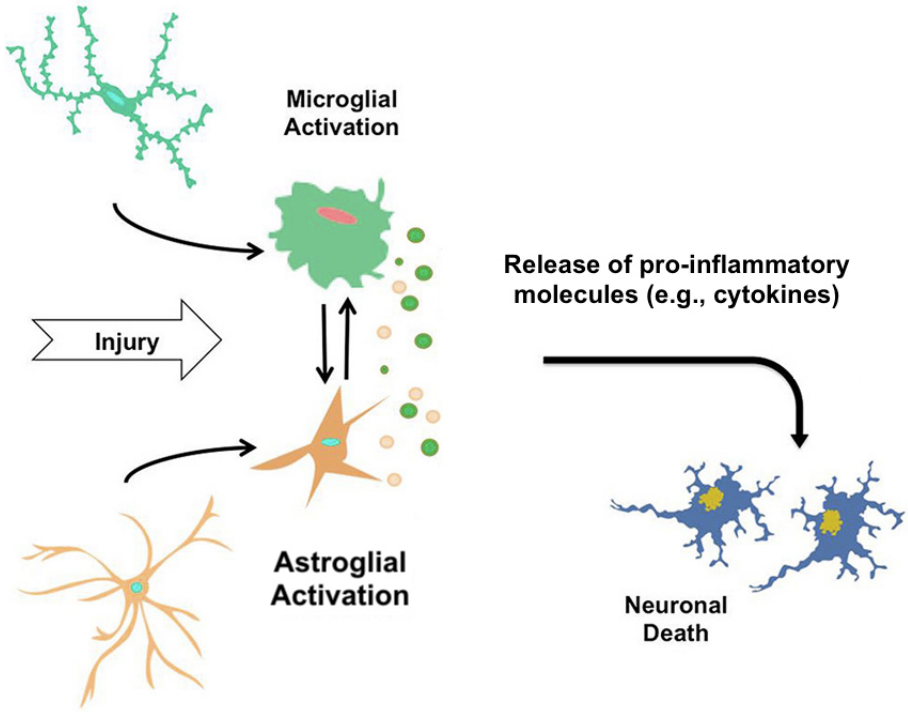

Figure 6. **Simplified depiction of neuroinflammatory process in AD. Adapted from (Morales et al., 2014).**

Genome wide association studies (GWAS) largely aided in the identification of the risk loci of AD, and a large number has been, in fact, detected in or around the genes that are expressed by microglia. In a recent study that involved more than 300,000 individuals, 49 single nucleotide polymorphisms (SNPs) that correlate with the risk of AD development have been discovered, and 29 of them were most highly expressed in microglia (Marioni et al., 2018). The highest (2- to 4-fold) risk of AD development is associated with the rare missense mutation in the Triggering

Receptor Expressed on Myeloid cells-2 (TREM-2), receptors that are mainly expressed on the surface of microglia cells (Guerreiro et al., 2013). Mutations in TREM-2 lead to insufficient activation of microglia and decrease its ability to clear Aß plaques. Therefore, loss of TREM-2 function appears to exacerbate the severity of AD (McQuade and Blurton-Jones, 2019).

1.3.4. Impairments in glucose metabolism

Glucose is a major source of energy not only in the periphery, but also in the brain. Through TCA, glycolysis and ETC complexes I to IV, glucose becomes metabolized to ATP to provide fuel for the brain. Glucose transporters (GLUTs) and brain insulin are crucial for glucose uptake from the vasculature and its usage by the brain cells, respectively (Arnold et al., 2018).

Glucose transport, therefore, mainly relies on GLUT1 and GLUT3. Along with the insulin-sensitive GLUT4, mainly expressed by cerebellar neurons, the insulin-independent GLUT1 is the main transporter of glucose transport through the blood-brain barrier into the brain and, specifically, into astrocytes (Leybaert et al., 2007). GLUT3 is responsible for the transport of glucose into neurons (Simpson et al., 2007). Reduced densities of GLUT1/3 are frequently found post-mortem in the brain of AD patients (Liu et al., 2008).

One of the key mechanisms of AD progression is the development of brain insulin resistance. It leads to neurofibrillary degeneration *via* two cooperating pathways: 1) phosphatidylinositide 3-kinase (PI3K) signaling activity and glycogen synthase kinase-3β (GSK-3β) overactivation and 2) decreased GLUT1 and GLUT3 expression and decreased intraneuronal glucose metabolism (Arnold et al., 2018; Croteau et al., 2018). The PI3K/protein kinase B pathway regulates the inhibitory phosphorylation of GSK-3β at serine 9 position (Kaytor and Orr, 2002). Decreased activity of this pathway leads to the excessive activity of GSK-3β, a major kinase that regulates tau phosphorylation (Deng et al., 2009).

One of the mechanisms for brain insulin resistance includes the activation of a multi-protein complex, mechanistic Target Of Rapamycin (mTOR) (Di Domenico et al., 2018). Activation of mTOR leads to the inhibition of autophagy in AD, which results in the accumulation of misfolded and aggregated proteins, damaged mitochondria and other organelles (Tramutola et al., 2015). Impaired autophagy-mediated neuronal death is a process that is found in the early stages of AD, both in the pre-dementia and MCI stages (Tramutola et al., 2015). Brain insulin resistance might also lead to deficits in neuronal glucose levels, coinciding with glucose hypometabolism and decreased ATP production (Di Domenico et al., 2018). The decreased ability of brain tissues to

utilize glucose shifts the cleavage of APP to amyloidogenic and elevates tau phosphorylation, thereby resulting in the accumulation of Aß and hyperphosphorylated tau (Grieb, 2016; Fig. 7).

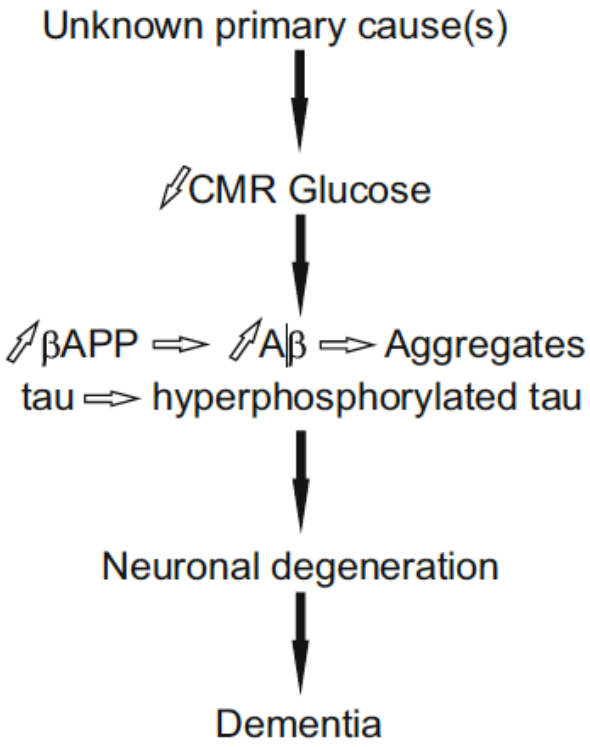

Figure 7. **The cerebral glucose hypometabolism cascade hypothesis of AD. ßAPP – amyloid precursor protein; Aß – amyloid beta; CMR – cerebral metabolic rate. Adapted from (Grieb, 2016).**

1.3.5. Apolipoprotein E4

Apolipoprotein E (APOE) plays a major role in cholesterol transport, response to brain injury, as well as in glucose metabolism (Dorey et al., 2014). A polymorphism in the APOE epsilon 4 allele (*APOE4*) is the single strongest genetic risk factor of sAD (Agosta et al., 2009). Strong evidence comes from *in vivo* and *in vitro* studies, suggesting that APOE4 participates in AD-associated neuronal degeneration. *APOE4* mice showed activation of the amyloid accumulation cascade that led to the degeneration of the neurons in the entorhinal cortex and in the hippocampus (Belinson et al., 2008).

In carriers of *APOE4* with a clinically established AD and cognitive impairment, a decrease in mitochondrial enzymatic activity is evident (Wilkins et al., 2017). Fragments of APOE4 are neurotoxic and may interact with mitochondria, resulting in its dysfunction and a lesser chance of survival (Muñoz et al., 2018).

APOE4 is primarily produced in glial cells, although in injury- and stress-related situations, its production can also occur in neurons (Xu, 2006). In post-mortem studies, the presence of the

APOE4 allele was shown to be significantly stimulating the accumulation of reactive glia in the frontal gyrus (Minett et al., 2016). Microglia and astrocytes that express *APOE4* induce gliosis in the brain parenchyma and promote a release of pro-inflammatory agents that result in synaptic death and neuronal loss.

1.3.6. Viral infections

Herpes simplex virus type 1 is a strong risk factor for AD, especially in *APOE4* carriers, where it might be reactivated by inflammatory and immunosuppressive events, resulting in the development of AD (Itzhaki, 2018). Implications on the role of pathogenic organisms in the progression of sAD has been studied for almost three decades, but large-scale multi-omic studies have only been completed recently. The results of one such study have shown that human herpes virus-6A and -7 play a major role in the regulation of genetic networks and may, therefore, initiate neuropathological processes that result in AD (Readhead et al., 2018).

1.3.7. Neurotransmitter dysfunction

1.3.7.1.Cholinergic neurotransmission

Acetylcholine is a major neurotransmitter of the CNS and cholinergic synapses are ubiquitous throughout the whole cortex, basal ganglia and basal forebrain (Mesulam, 2013). Autopsy studies of human AD patients have demonstrated that the impairment in the functioning of the cholinergic system occurs due to the degeneration of *nucleus basalis* of Meynert cholinergic neurons, as well as their axonal projections to the cerebral cortex (Davies and Maloney, 1976). Three major discoveries resulted in the development of the cholinergic hypothesis, namely: a) the discovery of presynaptic cholinergic depletion in the cerebral cortex (Davies and Maloney, 1976), b) the discovery of the *nucleus basalis* of Meynert in the basal forebrain as the major source of cortical cholinergic innervation, and its role in AD (Mesulam, 2013), and c) the demonstration that the antagonists of the cholinergic receptors weaken, while the agonists improve memory (Drachman and Leavitt, 1974). Recent data suggest that in sAD an abnormal interaction between different molecular pathways creates a malfunction and, ultimately, a collapse of the cholinergic system (Hampel et al., 2018). The key role of cholinergic transmission in higher brain functions, e.g., learning and memory, is marked by the presence of high density cholinergic synapses located in the striatum, limbic system, thalamus and neocortex (Hampel et al., 2018).

Current therapeutic strategies in the management of AD are based on the maintenance of the cholinergic function by attenuating the breakdown of acetylcholine using inhibitors of the

enzyme acetylcholinesterase (Massoud and Gauthier, 2010). Galantamine, donepezil and rivastigmine have been reported to significantly improve cognition in individuals with AD (Massoud and Gauthier, 2010). A meta-analysis on the use of galantamine, donepezil and rivastigmine reported a modest efficacy of these drugs in terms of stabilizing cognition, behavior, and global clinical change (Hansen et al., 2008).

1.3.7.2. Glutamatergic neurotransmission

Another major hypothesis of AD includes excessive excitatory glutamatergic neurotransmission that occurs through N-methyl-D-aspartate (NMDA) receptors. Normally, glutamatergic neurotransmission mediates calcium ion (Ca^{2+}) influx and thereby promotes neuronal survival and synaptic plasticity. In AD, NMDA receptors become extensively and increasingly activated, a process termed excitotoxicity that results in Ca^{2+} overload, thus leading to cell death and neurodegeneration (Wang and Reddy, 2017). Memantine, a selective antagonist of the extrasynaptic NMDA receptors, symptomatically reduces excitotoxicity and is used *per se* or concomitantly with anticholinesterase drugs mentioned above (Wang and Reddy, 2017). Unfortunately, memantine has not shown any promising activity in reducing cognitive impairments and the progression of AD.

1.3.7.3. GABAergic neurotransmission

Although the role of GABAergic system in the etiopathogenesis of AD has long been considered to be minor, recent studies have highlighted the deficits of the primary inhibitory neurotransmitter of the CNS in the progression of the neurodegenerative disease. The imbalance in the functioning of excitatory glutamatergic and inhibitory GABAergic systems is believed to facilitate neurodegenerative events and synaptic dysfunction in AD (Calsolaro and Edison, 2016; Nava-Mesa et al., 2014; Palop and Mucke, 2010). GABA is produced by neurons through the conversion of glutamic acid with the aid of enzyme glutamic acid decarboxylase. Upon release, GABA can: 1) bind to its ionotropic receptor, GABA-A, and induce fast hyperpolarization or 2) bind to its metabotropic GABA-B receptor and induce a slow inhibitory postsynaptic current (Padgett and Slesinger, 2010). Influx of chloride ions leads to the hyperpolarization of the postsynaptic neuron and hence decreases the probability of the action potential firing. The role of GABA-A and GABA-B receptors are well documented and include sedative, tranquilizing and hypnotic effects. Chronic use of GABA-A receptor agonists, such as diazepam, has been attributed to the impairment of memory, e.g., anterograde amnesia.

However, recently, detailed analysis of the GABA receptors has been done and its complex interaction with its subunits and their heterogeneity was reported. There are 5 main subunits of the GABA-A receptors, as shown in Figure 8, there are numerous subunits that can be combined in order to create the ionotropic receptor. The repertoire of the 5 GABA-A receptor subunits are thought to underpin the expression of somewhat 20 to 30 distinct subtypes of GABA-A receptors, expressed heterogeneously throughout the mammalian CNS (Fritschy and Brünig, 2003). Nevertheless, it is now known that 19 different genes code for individual subunits of the large "family" of GABA-A receptor: α(1-6), β(1-3), γ(1-3), ρ(1-3), δ, ε, θ and π. According to the aminoacid homology, these can be further divided into subfamilies and the number of heteropentameric combinations is large. These subunits are further divided into subfamilies depending on their amino acid homology (Olsen and Sieghart, 2008).

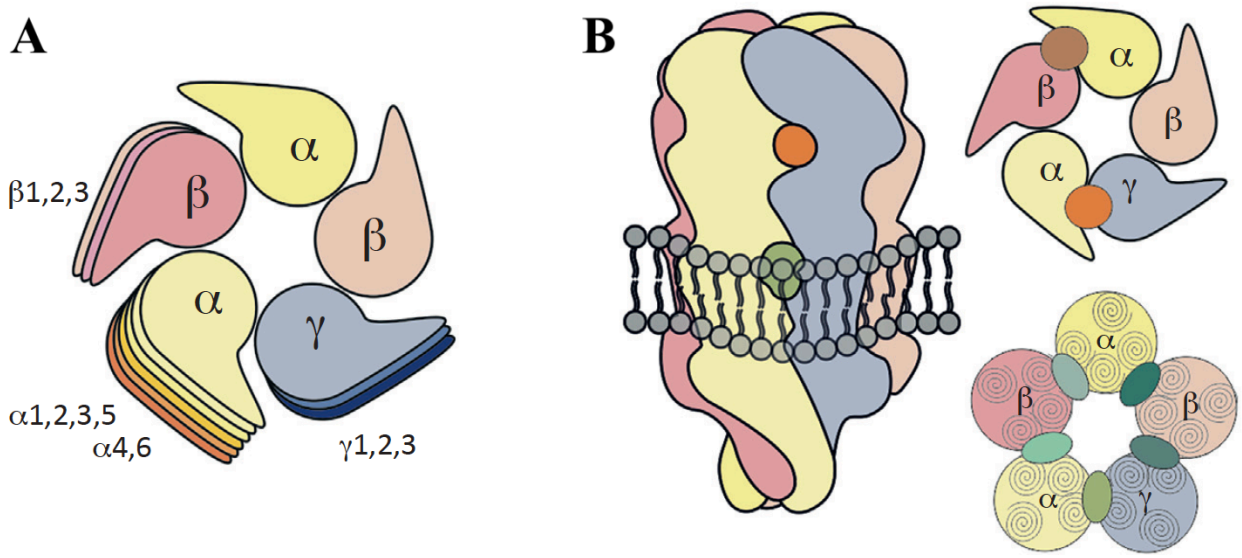

Figure 8. **GABA-A receptor subunit arrangement. Isoforms of the pentameric GABA receptor (A). Membrane-embedded GABA-A receptor (B) with the benzodiazepine binding site (orange), low-affinity site (green) and a view from outside of the cell that depicts the benzodiazepine binding site and a homologous site (brown). Adapted from (Sigel and Ernst, 2018).**

Complexity of GABA-A receptors is further observed at the synapse level: γ-subunit-containing GABA-A receptors are mainly localized post-synaptically, whereas δ-subunit-containing are predominantly localized extra-synaptically. Furthermore, GABA receptors are also localized on the glial cell surface (Fig. 9). Micromolar concentrations of the GABA and GABA-A receptor agonist muscimol displayed 8- to 22-fold higher potency at high-affinity extra-synaptic receptors than at synaptic receptors (Ahring et al., 2016).

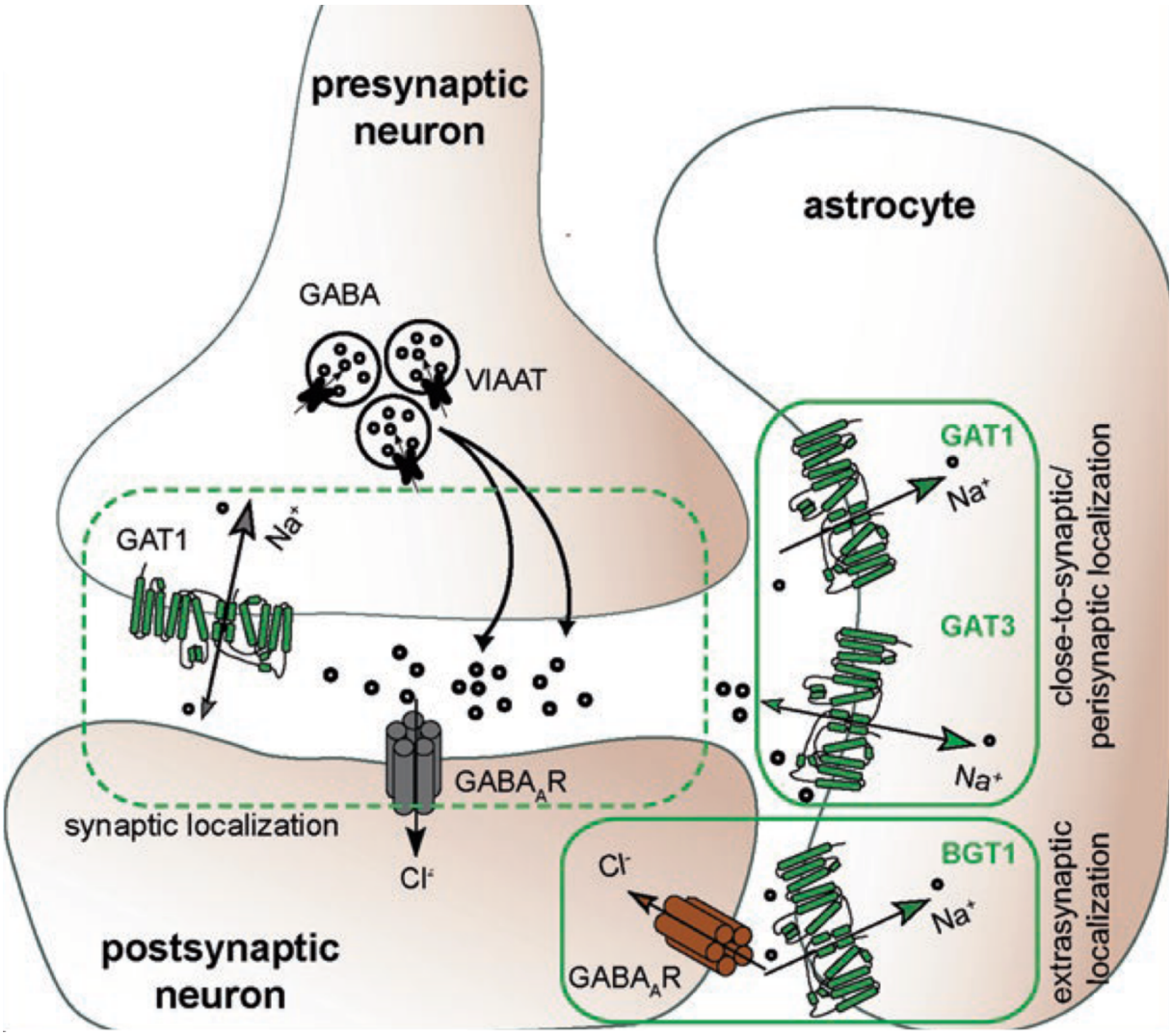

Figure 9. **Localization of GABA receptors. BGT – betaine-GABA transporter; Cl^- – chlorine ions; $GABA_AR$ – GABA-A receptor; GAT – GABA transporter; VIAAT – vesicular inhibitory amino acid transporter; Na^+ – sodium ions. Adapted from (Lie et al., 2017).**

GABA-B receptors are metabotropic, ubiquitously expressed receptors (Terunuma, 2018). Signaling that is mediated through GABA-B receptors involved G protein-activated potassium channels, adenylyl cyclase and voltage-gated Ca^{2+} channels (Bettler et al., 2004). The result of such signaling is the modulation of neuronal excitability and inhibition of neurotransmitter release (Bettler et al., 2004). There is a certain complexity of the GABA-B receptor and its subunits. GABA-B (1a,2) receptors are located pre-synaptically, whereas GABA-B (1b,2) receptors are predominantly expressed post-synaptically (Gassmann and Bettler, 2012; Marshall et al., 1999; O'Leary et al., 2014). The only selective GABA-B receptor agonist on the market is baclofen, which is used to treat spasticity and as a muscle relaxant in patients that suffer from multiple sclerosis, cerebral palsy and hemi- or tetraplegia (Froestl, 2010). Baclofen therapeutically acts by

inhibiting the release of excitatory neurotransmitters and neuropeptides in spinal cord, owing to its anti-spastic effects. The unwanted effects of baclofen include sedation, motor impairment and the development of tolerance. Structure of the GABA-B receptors is shown in Figure 10.

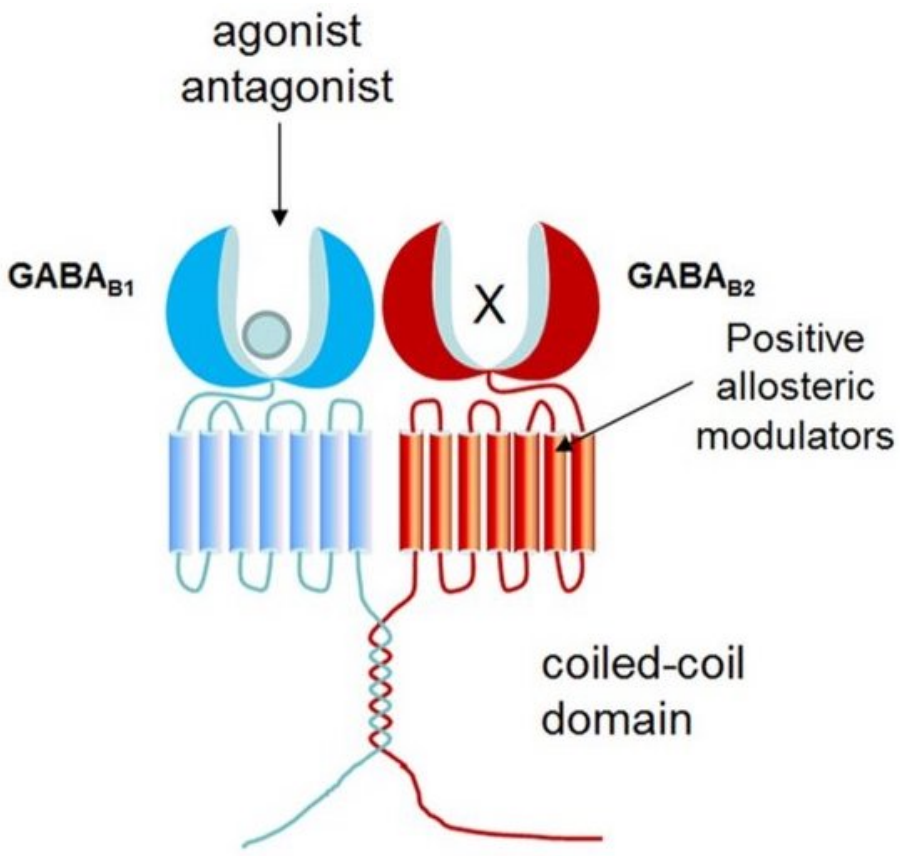

Figure 10. **Structural organization of the GABA-B receptor. 7-TM – 7-transmembrane domain. Adapted from (Xu et al., 2014).**

GABA participates in intercommunication with both glutamatergic and cholinergic neurotransmitter systems in the hippocampus and neocortex, the brain regions that are involved in providing synaptic plasticity and formation of memory (Ellender and Paulsen, 2010; Lawrence, 2008). Recent data highlight that GABA plays the lead role in learning and memory processes (Heaney and Kinney, 2016; Lee et al., 2011) and also regulates immune signaling (Lee et al., 2011). Processing of information in the brain relies on the spatial and temporal control of the way action potentials are transmitted between neural populations so that they fire action potentials in a coordinated manner (Panzeri et al., 2015). Specific neuronal populations are recruited and modulated by differential inhibitory neurons, whose heterogeneity corresponds to their ability to effectively and selectively regulate all compartments of the cells that these neurons target (Roux and Buzsáki, 2015). Inhibitory neurons participate in the regulation of all aspects of cell signal

transmission, starting from the input generation and ending with the output production. These neurons oversee the computations at the synaptic, cellular and network levels (Roux and Buzsaki, 2015). If one of these processes becomes dysregulated, a series of deleterious events might follow, resulting in cognitive and behavioral deficits (Palop and Mucke, 2010). The highest diversity of inhibitory neurons is observed in the hippocampal and neighboring regions, where more than 20 different neuronal cell types exist. Control provided by inhibitory neurons occurs in response to several sensory stimuli (Roux and Buzsaki, 2015), during higher order executive function (memory encoding or recall) performance (Ognjanovski et al., 2017) or specific behavioral states, e.g., mobility.

Hippocampus is a particularly important region where GABA produces its effects. Neurodegeneration in AD is partly evident as brain atrophy in the temporal lobe, specifically in the hippocampus. Loss of hippocampal pyramidal neurons was described in preclinical AD models (Eimer and Vassar, 2013; Fuhrmann et al., 2010). Adult neurogenesis takes place within the dentate gyrus (DG) both in rodents and in humans (Ming and Song, 2011) and it has been implied in AD among other several pathological processes (Mu and Gage, 2011). The DG is a compartment of hippocampus that is particularly vulnerable to amyloidosis, as shown by multiple studies (Chin, 2005; Palop, 2005). Both glutamatergic and GABAergic inputs regulate adult neurogenesis in the DG throughout postnatal development in a time-dependent fashion (Ming and Song, 2011; Toni et al., 2008). A knockin and expression of the *APOE4* gene resulted in a reduction of GABAergic interneurons and synapses in the DG, coinciding with a lack of mature adult-born granule cells (Li et al., 2010). Increase in neural progenitor cell proliferation and insufficient maturation of the newborn granule cells were observed in APP knockout mice, a model characterized by impairments in GABAergic synaptic transmission (Wang et al., 2014).

Inhibitory neurons are the pillars of adequate functionality in neuronal networks. Lack of sufficient inhibitory control might cause abnormal network activity patters that could lead to behavioral and cognitive impairments. Molecular and cellular level pathological changes in glutamatergic and GABAergic signaling might be reflected on a larger scale as abnormalities in the activity of the networks. Aberrant signaling of GABA has been well documented in AD (De Strooper and Karran, 2016; Jo et al., 2014; Kim and Yoon, 2017; Li et al., 2016; Wu et al., 2014). Excessive release of GABA by astrocytes of the DG was observed in both *APOE4* knockin and APPswe/PS1de9 mice (Jo et al., 2014; Wu et al., 2014). As a result, tonic inhibition by GABA was increased and a deficit in long-term potentiation was present. The reduction of tonic GABA inhibition and in GABA synthesis rescued spatial reference memory (Jo et al., 2014) and working memory (Wu et al., 2014), respectively. An increase in GABA synthesis and release from

astrocytes might occur as a compensatory action in response to the hyperexcitation. A schematic representation of GABAergic dysfunction in AD is shown in Figure 11.

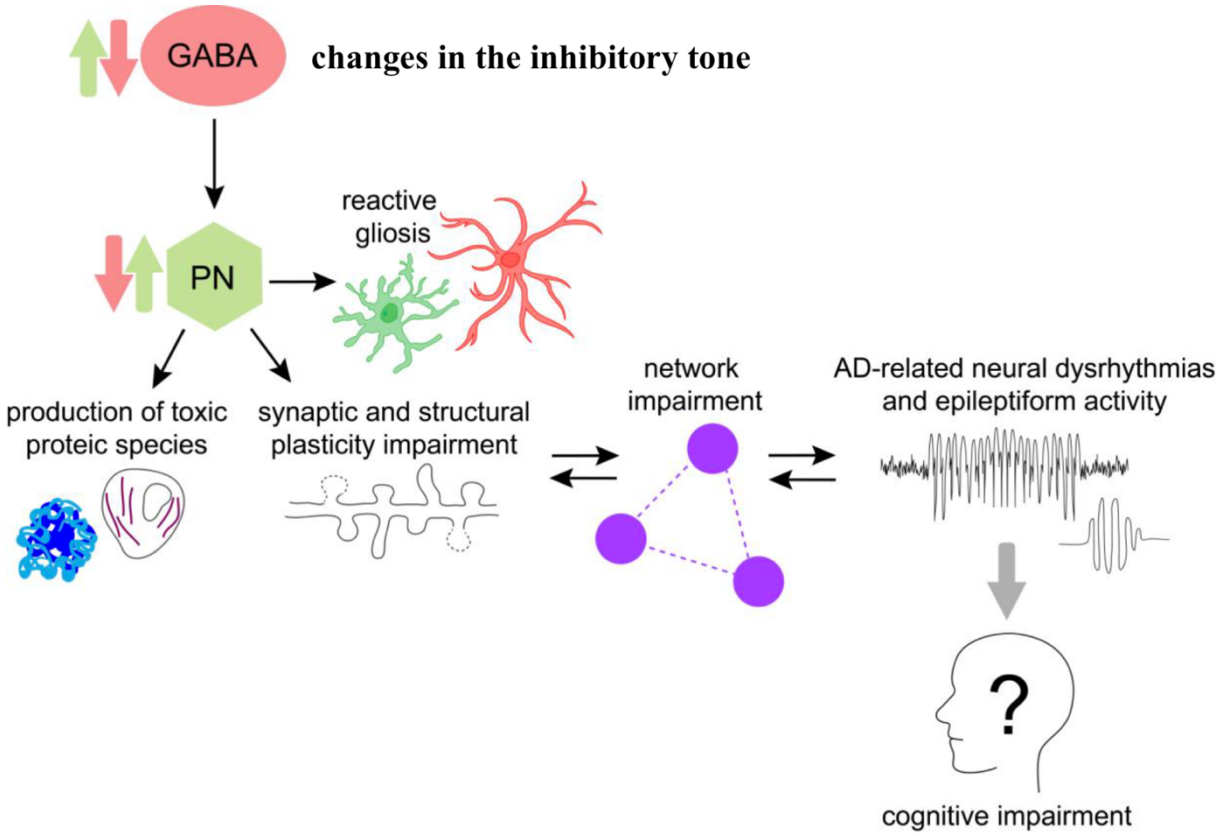

Figure 11. **Schematic depiction of the GABAergic dysfunction in AD. PN – principal neurons. Adapted from (Giovannetti and Fuhrmann, 2019).**

A decrease in GABA uptake was documented a long time ago using synaptosomal preparations from AD brains (Hardy et al., 1987) and radioactive labeling (Simpson et al., 1988) that allowed to conclude that a loss of GABAergic synapses was evident. Recently, deficits in GABA amounts and GABA receptor levels in AD have also been described by several authors (Calvo-Flores Guzmán et al., 2018; Govindpani et al., 2017; Kwakowsky et al., 2018). Different subunits of GABA-A receptors were studied in the prefrontal, entorhinal and temporal cortex using quantitative polymerase chain reaction method; a decrease in the number of receptors have been observed in these regions (Howell et al., 2000; Limon et al., 2012; Luchetti et al., 2011).

Activation of glia and as a response to the dysregulation of neural activity is a major factor that further exacerbates neurodegeneration. Although the interaction between GABAergic and glial cells has not been extensively studied, several studies have demonstrated that GABAergic transmission is associated with immune processes. GABA-B receptors of the $G_{i/o}$ subclass are expressed on microglial cell surface and are upregulated when microglia become activated (Kuhn et al., 2004). Furthermore, both GABA-A and GABA-B receptors regulate anti-inflammatory

processes. It has been demonstrated that upon release from astrocytes into the extracellular fluid, GABA is able to diminish astro- and microglia-induced release of interleukin-6 and tumor necrosis factor α that occurs through GABA-B receptor (Lee et al., 2011). Moreover, GABA was proven to inhibit inflammatory reactions governed by activated microglia and astroglia (Carson et al., 2006; Karve et al., 2016; Lee et al., 2011). Agonist of the GABA-B receptors baclofen reduced intracellular inflammatory pathways by 40 to 60% (Lee et al., 2011). Overall, anti-inflammatory effects of GABA receptor agonists were previously documented in multiple models of inflammation.

1.4. Models of AD

There are hundreds of different models of fAD, and they replicate the familial form of the disease. These models are generally transgenic and include overproduction, knockout or knockin of the genes that are involved in the accumulation of Aß, tau hyperphosphorylation and others. However, sAD has also been successfully modeled with the use of non-transgenic animals.

Non-transgenic models of AD are mostly obtained by administering a neurotoxic substance, e.g., Aß42, streptozocin (STZ), alloxan directly into the animal brain. STZ is a glucosamine-nitrosourea compound derived from soil bacteria and firstly developed as an anti-cancer agent, until the discovery of its diabetogenic properties in 1963. Single bilateral intracerebroventricular (icv) STZ injection produces multiple effects that resemble the molecular, pathological, and behavioral features of sAD that cannot be mimicked by the transgenic mice models of fAD (Grieb, 2016). As in the fAD models, the ultimate result is the Aβ pathology and neurodegeneration. However, the first effects produced by a single subdiabetogenic dose (3 mg/kg) were impaired insulin signaling, overactivation of glycogen synthase kinase-3β and significantly lower levels of major brain GLUT 1 and GLUT3 (Deng et al., 2009). Chronic decrease in cerebral glucose uptake led to several AD-like pathophysiological changes such as brain insulin resistance, decreased brain glucose metabolism (Grieb, 2016; Kamat et al., 2016). Glial activation, tumor necrosis factor-α and the generation of free radicals was the next major event that took place in the icv STZ model and produced progressive deterioration of memory function (Rai et al., 2014). Concomitantly, brain mitochondrial abnormalities and brain tissue oxidative stress (Tiwari et al., 2009) were detected, leading to caspase-mediated apoptotic cell death (Chen et al., 2013; Saxena et al., 2011). The mentioned behavioral and neurodegenerative responses appeared at distinct time courses ranging from 1 h to 15 days (Santos et al., 2012). Moreover, five weeks after STZ injection, decreased brain weight, significant accumulation of hippocampal Aβ and elevated

levels of hippocampal and cortical hyperphosphorylated tau were reported (Correia et al., 2013; Grieb, 2016). The schematic representation of STZ mechanism of action is shown in Figure 12.

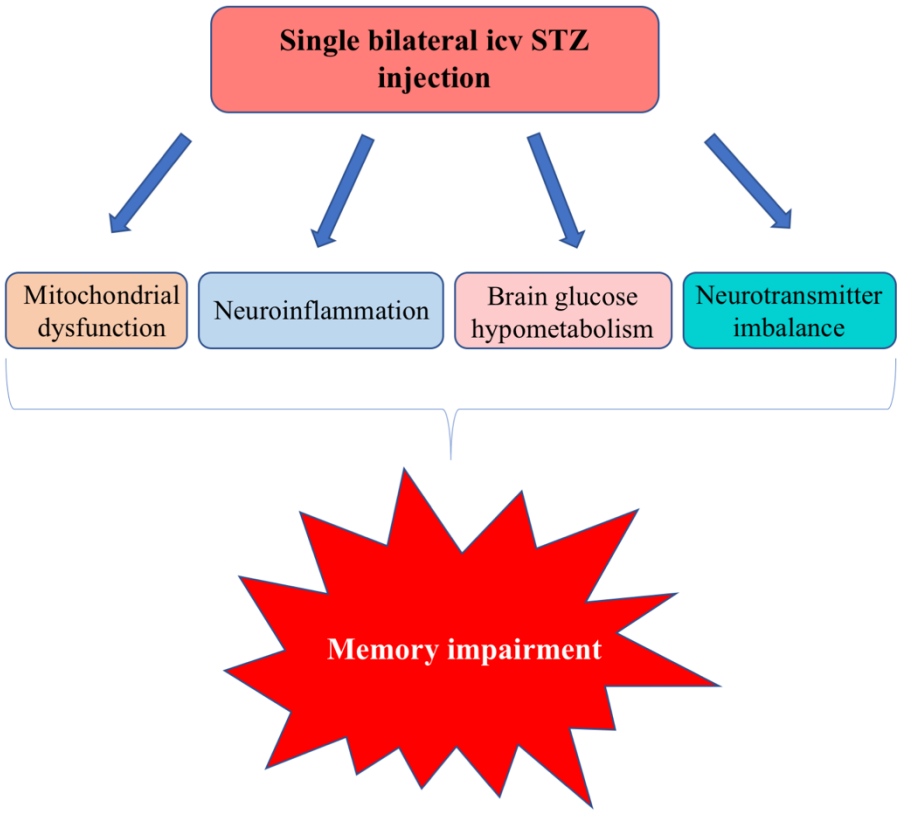

Figure 12. **The effects of intracerebroventricular (icv) injection of streptozocin (STZ). Adapted from (Kamat, 2015).**

2. METHODS

2.1. Animals

Male Wistar rats (280 ± 20 g) were obtained from the Laboratory Animal Center, University of Tartu, Estonia. All efforts were made to minimize animal suffering and reduce the number of animals used. The experiments were conducted in accordance with the EU Directive 2010/63/EU and local laws and policies on the protection of animals used for scientific purposes. The animal protocol used in the present study was approved by the Animal Ethics Committee of the Food and Veterinary Service, Riga, Latvia. The animals were housed in polypropylene cages (5 rats per cage) with food (R70, Lantmännen, Sweden) and tap water provided *ad libitum* in a controlled laboratory environment (temperature 22±2 °C, humidity 50–60%, 12/12 h light/dark cycle). The exclusion criteria for the behavioral and biochemical tests were as follows: 1) changes in behavior (aggressiveness, changes in breathing (tachypnea/dyspnea), decrease in movement, abnormal gait, inability to be handled); 2) negative impact of environment (diarrhea with/without blood); and 3) worsening of visual appearance (unkempt coat, weight loss more than 20%).

2.2. Chemicals and antibodies

The following chemicals were purchased from Sigma-Aldrich (USA): 3,3'-diaminobenzidine (DAB, cat. nr. D5905), anti-GFAP antibody (cat. nr. G3893), anti-SYP1 antibody (cat. nr. S6758), bovine serum albumin (BSA, cat. nr. 422351S), di-2-ethylhexyl phthalate (DEHP, cat. nr. D201154), ethopropazine (cat. nr. E5406), ExtrAvidin Peroxidase Staining Kit (cat. nr. EXTRA2), 4-(2-hydroxyethyl)-1-piperazine ethanesulfonic acid (HEPES, cat. nr. H3375), Mayer's hematoxylin solution (cat. nr. MHS16), muscimol (cat. nr. M1523), STZ (cat. nr. S0130) and Triton X-100 (cat. nr. X100). Anti-Iba-1 antibody (cat. nr. 019-19741) was supplied by Wako (Japan). Goat anti-rabbit immunoglobulins (cat. nr. ab205718) were purchased from Abcam (USA). S-acetylthiocholine iodide (cat. nr. A16802) and nickel ammonium sulfate hexahydrate (cat. nr. 12519) was obtained from Alfa Aesar (USA). Copper sulphate (cat. nr. 102790), potassium hexacyanoferrate (III) (cat. nr. 104973) and sodium citrate (cat. nr. 106448) were purchased from Merck-Millipore (USA). Anti-Bax antibody (cat. nr. sc-7480), anti-Bcl2 antibody (cat. nr. sc-7382), anti-caspase 3 (CASP 3) antibody (cat. nr. sc-7272) and anti-GAD67 antibody (cat. nr. sc-28376) were procured from Santa Cruz Biotechnology (USA). Invitrogen™ 3-(4,5-dimethyl-2-thiazolyl)-2,5-diphenyl-2H-tetrazolium bromide (MTT, cat. nr. M6494), Invitrogen™ Molecular Probes, 2,7-dichlorofluorescein (DCF) diacetate (cat. nr. D399), Gibco™ Dulbecco's modified Eagle medium (DMEM, cat. nr. 670087), Gibco™ horse serum (cat. nr.

16050122), Gibco™ fetal bovine serum (cat. nr. 16000044), phosphate buffered saline (PBS, cat. nr. 70011-044), trypsin-ethylenediaminetetraacetic acid solution (cat. nr. 25300062), penicillin-streptomycin-glutamine mixture (cat. nr. 10378016) were purchased from ThermoFisher Scientific (USA). Anti-p53 antibody (cat. nr. 9286) was purchased from Cell Signaling Technology (The Netherlands). Artificial cerebrospinal fluid (aCSF) was prepared *ex tempore* (mmol/l): 147 mM NaCl, 2.9 mM KCl, 1.6 mM $MgCl_2$, 1.7 mM $CaCl_2$ and 2.2 mM d-glucose were dissolved in water for injection. Gammapyrone was synthesized at the Laboratory of Membrane Active Compounds of the Latvian Institute of Organic Synthesis (Riga, Latvia). Diazepam solution (5 mg/ml) was obtained from JSC "Grindeks" (Latvia).

2.3. *In vivo* experiments

2.3.1. Drug treatments

2.3.1.1. Treatment with muscimol

The rats were randomly divided into six groups of 10 animals each. The groups were injected intraperitoneally (ip) with either saline (1 ml/kg) or muscimol (M, 0.01 and 0.05 mg/kg, dissolved in saline) for 3 consecutive days prior to the icv injection of STZ or aCSF and during 4 consecutive water maze training days. The following groups were used in the muscimol experiments: 1) ip saline and icv aCSF (Control); 2) ip saline and icv STZ (STZ); 3) ip muscimol 0.01 mg/kg and icv aCSF (M 0.01 + aCSF); 4) ip muscimol 0.05 mg/kg and icv aCSF (M 0.05 + aCSF); 5) ip muscimol 0.01 mg/kg and icv STZ (M 0.01 + STZ); and 6) ip muscimol 0.05 mg/kg and icv STZ (M 0.05 + STZ).

2.3.1.2. Treatment with diazepam

The rats were randomly allocated to one of the six groups (n=10) and received ip injections of either saline (1 ml/kg) or diazepam (DZP, 0.05 and 1 mg/kg). Administration of saline or diazepam was done for 3 consecutive days prior to the icv injection of STZ or aCSF, as well as on experimental days 5-22.The groups were the following: 1) ip saline and icv aCSF (Control); 2) ip saline and i.c.v. STZ (STZ); 3) ip diazepam 0.05 mg/kg and icv aCSF (DZP 0.05 + aCSF); 4) ip diazepam 1 mg/kg + icv aCSF (DZP 1 + aCSF); 5) ip diazepam 0.05 mg/kg and icv STZ (DZP 0.05 + STZ); 6) ip diazepam 1 mg/kg + icv STZ (DZP 1 + STZ).

2.3.1.3. Treatment with baclofen

The rats were randomly divided into six groups of 10 animals each. The groups received ip injections of either saline (1 ml/kg) or baclofen (BCL, 0.025 and 0.05 mg/kg, dissolved in saline) for 3 consecutive days prior to the icv injection of STZ or aCSF and during 4 consecutive water maze training days (30 min prior to the test). The following groups were used: 1) ip saline and icv aCSF (Control); 2) ip saline and icv STZ (STZ); 3) ip baclofen 0.025 mg/kg and icv aCSF (BCL 0.025 + aCSF); 4) ip baclofen 0.05 mg/kg and icv aCSF (BCL 0.05 + aCSF); 5) ip baclofen 0.025 mg/kg and icv STZ (BCL 0.025 + STZ); and 6) ip baclofen 0.05 mg/kg and icv STZ (BCL 0.05 + STZ).

2.3.1.4. Treatment with gammapyrone

The rats were randomly divided into six groups of 10 animals each and received ip injections of either saline (1 mL/kg) or gammapyrone (0.1 and 0.5 mg/kg). Saline and gammapyrone were injected once daily for 3 consecutive days prior to the icv injection of STZ or aCSF, and on experimental days 15-22 (30 min prior to the test). The groups were the following: 1) saline ip and icv aCSF (Control); 2) saline ip and icv STZ (STZ); 3) gammapyrone 0.1 mg/kg ip and icv aCSF (GMP 0.1 + aCSF); 4) gammapyrone 0.5 mg/kg + icv aCSF (GMP 0.5 + aCSF); 5) gammapyrone 0.1 mg/kg ip and icv STZ (GMP 0.1 + STZ); 6) gammapyrone 0.5 mg/kg + icv STZ (GMP 0.5 + STZ).

2.3.2. Stereotactic surgery

On experimental day 4, animals were anaesthetized with isoflurane (3-3.5% for induction and 2% for maintenance) in N_2O and O_2 (70%/30% for induction and 50%/50% for maintenance). Animals were then fixed on a stereotaxic frame (Stoelting Inc., USA). The head was shaved and sterilized with an alcohol pad, and a sagittal incision in the midline was made. Two lateral holes were drilled in the skull using the following coordinates (Paxinos and Watson, 2007): −0.7 mm anteroposterior, 1.7 mm mediolateral and −4.0 mm dorsoventral relative to bregma. Using Hamilton microsyringe, STZ was injected in two lateral ventricles (750 µg in 10 µl aCSF for each animal) at 1 µl/min and 5 µl per ventricle. Control group received bilateral injections of aCSF (5 µl/ventricle). For the diffusion of the substance, the microsyringe was left in place for 2 min after each infusion. A 14-day resting period was implemented for the development of cognitive deficiency.

2.3.3. Open field test

Open field test was used to assess the changes in animal locomotor activity and included a circular arena (diameter 100 cm, wall height 40 cm). Center zone was 33 cm in diameter. The animals were acclimated to the behavioral room (experimental lights on and doors shut) for 30 min. Then, each animal was gently placed inside the arena for 10 min. After each test, the arena was cleaned with 70% ethanol and dried with paper towel. A video tracking device coupled with EthoVision XT 11.0 (Noldus, The Netherlands) was used to record the motility parameters: a) total distance traveled (cm) and b) total time spent in the center zone (cm/s).

2.3.4. Morris water maze (MWM) test

MWM test was carried out to assess the spatial learning and memory of the rats 14 days after the STZ injection. The apparatus (Ugo Basile, Italy) consisted of a blue circular tank (diameter 180 cm) filled with water (23 ± 1°C) to a depth that would cover the plexiglass platform (diameter 30 cm, height 10 cm) for 1-2 cm. Each animal underwent 4 trials (120 s maximum for each trial) per day for 4 consecutive days. The animals were trained to find the hidden platform from different starting points in the pool after being gently put in the water facing the wall of the pool. As soon as the animal found the platform, it was given 15 s to stay on it to learn the location. The intertrial period was 10 min. After 4 training days, the probe trial was carried out. In this case, the platform was removed from the pool and each animal had to swim for 120 s in the pool. EthoVision XT 11.0 video tracking software (Noldus, The Netherlands) was used to record:

- during the trainings: 1) rat escape latency, i.e., time in seconds for each animal to find the platform after being put in the pool and 2) rat swimming speed;
- during the probe trial: 1) time spent in the target quadrant and 2) the number of platform zone crossings.

2.4. *Ex vivo* experiments

2.4.1. Immunohistochemistry

On the next day after the probe trial, rats were deeply anaesthetized with ketamine (150 mg/kg) and xylazine (15 mg/kg), then transcardially perfused with ice-cold saline for 10 min. After the perfusion, animals were decapitated, and the brains were removed and fixed in 4% paraformaldehyde for 24 h. After fixation, the brains were placed in 30% sucrose for 48 h for cryoprotection and subsequently placed in an antifreeze solution.

Brain samples (4 per group) were then cut using CM1850 cryostat (Leica, USA) into 30-µm sections (AP plane: Bregma −2.92 mm to −3.48 mm) at -27°C. Free floating brain sections were rinsed 3 times in PBS and 0.1% Triton X-100 solution, incubated in citrate buffer (pH 6.0) at 95°C for 10 min to improve antigen retrieval (for GAD67, Iba-1 and SYP1), cooled to room temperature (20°C) and blocked with a 5% bovine serum albumin solution at room temperature for 1 h to avoid the formation of background staining. Sections were then stained with respective primary antibody (1:500 for GAD67, 1:1000 for GFAP and SYP1, 1:2000 for Iba-1). After incubation with the primary antibody, the sections were rinsed in PBS-T 3 times and transferred to a solution containing the biotinylated mouse immunoglobulins (dilution 1:500) raised against GAD67, GFAP and SYP1. The Iba-1 sections were incubated with goat anti-rabbit immunoglobulins conjugated with horseradish peroxidase (1:2000) for 2 h. After incubation with the secondary antibody, the GAD67, GFAP and SYP1 sections were rinsed and incubated with mouse ExtrAvidin Peroxidase (1:1000) for 1.5 h. After rinsing, the sections were incubated with PBS solution containing 2.5% DAB, 0.2% H_2O_2 and 5% nickel ammonium sulfate for 30 s (Iba-1), 1 min (GAD67 and GFAP) and 2 min (SYP1). For Iba-1 and SYP1, the sections were also counterstained for 1 min in hematoxylin solution. All stained sections were mounted on slides and coverslipped. Negative control sections were also stained using the same protocol but without the primary antibody. All experiments were done in duplicate.

2.4.2. Histochemistry

For each brain, 4 samples per animal was used to obtain 30 µm thick slices (AP plane: Bregma −2.92 mm to −3.48 mm). Histochemical detection of AChE-containing nerve axon density in the anterior cingulate cortex and hippocampal CA1 region was performed using a previously described method (Karnovsky and Roots, 1964), which was optimized and described elsewhere (Kadish and Van Groen, 2002). Briefly, brain sections (5 brain samples per group) were rinsed with a 0.1 M maleate buffer (pH 6.0). Subsequently, the sections were incubated with 0.1 M maleate buffer containing 86.5 mM S-acetylthiocholine iodide, 30 mM ethopropazine, 30 mM copper sulfate, and 100 mM sodium citrate and 0.03 mM potassium hexacyanoferrate for 2 h. Subsequently, the staining was intensified by incubating the sections with 2.5% DAB, 0.2% H2O2 and 5% nickel ammonium sulfate for 2 min in 0.05 M Tris buffer (pH 7.6). All experiments were done in duplicate.

2.4.3. Quantification

The mounted brain sections were digitized using a Pannoramic MIDI II Scanner (3DHISTECH, USA) with a 20 × lens. The corresponding regions were then selected, and images were captured using Pannoramic Viewer (3DHISTECH, USA). The optical densities of expressed proteins were measured in the anterior cingulate cortex and the *stratum radiatum* of hippocampal *cornu ammonis* 1 (CA1) region (AChE, GAD67, GFAP and Iba-1). The latter structure was chosen because of previously found more pronounced loss of CA1 neurons associated with AD (West et al., 2006; Zarow et al., 2005). SYP1 density was measured in the hippocampal CA1, CA3 and DG. All measurements were made in duplicate. Both immunohistochemical and histochemical data were quantified using an open-source image processing software (Fiji, Germany). A region of interest (same size for all samples) was chosen, and an automatic threshold, in arbitrary units (au), was used to detect pixel density. Densitometry was reported as the mean intensity per studied region of interest.

2.5. *In vitro* assays

2.5.1. Binding to GABA-A receptors

The experiment was accepted in accordance with Eurofins validation Standard Operating Procedure and performed by CEREP (France). Gammapyrone was tested at 1 μM, 10 μM and 100 μM concentrations and agonist radioligand [3H]muscimol – at a 15 nM concentration for 120 min at room temperature to assay the binding to the GABA-A1 receptor (α1,β2,γ2) obtained from human recombinant cells (Wang, 2001). Compound binding was detected using scintillation counting and was calculated as percent inhibition of the binding of a radioactively labelled ligand specific for the GABA-A receptor. Experiment was done two times, with each assay conducted in duplicate. Inhibition or stimulation higher than 50% were considered significant.

2.5.2. Binding to GABA-B receptors

The brains from adult male Wistar rats (180 ± 20 g) were removed, embedded in cryoglue and cut into 10-μm thick adjacent coronal sections (thalamic nuclei, cerebellum and hippocampus) and membranes were prepared as described previously (Bischoff et al., 1999; Dambrova et al., 2008). In brief, membranes were incubated with the GABA-B receptor-selective radioligand [3H]-CGP 54626 (2 nM) and competing drugs (baclofen and gammapyrone) in 200 μl of Krebs-Henseleit (KH) buffer for 90 min at room temperature. Gammapyrone was tested at

1 μM, 10 μM and 100 μM concentrations. Non-specific binding for each assay was determined in the presence of 10 mM baclofen. The bound and free radioligands were separated by rapid filtration under a vacuum using Millipore GF/C filter paper (Merck Millipore, USA). The filters were washed three times with 0.25 ml of KH buffer. Radioactivity of the samples was measured with a liquid scintillation counter (Wallac MicroBeta TriLux, PerkinElmer, USA). Each experiment was performed twice, and each assay was conducted in duplicate. Significant inhibition or stimulation was considered to be that of 50% or higher.

2.5.3. Cell culture

Rat PC12 cells (TCC® CRL-721™, USA) were cultured in DMEM, supplemented with 10% horse serum, 5% PBS, 1% L-glutamine (200 mM), 1% of mixture penicillin (100 international units/ml) and streptomycin (100 μg/ml) at 37°C in a CO_2 incubator. Before the experiments, cells were differentiated by culturing in serum-free medium containing 50 ng/ml nerve growth factor for 5 days. Protein concentration was quantified by using Bradford colorimetric protein determination at 595 nm (Bradford, 1976). All experiments in PC12 cells were done in collaboration with the research group lead by Professor Vittorio Calabrese, Department of Biomedical and Biotechnological Sciences, University of Catania, Italy.

2.5.4. Cell viability and toxicity assay

Cell viability was determined by the MTT assay, based on the ability of living cells to metabolize the yellow tetrazolium salt to a blue formazan via mitochondrial succinate dehydrogenase which is a member of mitochondrial electron transfer system complex. Gammapyrone was added at concentrations 1, 10 and 100 μM. Based on the results obtained from the cell viability assay, 1 μM was the concentration of gammapyrone chosen to perform DEHP toxicity tests.

PC12 cells (2.5×10^5 cells/well in a 96-well plate) were incubated at 37°C after pretreatment with gammapyrone (1 μM) for 2 h and then incubated with DEHP (83 μM) for 24 h. A negative control containing only cells was also evaluated. After treatment with gammapyrone, the cells were incubated with 5 mg/ml MTT for 3 h at 37°C, the medium was carefully removed after the incubation and the formazan crystals were dissolved in 150 μl dimethyl sulfoxide. Absorbance of formazan reduction product was measured by spectrophotometry at 570 nm using an ELx800™ microplate reader (BioTek Instruments, USA). The results were expressed as the percentage of

MTT reducted relative to the absorbance measured from negative control cells. All assays were performed in triplicate.

2.5.5. Determination of reactive oxygen species (ROS)

To estimate the levels of endogenous ROS production in control and experimental cells, the nonfluorescent probe DCF diacetate was used. It diffuses passively into the intracellular matrix of cells and undergoes cleavage by esterases to form impermeable $DCFH_2$ that does not leave the cell (McLennan and Esposti, 2000). Then, in a ROS-dependent oxidation, fluorescent DCF is formed from $DCFH_2$ (Chen et al., 2010), was used. PC12 cells were seeded on 24-well culture plates (Polylabo, France) at 10^5 cells/well and incubated for 24 h. Then, the cells were incubated with DEHP alone or combined to gammapyrone (1 µM) for 24 h at 37°C. After treatment, cells were incubated with 20 µM DCF diacetate for 30 min at 37°C and washed twice with PBS to remove the excess probe. The intracellular production of ROS was measured by fluorometric detection of DCF oxidation on a fluorescence and luminescence reader (FLx800, BioTek Instruments, USA) with an excitation wavelength of 485 nm and emission wavelength of 522 nm.

2.5.6. Measurement of mitochondrial membrane potential (MMP)

Changes in MMP were determined by the mitochondrial-specific incorporation of a cationic fluorescent dye Rhodamine-123 (Rh-123) (Debbasch et al., 2001). The cells were seeded in 96-well culture plates and were treated with DEHP alone or combined with gammapyrone (1 µM) for 24 h. Then, cells were rinsed with PBS, and 100 µL of Rh-123 (1 µM) in PBS was added on the plates. Cells were incubated (37°C, 5% CO_2) for 15 min. Next, the PBS solution containing Rh-123 that was not taken up by the cells was washed and replaced by fresh PBS, and fluorometric detection was done. The results were expressed as the intracellular Rh-123 uptake. All assays were performed in triplicate.

2.5.7. Preparation of mitoplasts

PC12 cells were collected by trypsinization, pelleted by centrifugation at 500 × g and resuspended in PBS (pH 7.4). The cell suspension was exposed to 2 mg digitonin/mg cellular proteins for 10 min on ice. The mitoplast fraction, obtained by digitonin cell disruption, was pelleted at 14000 × g and resuspended in PBS (Signorile et al., 2014).

2.5.8. Enzymatic spectrophotometric assay of mitochondrial complexes

Mitoplasts were exposed to ultrasound energy for 15 s at 0°C. The reduced nicotinamide adenine dinucleotide (NADH):ubiquinone oxidoreductase (complex I) activity was measured by quantifying the oxidation of 100 μM NADH at 340–425 nm ($\Delta\varepsilon$ = 6.81 $mM^{-1} \cdot cm^{-1}$), using 50 μg of mitoplast proteins in the presence of 40 mM potassium phosphate buffer (pH 7.4) containing 5 mM $MgCl_2$, 3 mM KCN, 1 μg/ml antimycin A and 200 μM decylubiquinone. The activity was corrected for the residual activity measured in the presence of 1 μg/ml rotenone (Piccoli et al., 2006). Activity of succinate-cytochrome c oxidoreductase (complexes II+III) was measured at 550–540 nm ($\Delta\varepsilon$ = 19.1 $mM^{-1} \cdot cm^{-1}$) as the initial rate of cytochrome c reduction. Proteins (100 μg/ml) were incubated for 10 min in the assay buffer (25 mM potassium phosphate, pH 7.2, 5 mM $MgCl_2$) in the presence of 20 mM succinate, 3 μg/ml rotenone, 2 mM KCN and 65 mM decylubiquinone. The reaction started by the addition of 20 μM cytochrome c and was corrected by the residual activity measured in the presence of 2 μg/ml antimycin A. Activity of cytochrome c oxidase (complex IV) was measured by quantifying the oxidation of 10 μM ferrocytochrome c at 550–540 nm ($\Delta\varepsilon$ = 19.1 $mM^{-1} \cdot cm^{-1}$). Enzymatic activity was measured in 10 mM PBS using 30 μg of mitoplast proteins (Cooperstein and Lazarow, 1951).

2.5.9. Measurement of mitochondrial ATP production rate

The rate of ATP production by oxidative phosphorylation was determined in digitonin-permeabilized cells, essentially as described elsewhere (Valenti et al., 2013). Briefly, aliquots of trypsinized fibroblasts washed with PBS were suspended in 1 ml of medium containing 210 mM mannitol, 70 mM sucrose, 20 mM Tris/HCl, 5 mM KH_2PO_4/K_2HPO_4 (pH 7.4), 3 mM $MgCl_2$ in the presence of the ATP detecting system (ATP-ds). The ATP-ds consisted of 2.5 mM glucose, 2 units hexokinase, 1 unit glucose 6-phosphate dehydrogenase (G6P-DH) and 0.25 mM nicotinamide adenine dinucleotide phosphate ($NADP^+$), with 3 μM rotenone as toxin and 5 mM succinate as energy substrate, as well as 10 μM diadenosinepentaphosphate as the adenylate kinase inhibitor (Lienhard and Secemski, 1973).

After 5 min of incubation with digitonin (30 μg/10^6 cells) at 37°C, the reduction of $NADP^+$ in the extramitochondrial phase, which reveals ATP formation from externally added adenosine diphosphate (ADP, 0.5 mM), was determined as the increase in absorbance at 340 nm. Care was taken to use enough hexokinase/G6P-DH coupled enzymes to ensure a nonlimiting ADP-regenerating system for the measurement of ATP production. The rate of ATP production by

Complex V was corrected for the residual ATP production measured in the presence of 2 μg/mg protein oligomycin.

2.5.10. Protein extraction and Western blot analysis

After the treatment schedule, PC12 cells (1×10^5) in 6-well plates were harvested, washed with PBS, and lysed in 100 μL lysis buffer (0.5 M HEPES containing 0.5% Nonidet-P40, 1 mM phenylmethylsulfonyl fluoride, 1 mg/ml aprotinin, 2 mg/ml leupeptin, pH 7.4) and incubated 20 min on ice before centrifugation. Protein concentrations were determined in cell lysates using the BioRad protein assay.

Equal amounts of proteins (30 μg) were separated on 12% sodium dodecyl sulphate–polyacrylamide gel electrophoresis and subsequently blotted onto polyvinylidene difluoride membranes (Millipore, USA). After blocking for 1 h in Tris-buffered saline containing 5% nonfat dry milk at 25°C, the blots were probed overnight with the following primary antibodies: Bax (1:500), Bcl2 (1:500), p53 (1:2000), CASP 3 (1:500) and β-actin overnight at 4°C. The blots were then washed and incubated for 1 h with the corresponding secondary antibodies: horseradish peroxidase-conjugated anti-mouse or anti-rabbit immunoglobulins (both 1:3000). Protein bands were visualized by using enhanced chemiluminescent substrate kit (GenScript, USA). Proteins levels were then determined by computer-assisted densitometric analysis using GS-800 densitometer (BioRad, USA). All assays were performed in duplicate.

2.6. Statistical analysis

GraphPad Prism® 6 software (GraphPad Software Inc., USA) was used to conduct the statistical analysis. All data were subjected to the Kolmogorov–Smirnov test for normality and an equal variance test. Data are presented as the mean ± standard deviation (S.D.) values. The Morris water maze training data were analyzed using two-way repeated measure analysis of variance (ANOVA) to account for inter-group variations (with group and training day as factors) and were followed by Bonferroni's (muscimol and baclofen data) or Holm-Sidak's (diazepam and gammapyrone data) multiple comparisons test. Data from the Morris water maze probe trial and open field data, as well as quantitative immunohistochemical and histochemical data, were analyzed using one-way ANOVA followed by Bonferroni's (muscimol and baclofen data) or Holm-Sidak's (diazepam and gammapyrone data) multiple comparisons test. *In vitro* data (in PC12 cells) were analyzed using one-way ANOVA followed by Tukey's multiple comparisons test. Statistical significance was set at $P < 0.05$.

3. RESULTS

3.1. Effects of GABA-A receptor agonist muscimol

3.1.1. In the MWM test

In the MWM trainings, a significant interaction was revealed in group and training day factors. The administration of STZ resulted in a longer escape latency than that of the controls starting from training day 2 to day 4 ($P < 0.0001$, Fig. 13.A). Treatment with both doses of muscimol shortened the escape latency of STZ-injected rats from training day 2 to day 4 ($P < 0.0001$) to the control group level. No significant differences were observed in swimming speed between groups on all training days (Fig. 13.B).

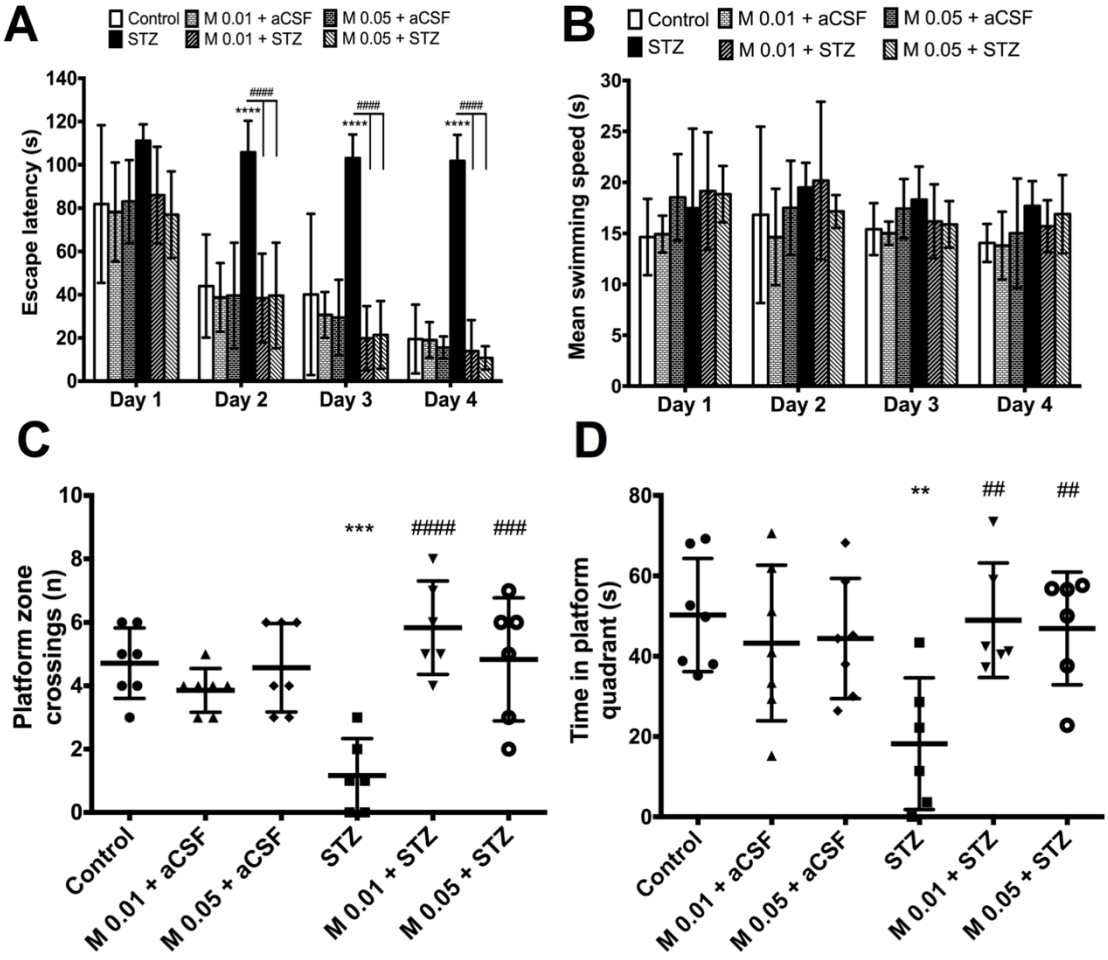

Figure 13. **Effects of muscimol (M) on the streptozocin (STZ) model and control rat escape latency (A), swimming speed (B), platform zone crossings (C) and time in platform quadrant (D). The data are shown as mean values ± S.D. (n=6-7/group). Two-way repeated measure ANOVA followed by Bonferroni's post-test. *****P*** **< 0.01, ******P*** **< 0.001 and *******P*** **< 0.0001 vs. Control; ##*P* < 0.01, ###*P* < 0.001 and ####*P* < 0.0001 vs. STZ.**

In the MWM probe trial, differences between groups were observed in platform crossings (Fig. 13.C) and in the time spent in the target quadrant (Fig. 13.D). STZ also produced impairments in spatial memory seen as decreased platform crossings ($P < 0.001$) and time spent in the platform quadrant ($P < 0.01$) compared to controls. Muscimol-treated STZ group rats showed a reversal of STZ-induced impairments by demonstrating significantly more platform crossings ($P < 0.001$) and longer time spent in the platform quadrant ($P < 0.01$). Muscimol *per se* did not significantly change rat performance in the MWM trainings and in the probe trial compared to the control group data.

3.1.2. On rat brain protein density

3.1.2.1. GFAP density

Significant differences were observed between groups in the density of GFAP staining in the cortex (Fig. 14.A and B), as well as in the hippocampus (Fig. 14.C and D). STZ induced an almost 3-fold increase in the density of GFAP staining in the cortex ($P < 0.0001$) and hippocampus ($P < 0.0001$) compared to the controls. Treatment with 0.01 and 0.05 mg/kg muscimol reversed STZ-induced increases in the density of cortical and hippocampal GFAP staining and restored its values to the levels observed in both structures in the control group ($P < 0.0001$). Muscimol at both doses did not change the cortical and hippocampal GFAP density in control group rats.

3.1.2.2. GAD67 density

Significant differences were observed between groups in cortical (Fig. 15.A and B) and hippocampal (Fig. 15.C and D) GAD67 staining density. STZ injection produced a slight, but significant (about 25%) decrease in the density of GAD67 staining in the cortex ($P < 0.01$) and hippocampus ($P < 0.0001$) compared to controls. At both tested doses, muscimol reversed STZ-induced decrease in GAD67 staining in the cortex ($P < 0.01$) and hippocampus ($P < 0.0001$). Muscimol treatments did not change cortical and hippocampal GAD67 staining compared to that of the control group.

3.1.2.3. AChE density

Significant differences were detected between groups in cortical (Fig. 16.A and B) and hippocampal (Fig. 16.C and D) AChE density. In the STZ group, a 3-fold increase in AChE density was observed in the cortex ($P < 0.0001$) and hippocampus ($P < 0.0001$) compared to the

control group rats. At both tested doses, muscimol reversed STZ effects in the cortex ($P < 0.0001$) and hippocampus ($P < 0.0001$). Muscimol *per se* did not alter cortical and hippocampal AChE density of the control group rats.

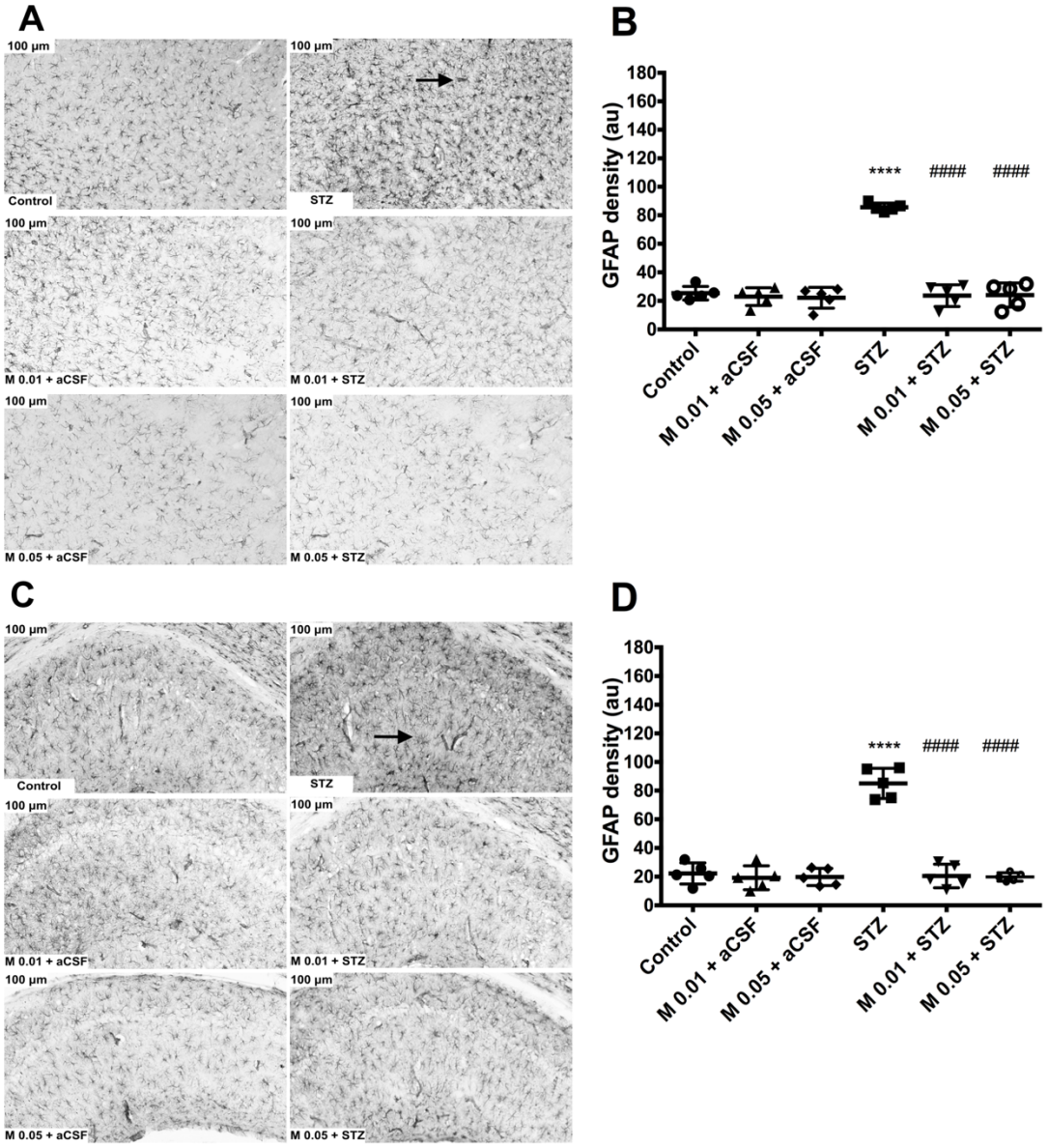

Figure 14. **Effects of muscimol (M) on glial fibrillary acidic protein (GFAP) density in streptozocin (STZ) model rats and control rats. Representative photomicrographs show GFAP staining in the rat anterior cingulate cortex (A) and hippocampal CA1 (C) at 200 × magnification. Black arrows indicate representative GFAP-positive cells. Bar graphs demonstrate cortical (B) and hippocampal (D) density measurements. The data are shown as mean values ± S.D. (n=5/group). One-way ANOVA followed by Bonferroni's post-test. *******P* < 0.0001 vs. Control; ####*P* < 0.0001 vs. STZ.**

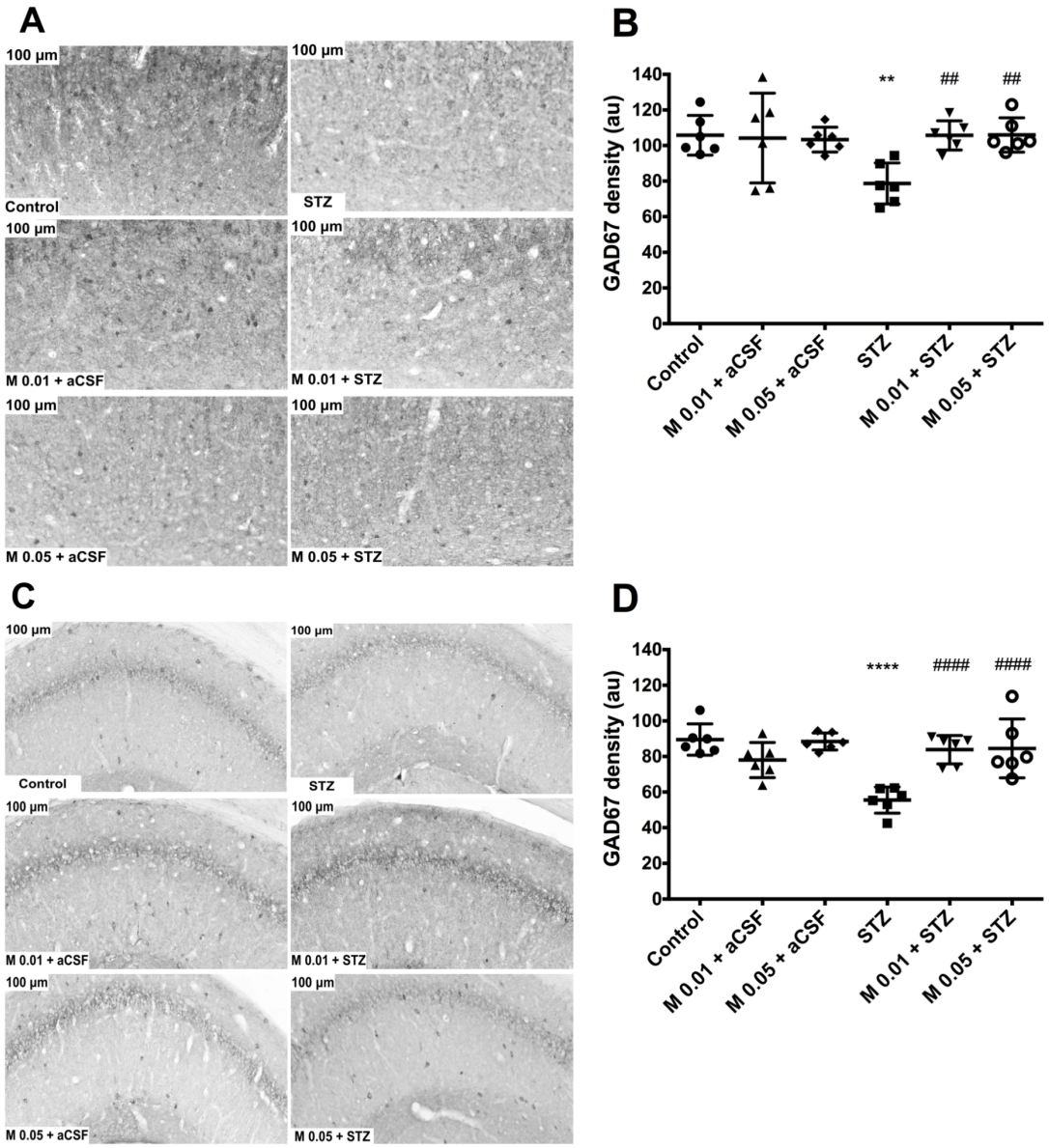

Figure 15. **Effects of muscimol (M) on glutamic acid decarboxylase 67 (GAD67) density in streptozocin (STZ) model rats and control rats. Representative photomicrographs show GAD67 staining in the rat anterior cingulate cortex (A) and hippocampal CA1 (C) at 200 × magnification. Bar graphs demonstrate cortical (B) and hippocampal (D) density measurements. The data are shown as mean values ± S.D. (n=6/group). One-way ANOVA followed by Bonferroni's post-test. *****P*** **< 0.01 and *******P*** **< 0.0001 vs. Control; ##*P* < 0.01 and ####*P* < 0.0001 vs. STZ.**

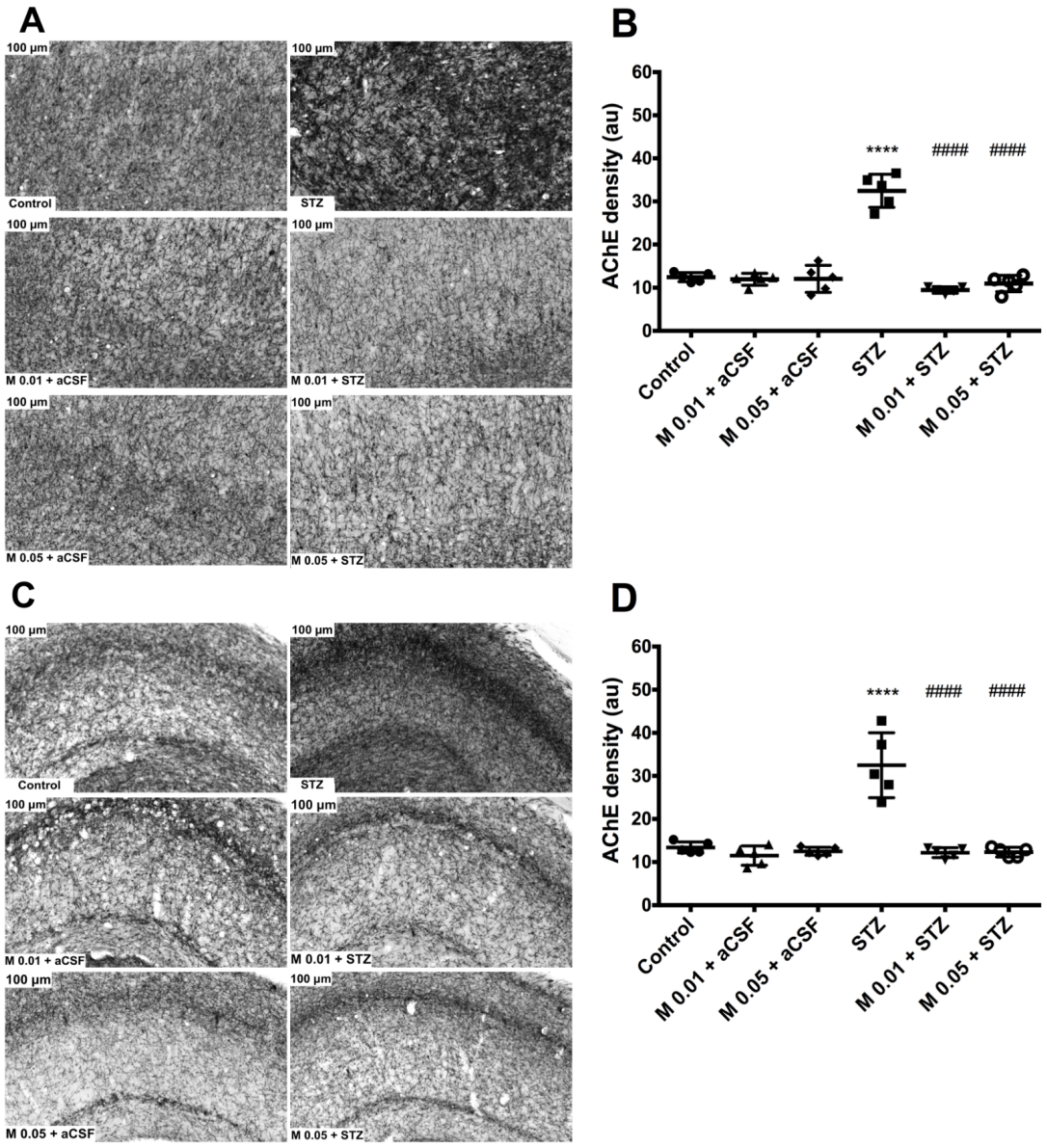

Figure 16. **Effects of muscimol (M) on acetylcholine esterase (AChE) density in streptozocin (STZ) model rats and control rats. Representative photomicrographs show AChE-positive nerve axons in the rat anterior cingulate cortex (A) and hippocampal CA1 (C) at 200 × magnification. Bar graphs demonstrate cortical (B) and hippocampal (D) density measurements. The data are shown as mean values ± S.D. (n=5/group). One-way ANOVA followed by Bonferroni's post-test. *******P* < 0.0001 vs. Control; ####*P* < 0.0001 vs. STZ.**

3.2. Effects of GABA-A receptor agonist diazepam

3.2.1. On behavior and locomotion

3.2.1.1. In the MWM test

Significant interaction was detected in the MWM training data in group and training day factors. Administration of i.c.v. STZ resulted in significantly longer escape latency on MWM training days 2-4 ($P < 0.001$) compared to the controls (Fig. 17.A). STZ rats treated with both diazepam doses demonstrated significantly shorter escape latencies on training day 2 ($P < 0.01$), training day 3 ($P < 0.0001$) and training day 4 (at 0.05 mg/kg – $P < 0.001$, at 1 mg/kg – $P < 0.01$) compared to the STZ group. Swimming speed in the experimental groups did not significantly differ from control group values in all training days (Fig. 17.B).

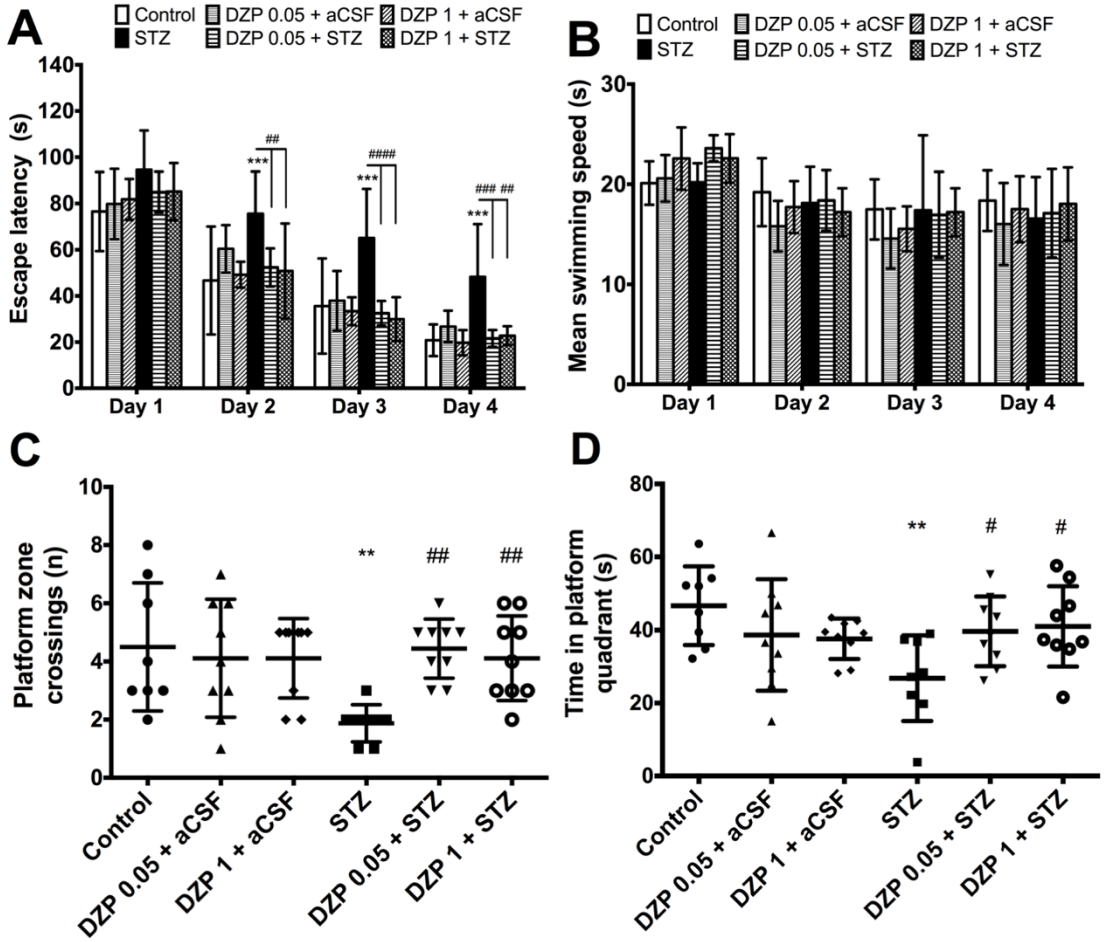

Figure 17. **Effects of diazepam (DZP) on the streptozocin (STZ) model and control rat escape latency (A), swimming speed (B), platform zone crossings (C) and time in platform quadrant (D). The data are shown as mean values ± S.D. (n=8-9/group). Two-way repeated measure ANOVA followed by Holm-Sidak's post-test. **$P < 0.01$ and ***$P < 0.001$ vs. Control; #$P < 0.05$, ##$P < 0.01$, ###$P < 0.001$ and ####$P < 0.0001$ vs. STZ.**

In the MWM probe trial, differences between groups were observed in platform crossings (Fig. 17.C) and in the time spent in the platform quadrant (Fig. 17.D). STZ group animals continued to show impaired search bias. A significantly lower amount of platform crossings ($P < 0.01$) and time spent in platform quadrant ($P < 0.01$) were observed in STZ-treated animals compared to the controls. STZ rats treated with 0.05 and 1 mg/kg diazepam had significantly more platform crossings ($P < 0.01$) and spent significantly more time in the platform quadrant ($P < 0.05$) vs. STZ. Diazepam *per se* did not significantly alter rat performance in the MWM trainings and in the probe trial compared to the control group data.

3.2.1.2. In the open field test

No significant differences were observed between groups in total distance walked: control – 933.3 cm; DZP 0.05 + aCSF – 856.2 cm; DZP 1 + aCSF – 695.9 cm; STZ – 839.2 cm; DZP 0.05 + STZ – 640.8 cm; DZP 1 + STZ – 689.2 cm. The time spent in the center zone also did not significantly differ between groups: control – 17.6%; DZP 0.05 + aCSF – 18.7%; DZP 1 + aCSF – 10.5%; STZ – 12.6%; DZP 0.05 + STZ – 13.2%; DZP 1 + STZ – 15%.

3.2.2. On rat brain protein density

3.2.2.1. GFAP density

Significant differences in GFAP density were observed in the anterior cingulate cortex (Fig. 18.A and B) and in the hippocampus (Fig. 18.C and D) of rats. Administration of STZ significantly increased rat GFAP density in the cortex ($P < 0.01$) and, similarly, in the hippocampus ($P < 0.01$) compared to the controls. Treatment with diazepam at both doses resulted in a significantly lower, control group level GFAP density values in the cortex (DZP 0.05 + STZ – $P < 0.01$; DZP 1 + STZ – $P < 0.05$) and in the hippocampus ($P < 0.01$) of STZ rats. Cortical and hippocampal density of GFAP did not differ between controls and animals treated with diazepam 0.05 mg/kg and 1 mg/kg *per se*.

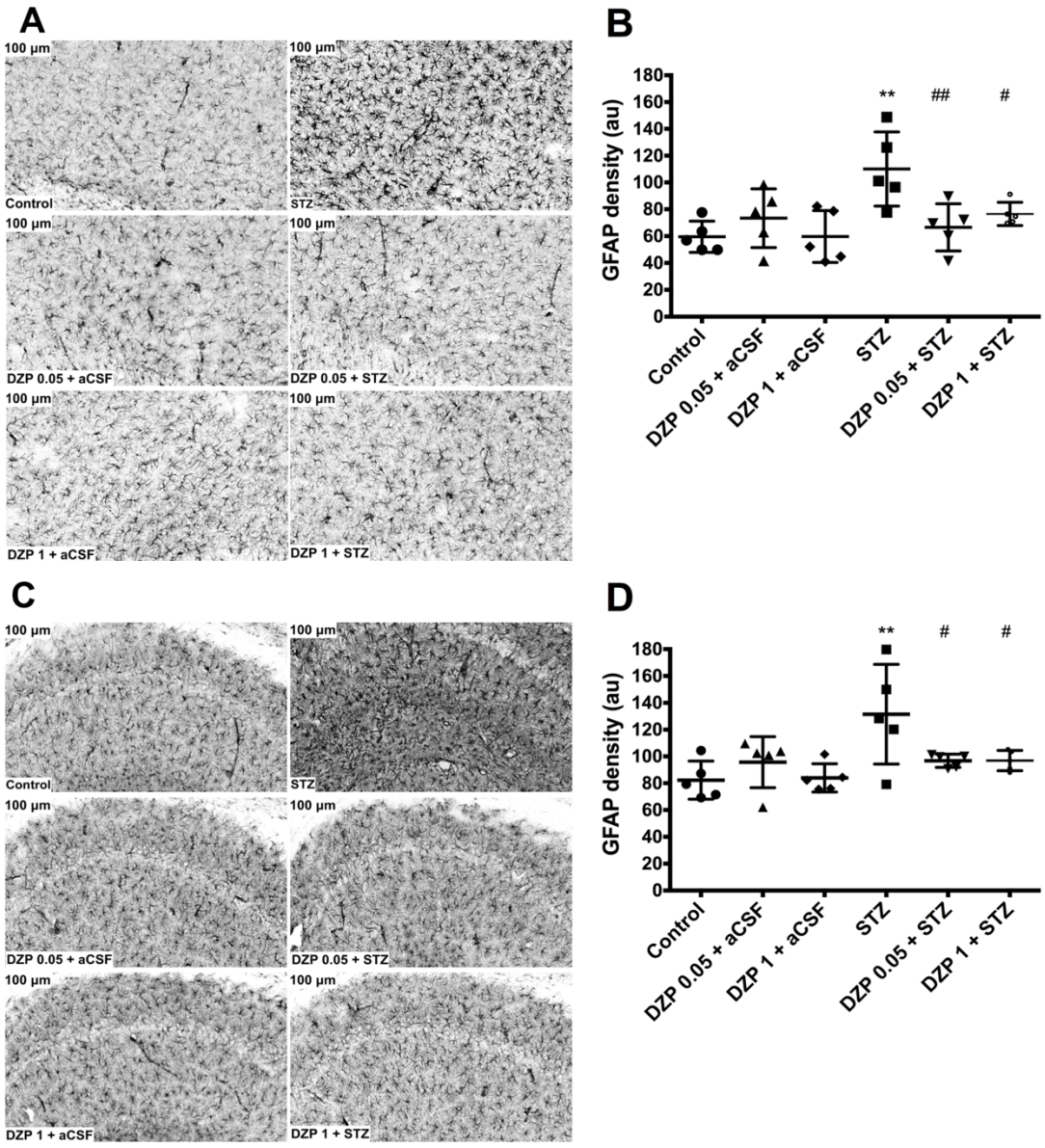

Figure 18. **Effects of diazepam (DZP) on glial fibrillary acidic protein (GFAP) density in streptozocin (STZ) model rats and control rats. Representative photomicrographs show GFAP staining in the rat anterior cingulate cortex (A) and rat hippocampal CA1 (C) at 200 × magnification. Bar graphs demonstrate cortical (B) and hippocampal (D) density measurements. The data are shown as mean values ± S.D. (n=5/group). One-way ANOVA followed by Holm-Sidak's post-test. *****P* < 0.01 vs. Control; #*P* < 0.05 and ##*P* < 0.01 vs. STZ.**

3.2.2.2. Iba-1 density

Significant differences in Iba-1 density were observed in the anterior cingulate cortex (Fig. 19.A and B) and in the hippocampus (Fig. 19.C and D). Administration of STZ significantly increased Iba-1 density in the cortex ($P < 0.001$) and in the hippocampus ($P < 0.001$) compared

to the controls. Treatment with diazepam at both doses resulted in a significantly lower Iba-1 density in the cortex ($P < 0.001$) and in the hippocampus ($P < 0.001$) vs. STZ. Treatment with both diazepam doses *per se* did not alter cortical and hippocampal Iba-1 density compared to the controls.

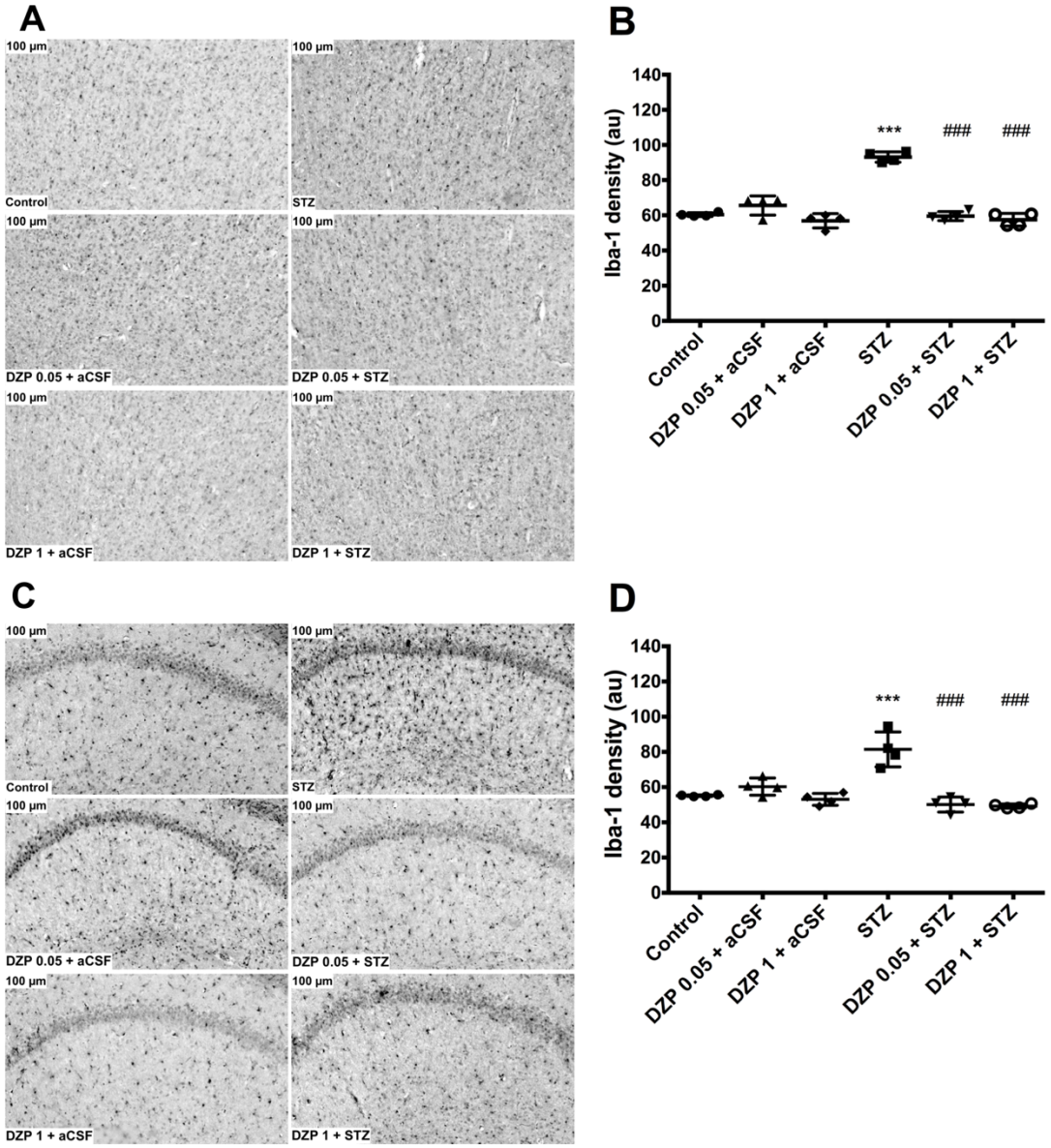

Figure 19. **Effects of diazepam (DZP) on ionized calcium-binding adapter molecule-1 (Iba-1) density in streptozocin (STZ) model rats and control rats. Representative photomicrographs show Iba-1 staining in the rat anterior cingulate cortex (A) and rat hippocampal CA1 (C) at 200 × magnification. Bar graphs demonstrate cortical (B) and hippocampal (D) density measurements. The data are shown as mean values ± S.D. (n=4/group). One-way ANOVA followed by Holm-Sidak's post-test. ******P* < 0.001 vs. Control; ###*P* < 0.001 vs. STZ.**

3.2.2.3. GAD67 density

Cortical (Fig. 20.A and B) and hippocampal (Fig. 20.C and D) density of GAD67 was significantly different between the groups. Animals that received icv STZ injections showed significantly lower GAD67 density in the cortex ($P < 0.05$) and in the hippocampus ($P < 0.01$) compared to the controls. STZ animals that were treated with diazepam at both doses protected against STZ-induced decrease in hippocampal ($P < 0.01$), but not cortical GAD67 density. Diazepam administration *per se* did not alter GAD67 density in the cortex and in the hippocampus compared to the controls.

3.2.2.4. AChE density

Significant inter-group differences were observed regarding density of AChE in the rat cortex (Fig. 21.A and B) and in the hippocampus (Fig. 21.C and D). In STZ rats, a significant increase in AChE density was observed in the cortex ($P < 0.05$) and hippocampus ($P < 0.01$) compared to the controls. Diazepam at both doses decreased AChE density in STZ rats to the control group values in cortical (DZP 0.05 + STZ – $P < 0.01$, DZP 1 + STZ – $P < 0.05$) and hippocampal ($P < 0.001$) regions. Treatment with diazepam *per se* did not produce significant differences in AChE density in the cortex and in the hippocampus compared to the controls.

3.2.2.5. Synaptic density

Significant inter-group differences were observed in SYP1 density in the rat hippocampal CA1 (Fig. 22.A-B), DG (Fig. 22.A and C), but not in CA3 (Fig. 22.A and D) regions. A significant decrease in SYP1 density was observed in the CA1 ($P < 0.005$), but not DG and CA3 of STZ-treated rats compared to the controls. Treatment of STZ rats with 0.05 mg/kg diazepam resulted in higher SYP1 density, comparable to the one observed in control group, in the CA1 ($P < 0.01$) and CA3 ($P < 0.01$), but not in DG region compared to the STZ group. Treatment with 1 mg/kg diazepam did not significantly alter SYP1 density in the three regions of the hippocampus compared to the STZ group. Treatment with diazepam *per se* did not produce significant differences in SYP1 density in the three hippocampal regions compared to the controls.

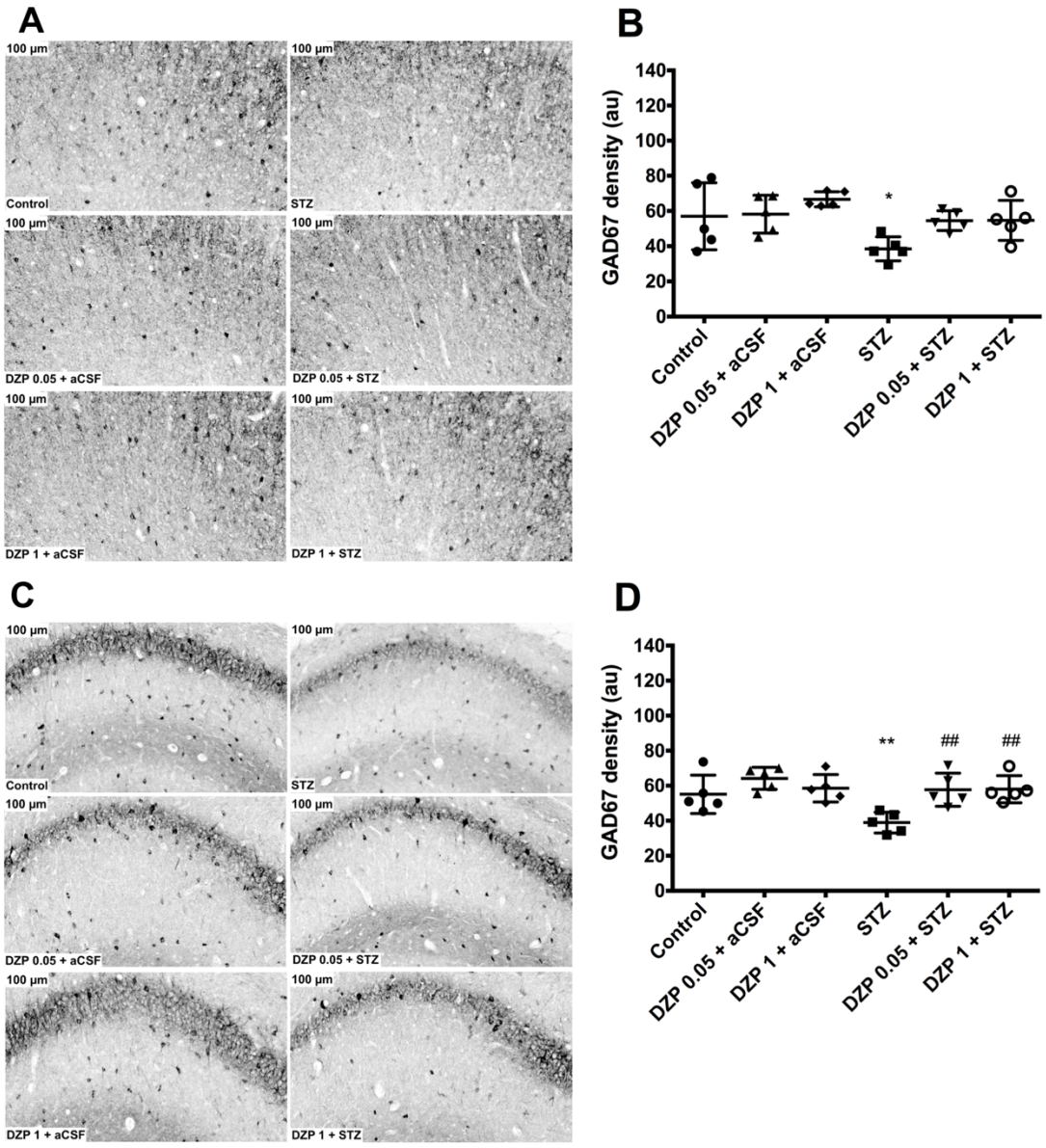

Figure 20. **Effects of diazepam (DZP) on glutamic acid decarboxylase 67 (GAD67) density in streptozocin (STZ) model rats and control rats. Representative photomicrographs show GAD67 staining in the rat anterior cingulate cortex (A) and rat hippocampal CA1 (C) at 200 × magnification. Bar graphs demonstrate cortical (B) and hippocampal (D) density measurements. The data are shown as mean values ± S.D. (n=5/group). One-way ANOVA followed by Holm-Sidak's post-test. ****P* < 0.05 and *****P*** **< 0.01 vs. Control; ##*P* < 0.01 vs. STZ.**

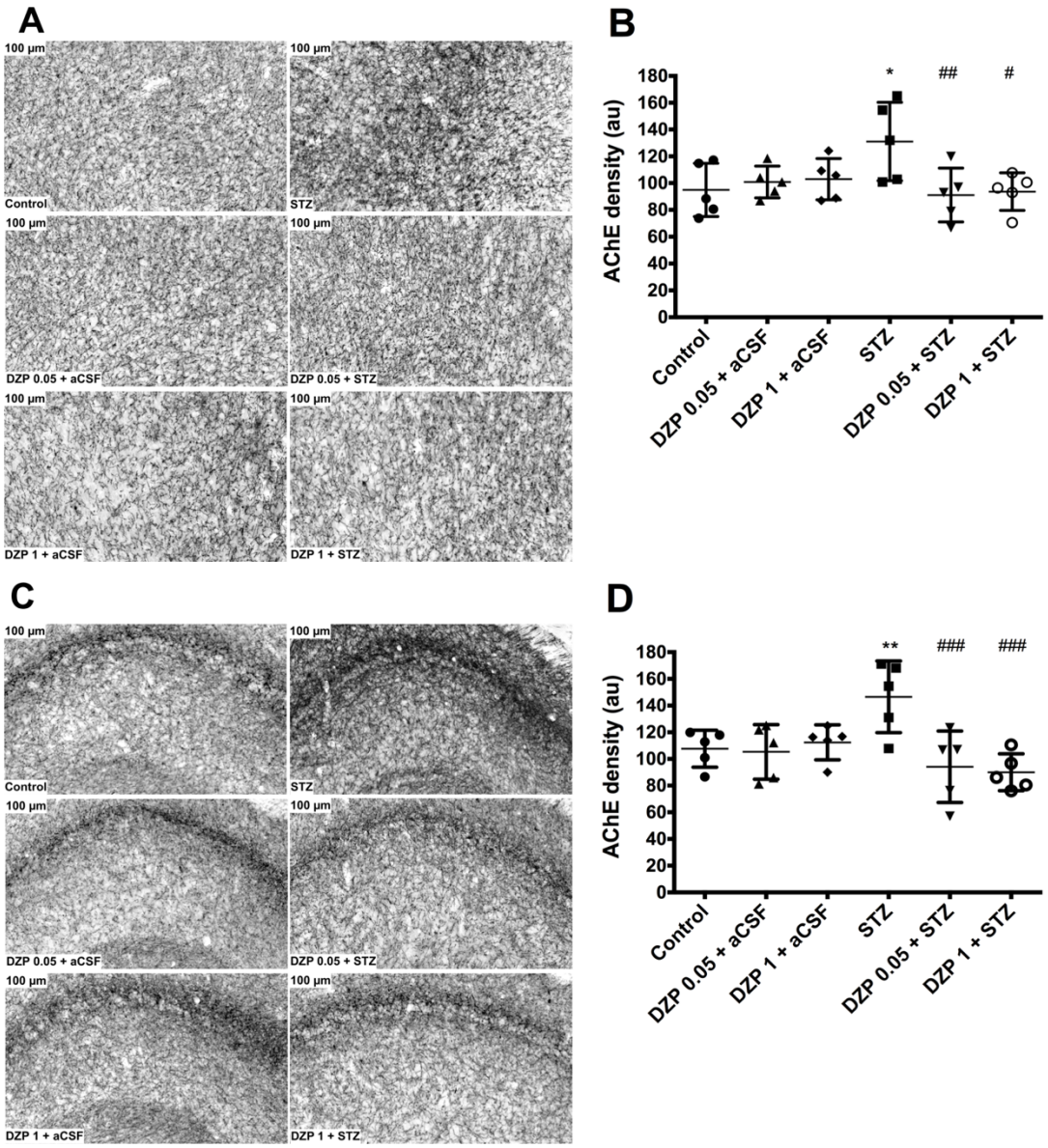

Figure 21. **Effects of diazepam (DZP) on acetylcholine esterase (AChE) density in streptozocin (STZ) model rats and control rats. Representative photomicrographs show AChE-positive axons in the rat anterior cingulate cortex (A) and rat hippocampal CA1 (C) at 200 × magnification. Bar graphs demonstrate cortical (B) and hippocampal (D) density measurements. The data are shown as mean values ± S.D. (n=5/group). One-way ANOVA followed by Holm-Sidak's post-test. ****P* < 0.05 and *****P*** **< 0.01 vs. Control; #*P* < 0.05, ##*P* < 0.01 and ###*P* < 0.001 vs. STZ.**

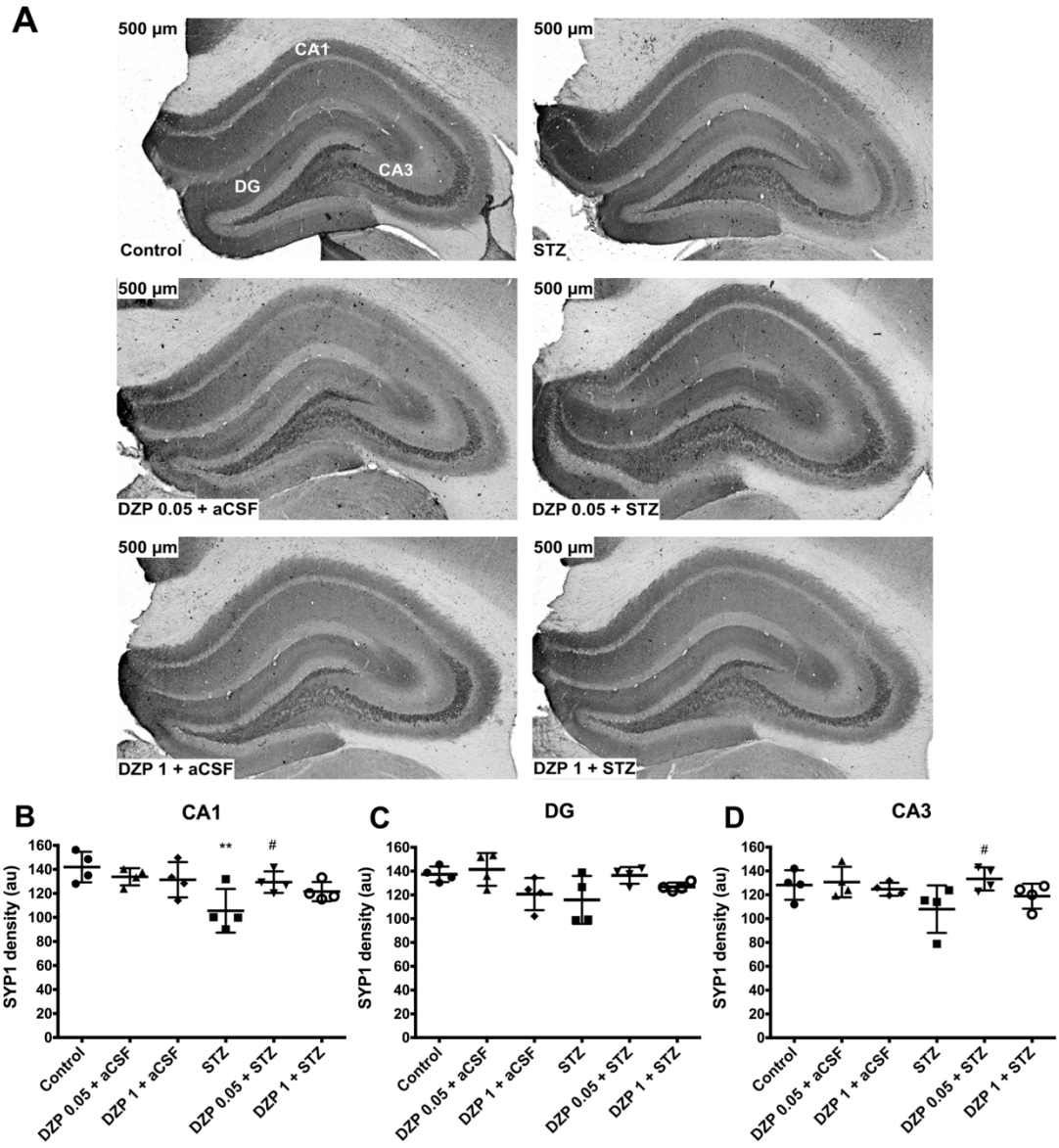

Figure 22. **Effects of diazepam (DZP) on synaptophysin 1 (SYP1) density in the hippocampus of streptozocin (STZ) model rats and control rats. Representative photomicrographs show SYP1 staining in the rat hippocampus (A) at 60 × magnification. Density measurements are shown for the hippocampal CA1 (B), dentate gyrus (C) and CA3 (D). The data are shown as mean values ± S.D. (n=4/group). One-way ANOVA followed by Holm-Sidak's post-test. *****P*** **< 0.01 vs. Control; #*P* < 0.05 vs. STZ.**

3.3. Effects of GABA-B receptor agonist baclofen

3.3.1. In the MWM test

In the MWM trainings, a significant interaction was revealed in group and training day factors. The administration of STZ resulted in a longer escape latency than that of the controls

starting from training day 2 ($P < 0.001$) and continued on training days 3-4 ($P < 0.0001$, Fig. 23.A). The administration of baclofen in 0.05 mg/kg dose prevented STZ-induced spatial learning impairments from training day 1 ($P < 0.01$) and in all remaining days (day 2: $P < 0.01$, day 3 and 4: $P < 0.0001$). Baclofen at 0.025 mg/kg dose produced similar effect on training days 2-4 ($P < 0.0001$). No significant differences were observed in swimming speed between groups in all training days (Fig. 23.B).

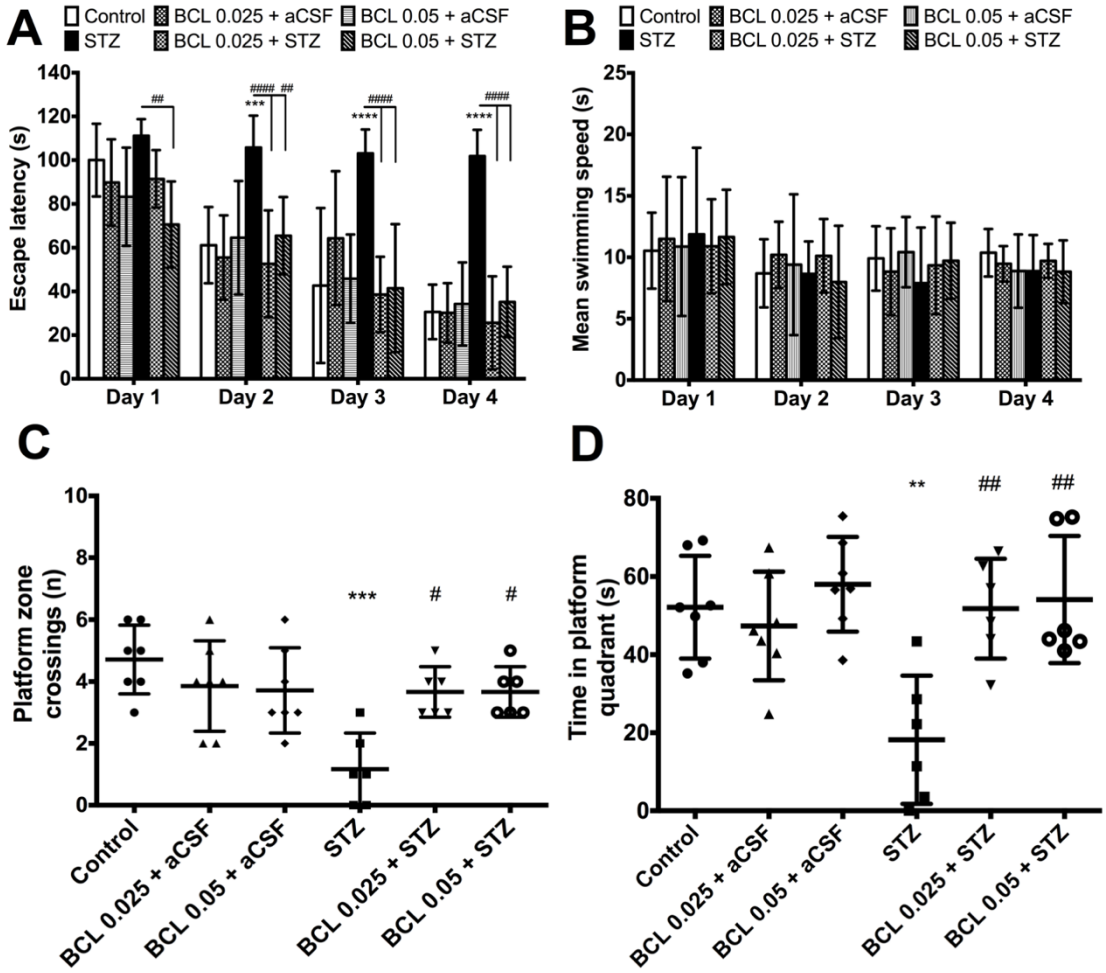

Figure 23. **Effects of baclofen (BCL) on the streptozocin (STZ) model and control rat escape latency (A), swimming speed (B), platform zone crossings (C) and time in platform quadrant (D). The data are shown as mean values ± S.D. (n=6-7/group). Two-way repeated measure ANOVA followed by Bonferroni's post-test. **$P < 0.01$, ***$P < 0.001$ and ****$P < 0.0001$ vs. Control; #$P < 0.05$, ##$P < 0.01$ and ####$P < 0.0001$ vs. STZ.**

In the MWM probe trial, significant differences between groups were observed in platform crossings (Fig. 23.C) and in the time spent in the platform quadrant (Fig. 23.D). STZ-injected rats crossed the platform significantly less times ($P < 0.001$) and spent significantly shorter time in

the platform quadrant ($P < 0.01$). STZ rats that were treated with both doses of baclofen displayed a reversal of STZ effects – significantly higher number of platform crossings ($P < 0.05$) and significantly longer time spent in the platform quadrant ($P < 0.01$). Baclofen *per se* did not significantly change control group rat performance in the MWM trainings and in the probe trial.

3.3.2. On rat brain protein density

3.3.2.1. GFAP density

Significant differences were observed between groups in the density of GFAP staining in the cortex (Fig. 24.A and B) and in the hippocampus (Fig. 24.C and D). STZ induced an almost 3-fold increase in the density of GFAP staining in the cortex ($P < 0.0001$) and hippocampus ($P < 0.0001$) compared to the controls. Treatments with both 0.025 and 0.05 mg/kg baclofen reversed STZ-induced increase in the density of cortical and hippocampal GFAP staining ($P < 0.0001$) and restored its values to the levels observed in both structures in the control group. In controls, baclofen *per se* did not produce changes in the cortical and hippocampal GFAP staining compared to that of the control group.

3.3.2.2. GAD67 density

Significant changes between groups were observed in the density of GAD67 staining in the cortex (Fig. 25.A and B) and hippocampus (Fig. 25.C and D). Injection of STZ induced a decrease in GAD67 density in the cortex ($P < 0.0001$) and hippocampus ($P < 0.0001$). At both tested doses, baclofen normalized the density of GAD67 staining in the hippocampus ($P < 0.05$), but not in the cortex of STZ rats. Treatment with baclofen *per se* did not produce significant changes in the density of cortical and hippocampal GAD67 staining in comparison to the control group data.

3.3.2.3. AChE density

Cortical (Fig. 26.A and B) and hippocampal (Fig. 26.C and D) density of AChE staining was significantly different between groups. Compared to controls, a significant increase in the density of AChE staining was observed in the cortex ($P < 0.0001$) and hippocampus ($P < 0.0001$) of STZ-treated animals. At both tested doses, baclofen attenuated STZ-induced effects by normalizing the density of cortical and hippocampal AChE staining ($P < 0.0001$). No significant changes in the density of AChE staining were observed in both structures of the rats treated with baclofen *per se* when compared to the control group.

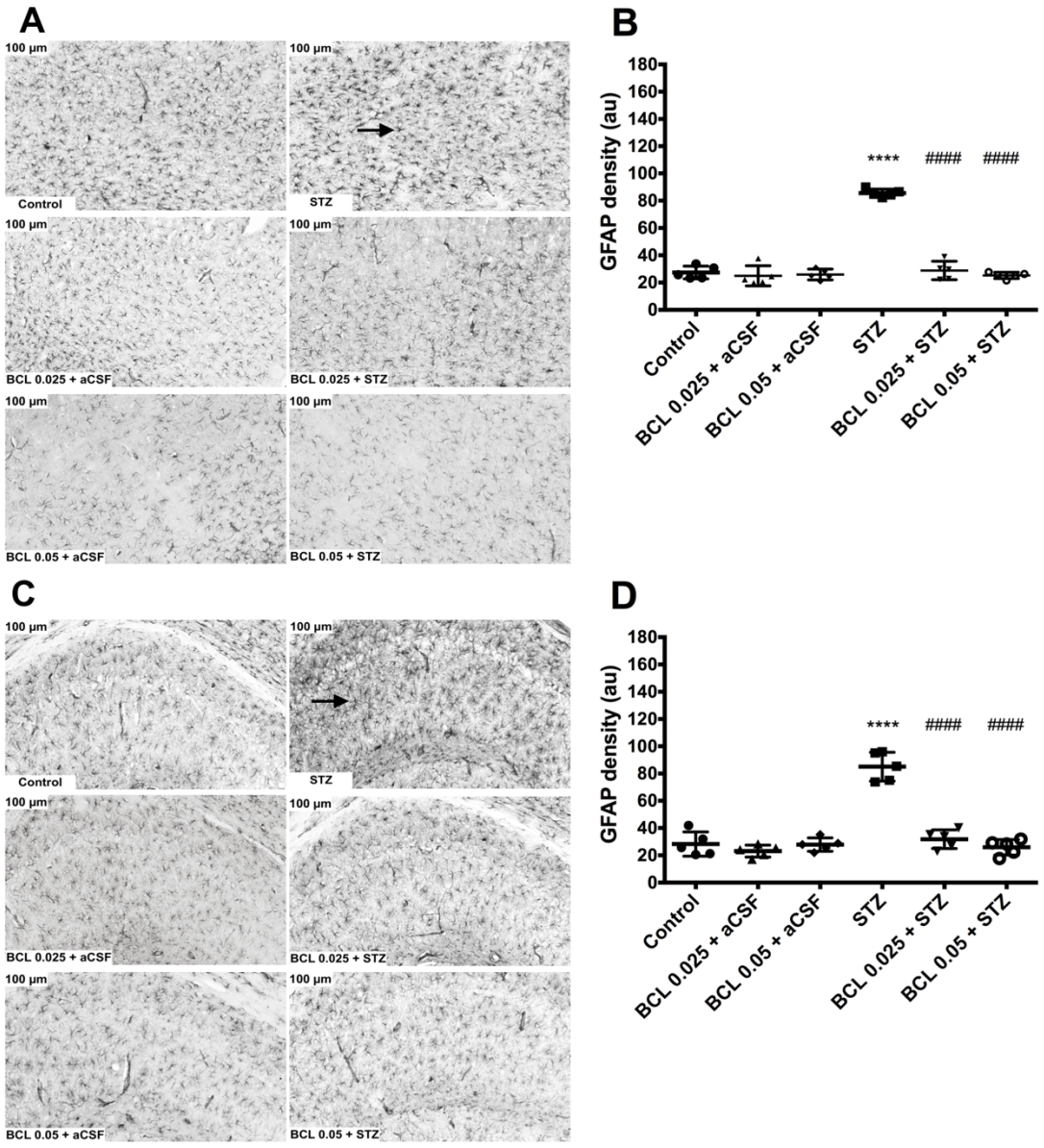

Figure 24. **Effects of baclofen (BCL) on glial fibrillary acidic protein (GFAP) density in streptozocin (STZ) model rats and control rats. Representative photomicrographs show GFAP staining in the rat anterior cingulate cortex (A) and hippocampal CA1 (C) at 200 × magnification. Bar graphs demonstrate cortical (B) and hippocampal (D) density measurements. Black arrows indicate representative GFAP-positive cells. The data are shown as mean values ± S.D. (n=5/group). One-way ANOVA followed by Bonferroni's post-test. *******P* < 0.0001 vs. Control; ####*P* < 0.0001 vs. STZ.**

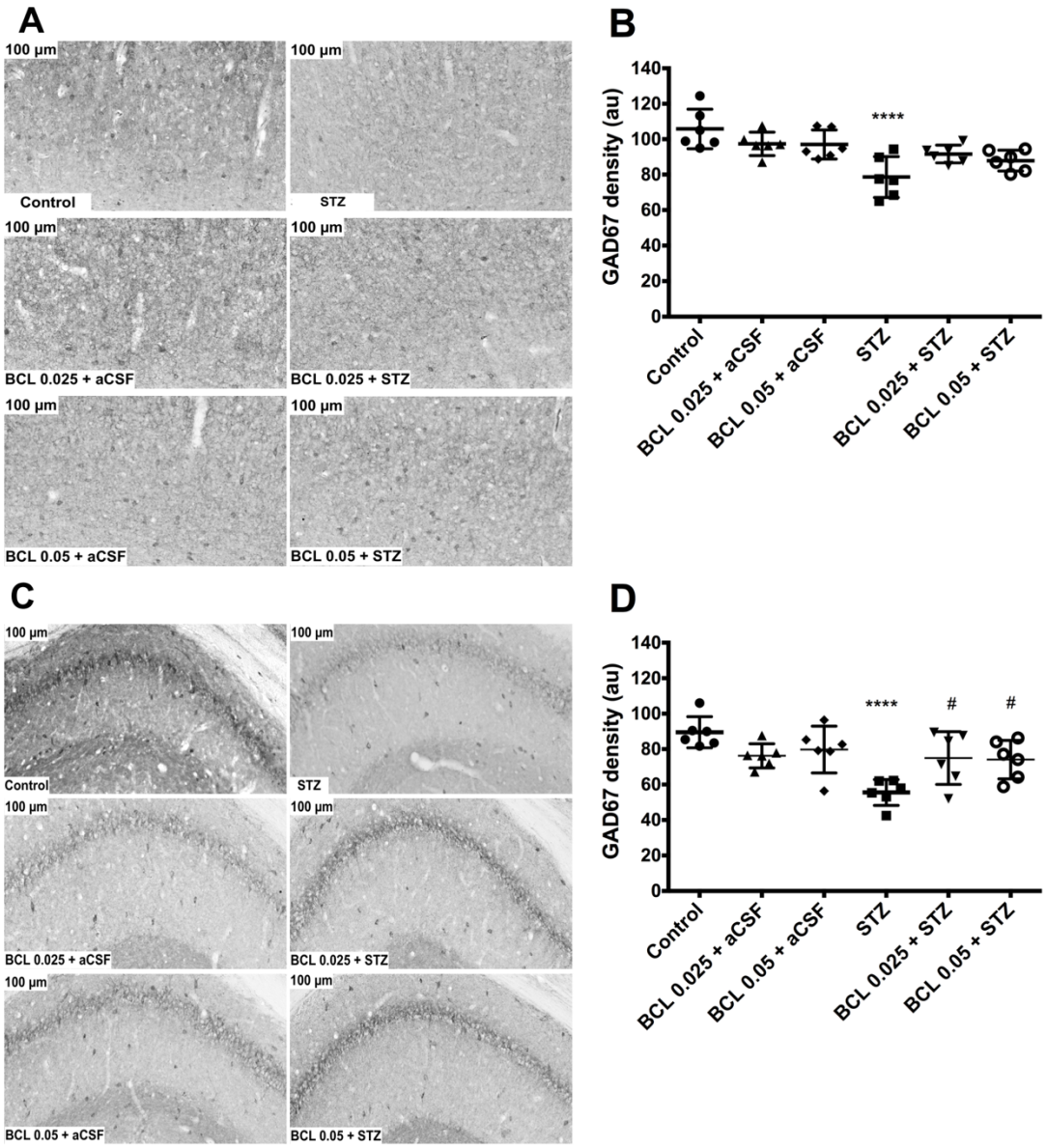

Figure 25. **Effects of baclofen (BCL) on glutamic acid decarboxylase 67 (GAD67) density in streptozocin (STZ) model rats and control rats. Representative photomicrographs show GAD67 staining in the rat anterior cingulate cortex (A) and hippocampal CA1 (C) at 200 × magnification. Bar graphs demonstrate cortical (B) and hippocampal (D) density measurements. The data are shown as mean values ± S.D. (n=6/group). One-way ANOVA followed by Bonferroni's post-test. *******P* < 0.0001 vs. Control; #*P* < 0.05 vs. STZ.**

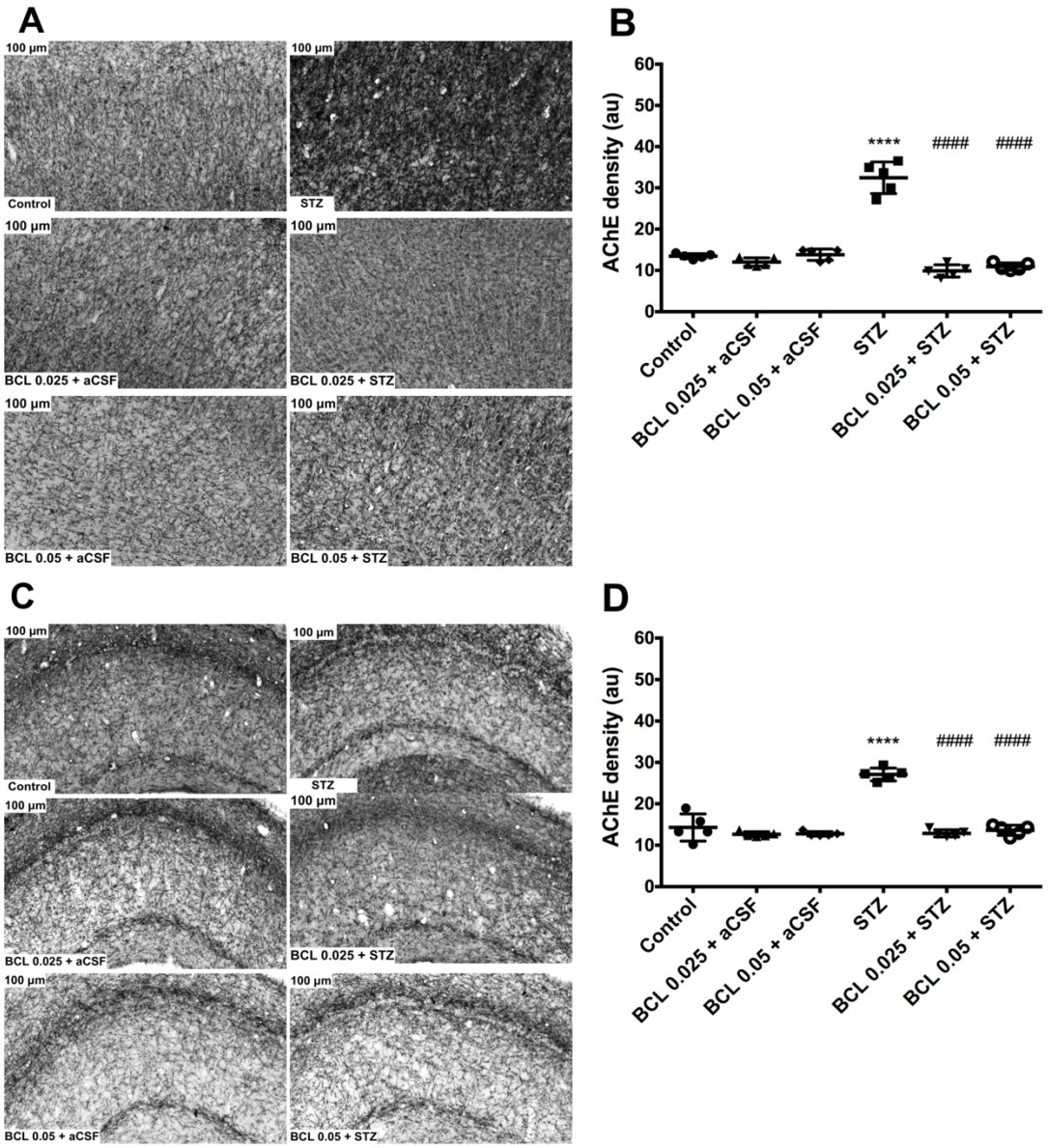

Figure 26. **Effects of baclofen (BCL) on acetylcholine esterase (AChE) density in streptozocin (STZ) model rats and control rats. Representative photomicrographs show AChE-positive nerve axons in the rat anterior cingulate cortex (A) and hippocampal CA1 (C) at 200 × magnification. Bar graphs demonstrate cortical (B) and hippocampal (D) density measurements. The data are shown as mean values ± S.D. (n=5/group). One-way ANOVA followed by Bonferroni's post-test. *******P* < 0.0001 vs. Control; ####*P* < 0.0001 vs. STZ.**

3.4. Effects of GABA-containing compound gammapyrone

3.4.1. On behavior and locomotion

3.4.1.1. In the MWM test

In the MWM trainings, a significant interaction was detected in group and training day factors. Administration of STZ resulted in significantly extended latency to reach the escape platform compared to controls on training day 2 ($P < 0.05$), day 3 ($P < 0.001$) and day 4 ($P < 0.0001$), as shown in figure 27.A. STZ rats treated with gammapyrone in dose 0.1 mg/kg demonstrated significantly shorter escape latency than STZ rats on training day 2 ($P < 0.05$), day 3 ($P < 0.01$) and day 4 ($P < 0.001$). Treatment with 0.5 mg/kg gammapyrone also resulted in significantly shorter escape latency of STZ rats vs. STZ group on training day 2 ($P < 0.001$), day 3 ($P < 0.01$) and day 4 ($P < 0.0001$). No significant differences were observed in swimming speed between groups in all training days (Fig. 27.B).

Significant differences between groups were discovered also in the MWM probe trial parameters: platform crossings (Fig. 27.C) and time spent in the platform quadrant (Fig. 27.D). Rats treated with STZ crossed the platform zone less ($P < 0.05$) and spent markedly less time in the platform quadrant ($P < 0.01$) than the controls. STZ animals treated with gammapyrone at 0.1 mg/kg demonstrated significantly more platform crossings ($P < 0.05$) as well as longer time spent in the platform quadrant ($P < 0.01$) in comparison to STZ group rats. STZ animals treated with gammapyrone at 0.5 mg/kg also showed more platform crossings ($P < 0.01$) and spent longer time in the platform quadrant ($P < 0.01$) compared to the STZ group. Gammapyrone at both doses *per se* did not significantly change rat performance in the MWM trainings and in the probe trial compared to the control group data.

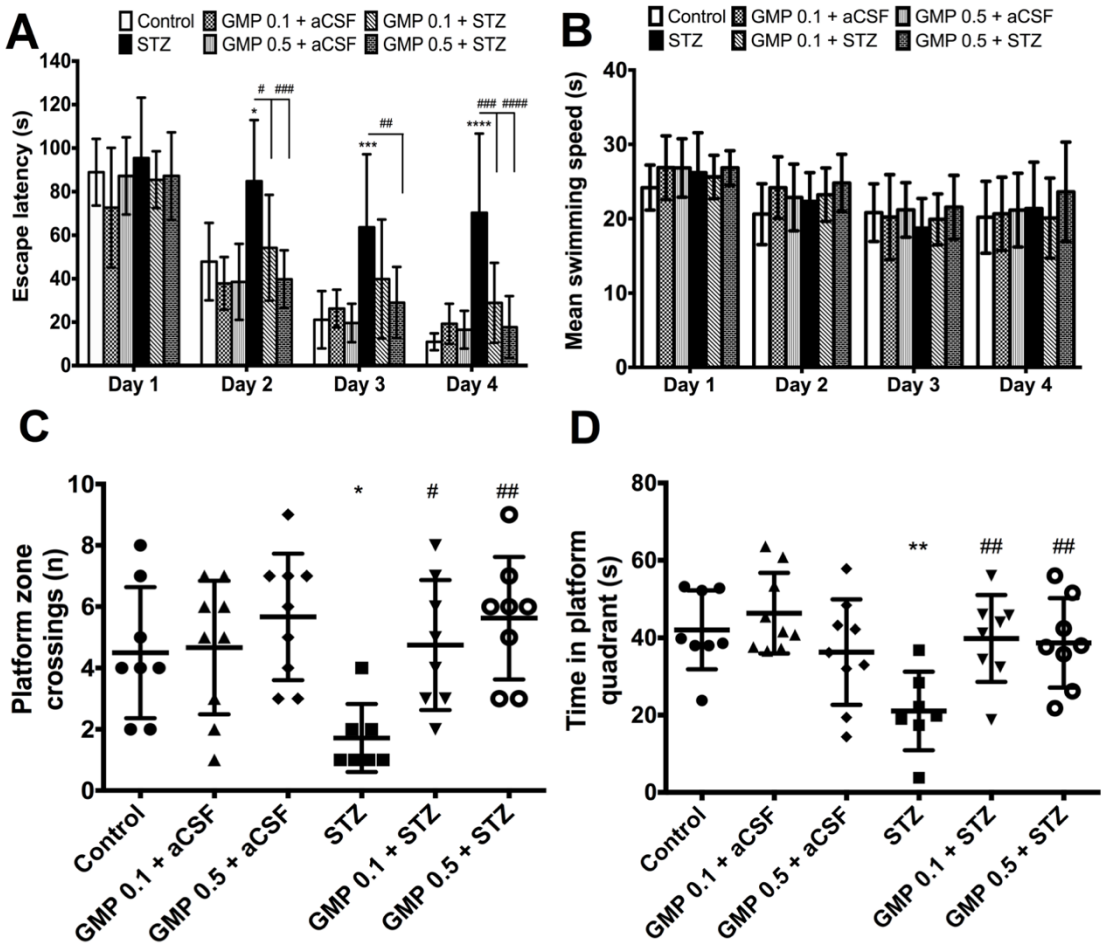

Figure 27. **Effects of gammapyrone (GMP) on the streptozocin (STZ) model and control rat escape latency (A), swimming speed (B), platform zone crossings (C) and time in platform quadrant (D). The data are shown as mean values ± S.D. (n=7-9/group). Two-way repeated measure ANOVA followed by Holm-Sidak's post-test. ****P* < 0.05, *****P*** **< 0.01, ******P*** **< 0.001 and *******P*** **< 0.0001 vs. Control; #*P* < 0.05, ##*P* < 0.01, ###*P* < 0.001 and ####*P* < 0.0001 vs. STZ.**

3.4.1.2. In the open field test

No significant differences were observed between groups in the total distance travelled and time spent in the center zone. For the total distance travelled, the mean values were as follows: control – 447.4 cm; GMP 0.1 + aCSF – 513.6 cm; GMP 0.5 + aCSF – 414.3 cm; STZ – 376.9 cm; GMP 0.1 + STZ – 638.5 cm; GMP 0.5 + STZ – 467.4 cm. For the time spent in the center zone, the mean values were as follows: control – 59.3 s; GMP 0.1 + aCSF – 71.6 s; GMP 0.5 + aCSF – 65.7 s; STZ – 68.4 s; GMP 0.1 + STZ – 106 s; GMP 0.5 + STZ – 59.6 s.

3.4.2. On rat brain protein density

3.4.2.1. GFAP density

Significant differences in GFAP density were found between groups in the cortex (Fig. 28.A and B) and in the hippocampus (Fig. 28.C and D). Compared to the controls, STZ induced a sharp, almost 2-fold increase in GFAP density in the cortex ($P < 0.0001$) and in the hippocampus ($P < 0.01$). A significantly lower (close to the control group values) cortical GFAP density was observed in STZ-injected rats treated with gammapyrone at 0.1 ($P < 0.0001$) and 0.5 mg/kg ($P < 0.001$) compared to the STZ-treated rats. Treatment with gammapyrone at both doses also significantly reversed STZ-increased GFAP density in the hippocampus ($P < 0.01$). Gammapyrone *per se* did not change cortical or hippocampal GFAP densities.

3.4.2.2. Iba-1 density

Significant differences in Iba-1 density were found between groups in the cortex (Fig. 29.A and B) and in the hippocampus (Fig. 29.C and D). STZ-injected animals demonstrated significant increase in Iba-1 density in the cortex ($P < 0.001$) and in the hippocampus ($P < 0.001$). This STZ-induce increase was prevented in the cortex by gammapyrone at 0.1 ($P < 0.05$) and 0.5 mg/kg ($P < 0.001$) compared to STZ-treated rats. Treatment with gammapyrone at both doses also significantly reversed STZ-induced increase in hippocampal Iba-1 density ($P < 0.01$ at 0.1 and $P < 0.001$ at 0.5 mg/kg). Neither of the gammapyrone treatments *per se* changed cortical or hippocampal Iba-1 density.

3.4.2.3. GAD67 density

Significant differences in GAD67 density between groups were detected in the cortex (Fig. 30.A and B) and hippocampus (Fig. 30.C and D). Injection of STZ caused a significant decrease in GAD67 density in the cortex ($P < 0.01$) and hippocampus ($P < 0.01$) in comparison to the controls. STZ rats treated with gammapyrone at 0.1 mg/kg showed significantly higher GAD67 density in the cortex ($P < 0.01$) and in the hippocampus ($P < 0.05$) compared to STZ group animals. At 0.5 mg/kg, gammapyrone also significantly increased STZ rat GAD67 density in the cortex ($P < 0.05$) and in the hippocampus ($P < 0.05$) compared to the STZ group data. Gammapyrone treatment *per se* did not change cortical or hippocampal GAD67 density.

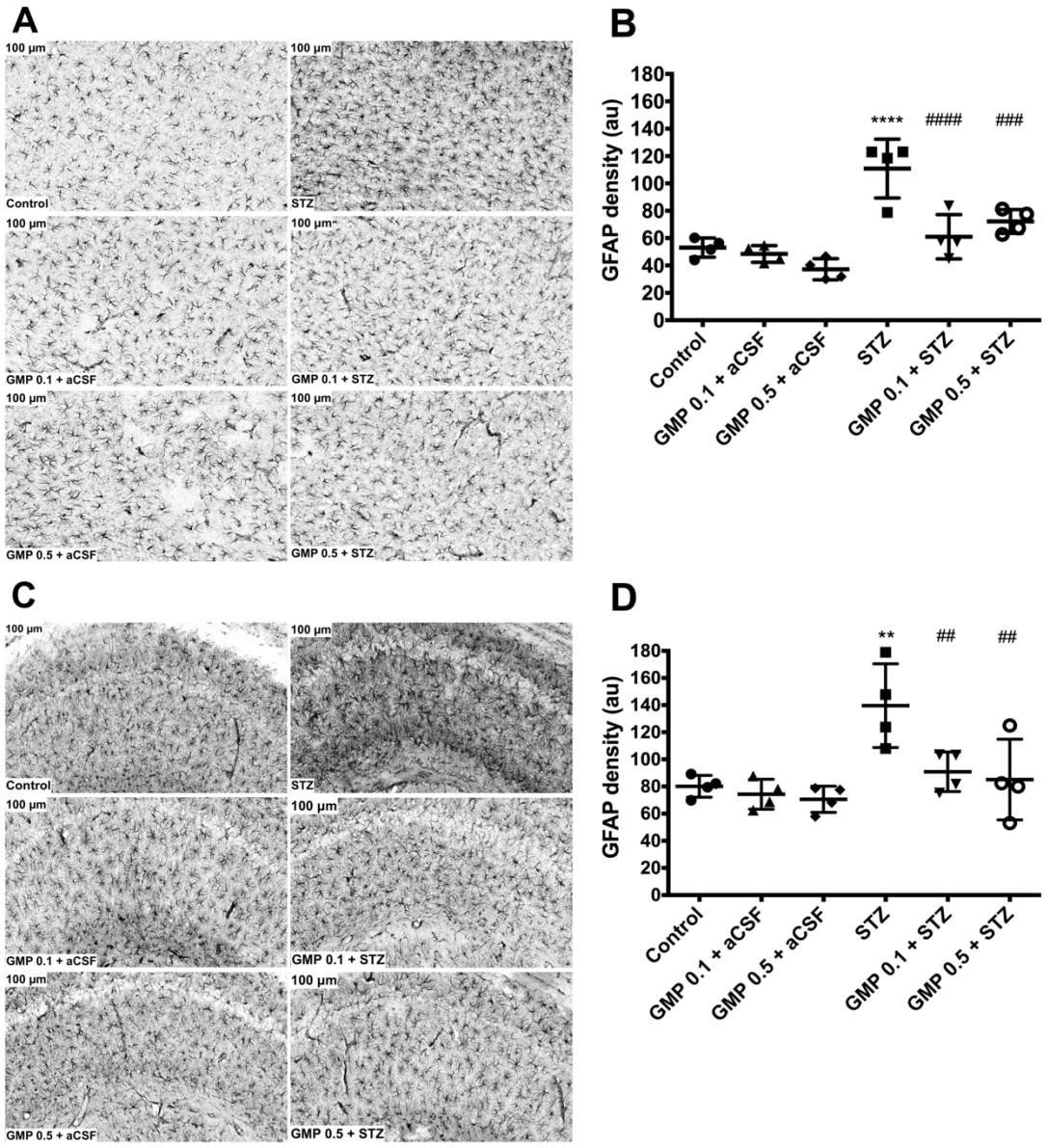

Figure 28. **Effects of gammapyrone (GMP) on glial fibrillary acidic protein (GFAP) density in streptozocin (STZ) model rats and control rats. Representative photomicrographs show GFAP staining in the rat anterior cingulate cortex (A) and hippocampal CA1 (C) at 200 × magnification. Bar graphs demonstrate cortical (B) and hippocampal (D) density measurements. The data are shown as mean values ± S.D. (n=4/group). One-way ANOVA followed by Holm-Sidak's post-test. *****P*** **< 0.01 and *******P*** **< 0.0001 vs. Control; ##*P* < 0.01, ###*P* < 0.001 and ####*P* < 0.0001 vs. STZ.**

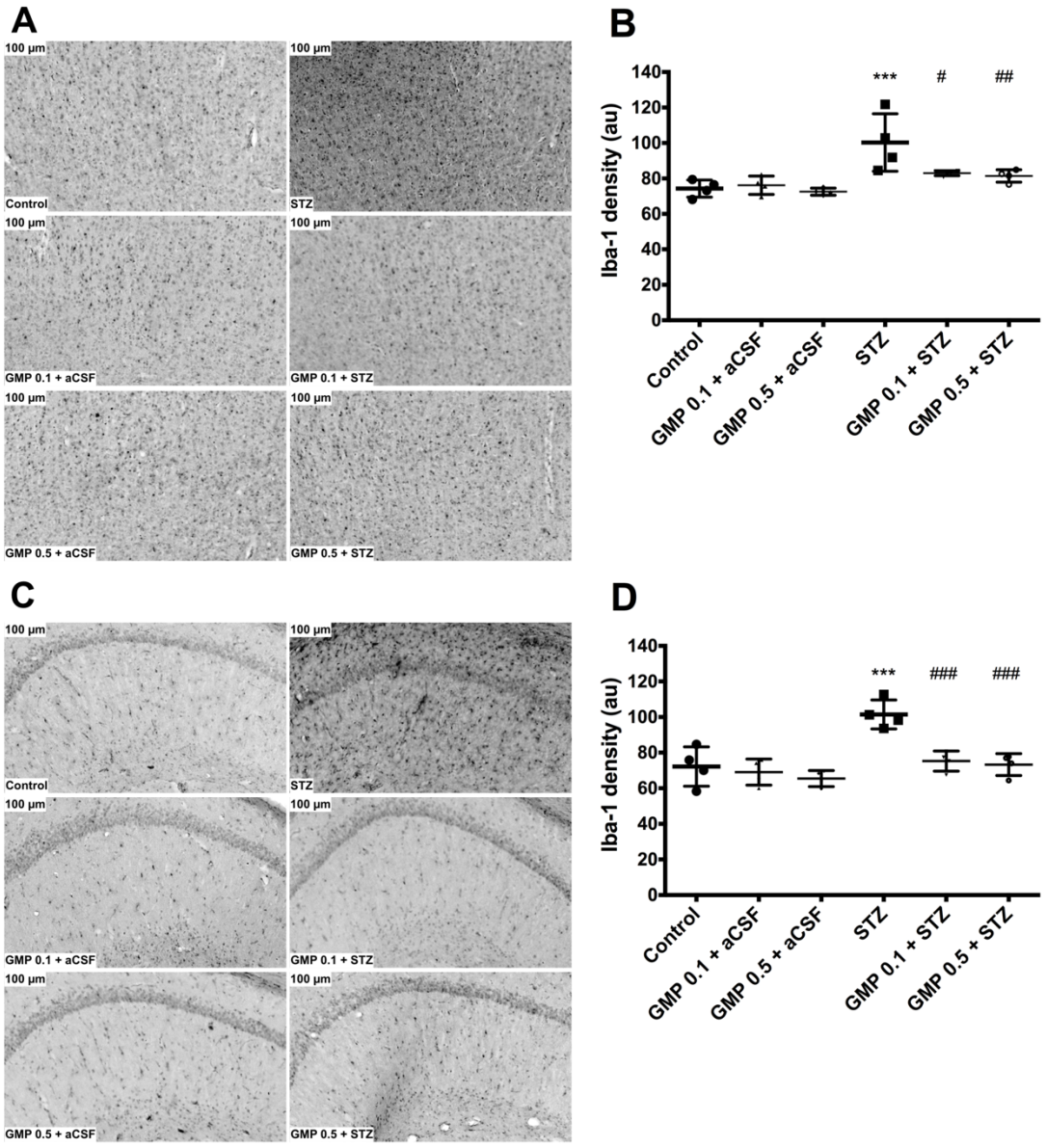

Figure 29. **Effects of gammapyrone (GMP) on ionized calcium-binding adapter molecule-1 (Iba-1) density in streptozocin (STZ) model rats and control rats. Representative photomicrographs show Iba-1 staining in the rat anterior cingulate cortex (A) and hippocampal CA1 (C) at 200 × magnification. Bar graphs demonstrate cortical (B) and hippocampal (D) density measurements. The data are shown as mean values ± S.D. (n=4/group). One-way ANOVA followed by Holm-Sidak's post-test. ******P* < 0.001 vs. Control; #*P* < 0.05, ##*P* < 0.01 and ###*P* < 0.001 vs. STZ.**

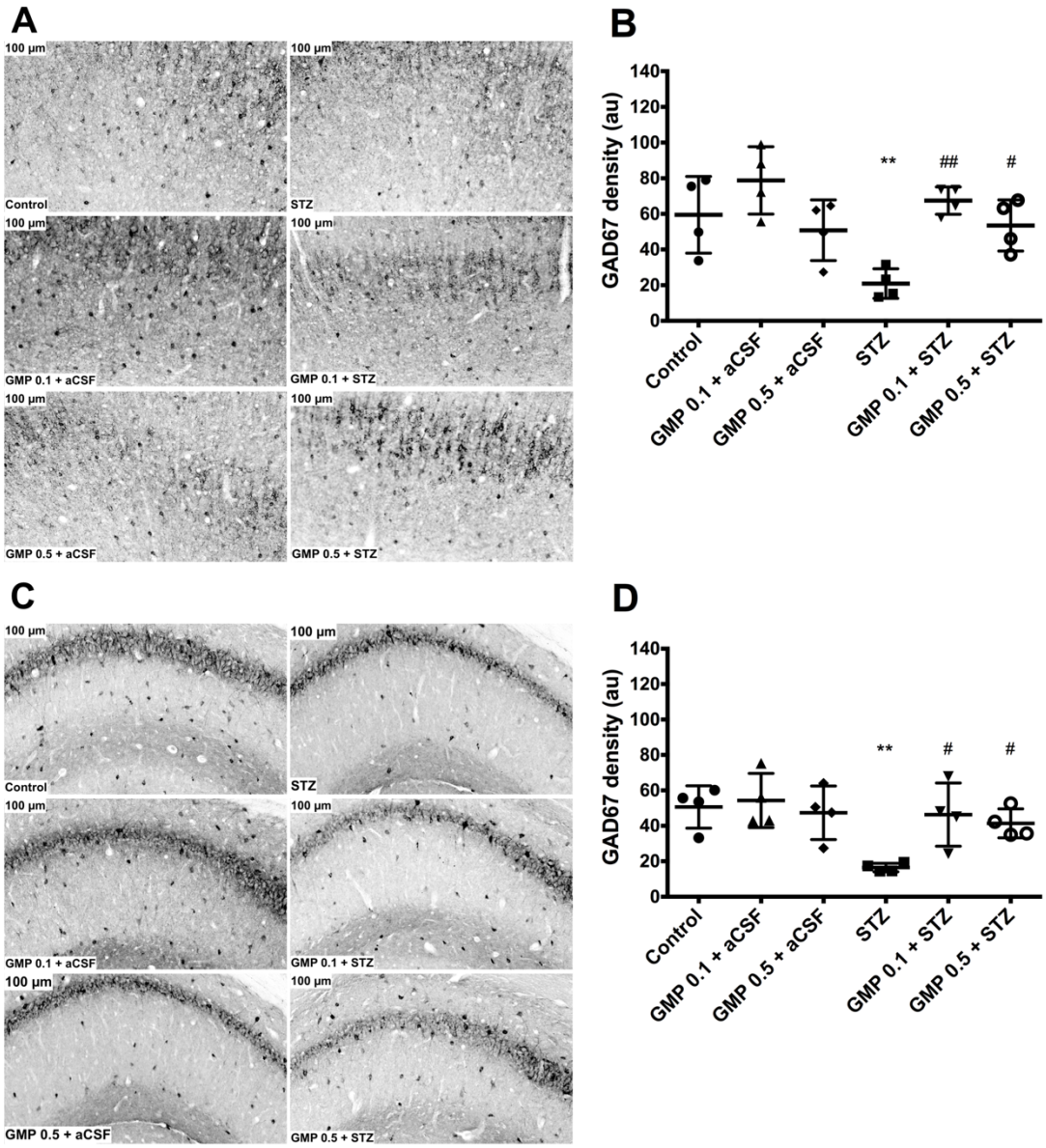

Figure 30. **Effects of gammapyrone (GMP) on glutamic acid decarboxylase 67 (GAD67) density in streptozocin (STZ) model rats and control rats. Representative photomicrographs show GAD67 staining in the rat anterior cingulate cortex (A) and hippocampal CA1 (C) at 200 × magnification. Bar graphs demonstrate cortical (B) and hippocampal (D) density measurements. The data are shown as mean values ± S.D. (n=4/group). One-way ANOVA followed by Holm-Sidak's post-test. *****P* < 0.01 and vs. Control; #*P* < 0.05 and ##*P* < 0.01 vs. STZ.**

3.4.2.4. AChE density

Cortical nerve axon density of AChE was significantly different between groups (Fig. 31.A and B), as well as hippocampal (Fig. 31.C and D). Administration of STZ resulted in a significant increase in AChE density in the rat cortex ($P < 0.05$) and hippocampus ($P < 0.01$) compared to

controls. Gammapyrone 0.1 mg/kg significantly reduced the STZ-induced elevation in AChE density in the cortex ($P < 0.001$) and hippocampus ($P < 0.001$) of STZ rats. At 0.5 mg/kg, gammapyrone produced similar effects on STZ-induced AChE elevation in the cortex and in the hippocampus ($P < 0.001$). Gammapyrone *per se* did not change AChE density in the cortical and hippocampal regions of the control group rats.

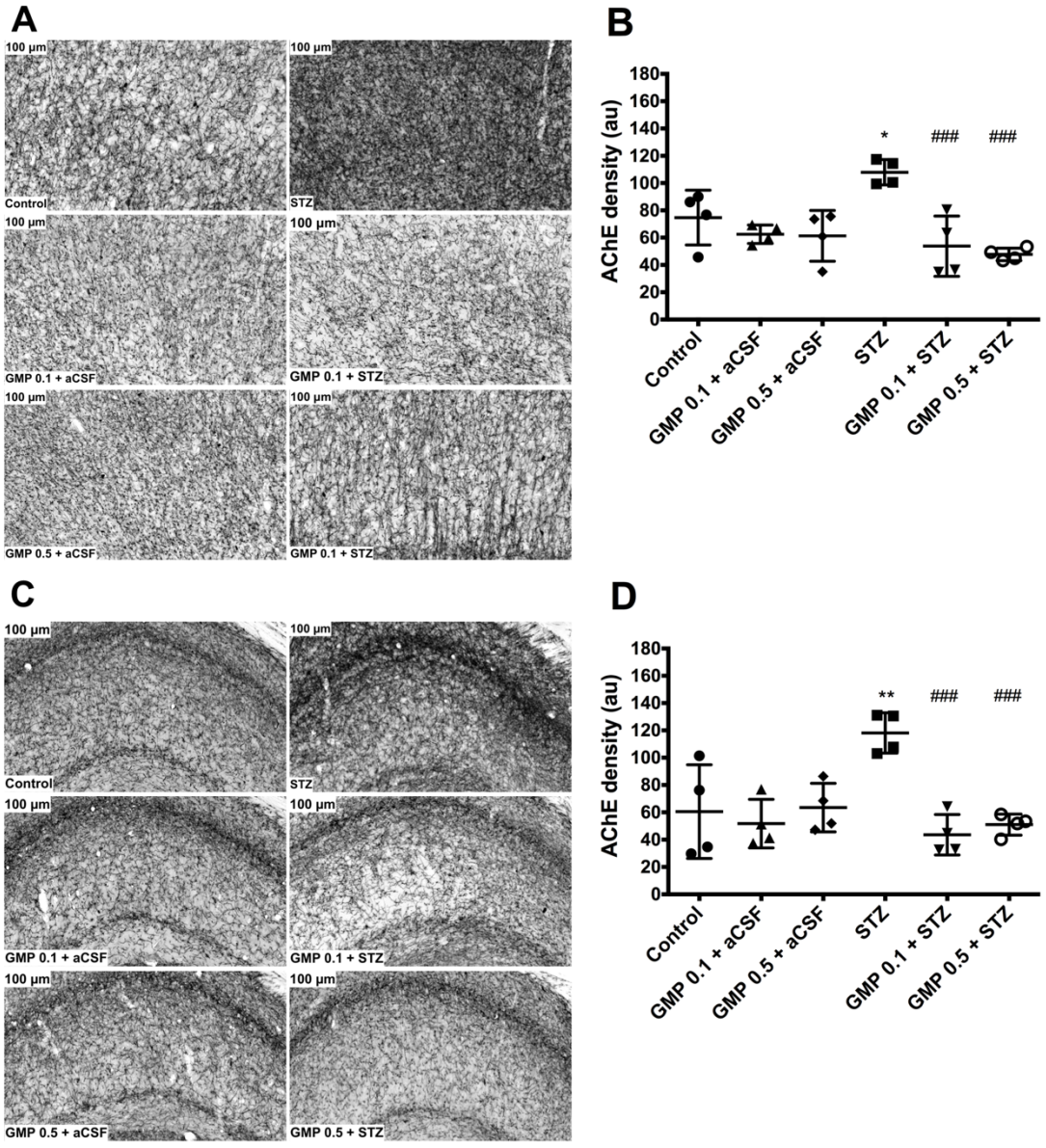

Figure 31. **Effects of gammapyrone (GMP) on acetylcholine esterase (AChE) density in streptozocin (STZ) model rats and control rats. Representative photomicrographs show AChE-positive nerve axons in the rat anterior cingulate cortex (A) and hippocampal CA1 (C) at 200 × magnification. Bar graphs demonstrate cortical (B) and hippocampal (D) density measurements. The data are shown as mean values ± S.D. (n=4/group). One-way ANOVA followed by Holm-Sidak's post-test. ****P* < 0.05 and *****P*** **< 0.01 vs. Control; ###*P* < 0.001 vs. STZ.**

3.4.3. Effects of gammapyrone *in vitro*

3.4.3.1. Binding to GABA-A and GABA-B receptors

Gammapyrone showed negligible inhibition of [3H]muscimol specific binding at 1 μM (5.4%), 10 μM (13.5%) and at 100 μM (19.3%) concentrations.

Gammapyrone also did not inhibit binding of selective GABA-B receptor antagonist [^{3}H]-CGP 54626 – at a concentration of 100 μM it displaced less than 10% of [^{3}H]-CGP 54626 binding (data not shown).

3.4.3.2. On cell viability in PC12 cells

Gammapyrone demonstrated negligible lowering of cell viability at 1-10 μM vs. basic level (0 μM), but a sharp decrease was observed at 100 μM ($P < 0.001$, Fig. 32.A). DEHP induced a two-fold decrease in cell viability compared to control ($P < 0.0001$, Fig. 32.B). At non-toxic concentration of 1 μM gammapyrone was capable to significantly improve the viability of DEHP-treated cells ($P < 0.05$, Fig. 32.B).

3.4.3.3. On ROS production, MMP and the activity of mitochondrial complexes in PC12 cells

In PC12 cells, treatment with DEHP resulted in significantly increased DCF oxidation ($P < 0.0001$, Fig. 33.A) and decreased uptake of Rh-123 compared to control ($P < 0.0001$, Fig. 33.B). DEHP also decreased the activity of all mitochondrial complexes (Fig. 34.A-D): complex I ($P < 0.0001$), complex II+III ($P < 0.0001$), complex IV ($P < 0.01$) and complex V ($P < 0.001$). In DEHP-treated cells, gammapyrone at 1 μM showed significantly lower fluorescence ($P < 0.0001$, Fig. 33.A), an increase in Rh-123 uptake ($P < 0.001$, Fig. 33.B), as well as significantly higher activities of all mitochondrial complexes ($P < 0.05$, Fig. 34.A-C, $P < 0.01$, Fig. 34.D) compared to the DEHP-treated cells. Gammapyrone *per se* demonstrated lower values of Rh-123 uptake ($P < 0.01$, Fig. 33.B).

3.4.3.4. On apoptosis markers

Western blot data demonstrated that DEHP induced a significant increase in the density of the apoptosis protein Bax ($P < 0.01$, Fig. 35.A and B), significantly reduced the density of Bcl2 ($P < 0.0001$, Fig. 35.A and C) and produced a sharp increase in CASP 3 ($P < 0.0001$, Fig. 35.D and E) and p53 ($P < 0.001$, 35.F and G). Gammapyrone was able to significantly reduce the

DEHP-induced increase in the density of Bax ($P < 0.01$), CASP 3 and p53 ($P < 0.0001$), but did not change Bcl2 density. Gammapyrone *per se* did not alter the densities of Bax, Bcl2 and CASP 3, but significantly decreased p53 density compared to the control ($P < 0.01$).

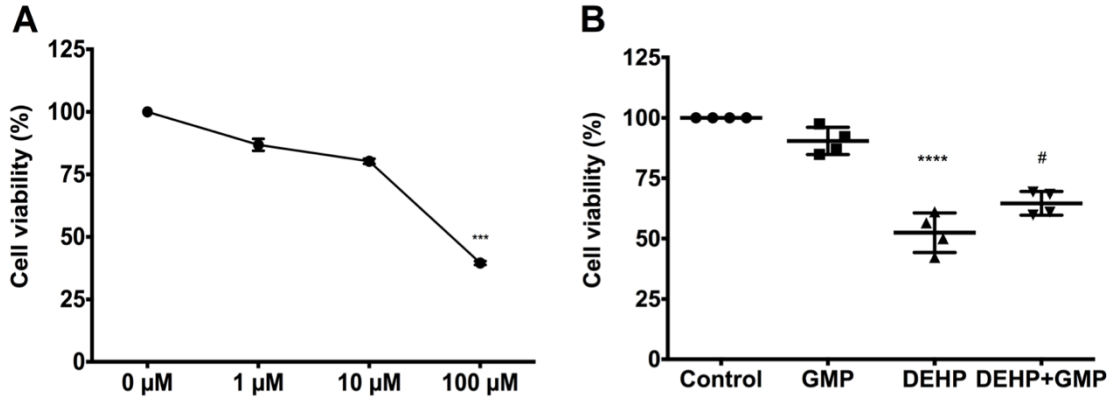

Figure 32. **Effects of gammapyrone (GMP) on PC12 cell viability at 0-100 µM concentrations (A) and, at 1 µM in the di-2-ethylhexyl phthalate (DEHP) model (B). Non-treated PC12 cells were the control. The data are shown as mean values ± S.D. (n=4/group). One-way ANOVA followed by Tukey's multiple comparisons test. ******P* < 0.001 and *******P* < 0.0001 vs. Control; #*P* < 0.05 vs. DEHP.**

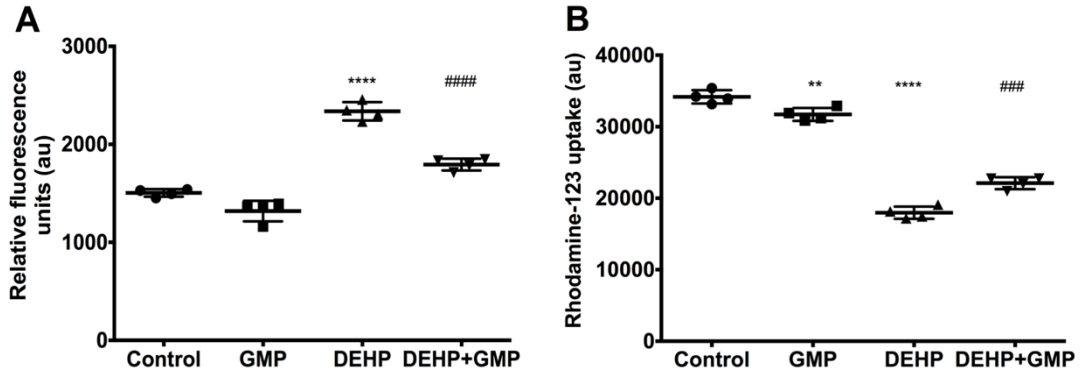

Figure 33. **Effects of 1 µM gammapyrone (GMP) on 2,7-dichlorofluorescein (DCF) oxidation (A) and Rhodamine-123 (Rh-123) uptake (B) in PC12 cells treated with di-2-ethylhexyl phthalate (DEHP). The data are shown as mean values ± S.D. (n=4/group). One-way ANOVA followed by Tukey's multiple comparisons test. *****P* < 0.01 and *******P* < 0.0001 vs. Control; ###*P* < 0.001 and ####*P* < 0.0001 vs. DEHP.**

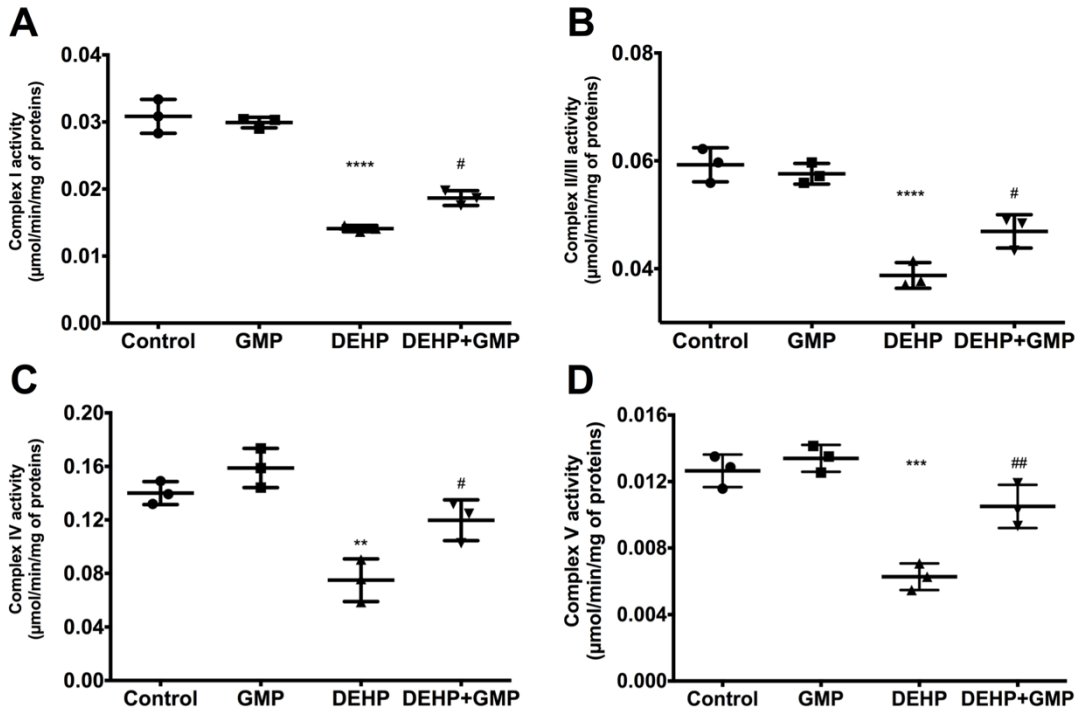

Figure 34. **Effects of 1 µM gammapyrone (GMP) on the activity of mitochondrial complexes I, (A), II/III (B), IV (C) and V (D) in PC12 cells treated with di-2-ethylhexyl phthalate (DEHP). The data are shown as mean values ± S.D. (n=3/group). One-way ANOVA followed by Tukey's multiple comparisons test. *****P*** **< 0.01, ******P*** **< 0.001 and *******P*** **< 0.0001 vs. Control; #*P*** **< 0.05 and ##*P*** **< 0.01 vs. DEHP.**

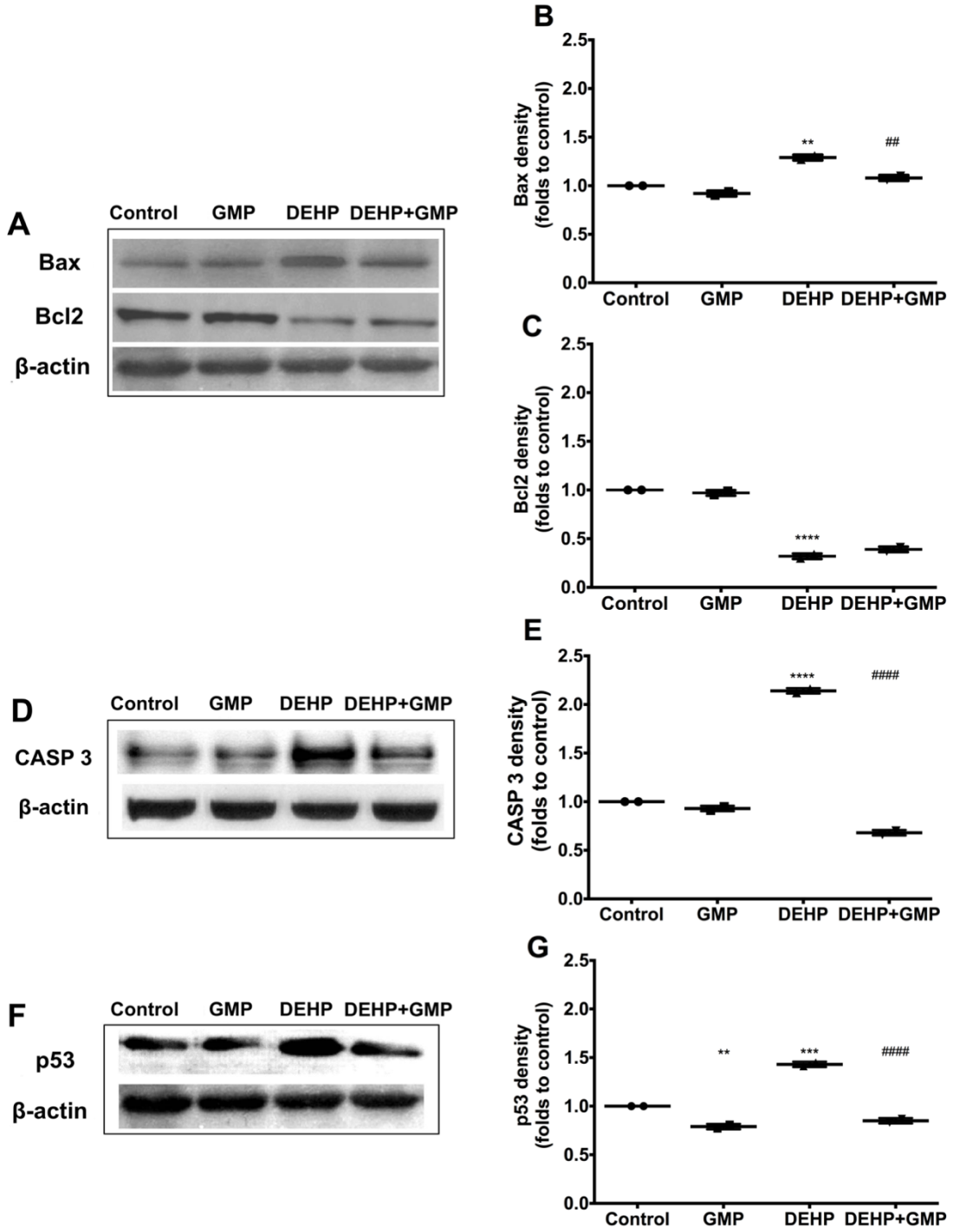

Figure 35. **Effects of 1 µM gammapyrone (GMP) in PC12 cells on the expression of apoptosis markers Bax and Bcl2 (A), CASP 3 (D) and p53 (F) after di-2-ethylhexyl phthalate (DEHP)-induced toxicity. Bar graphs demonstrate density measurements of Bax (B), Bcl2 (C), CASP 3 (E) and p53 (G). Graphs demonstrate the ratio for density normalization of the markers to the β-actin. The data are shown as mean values ± S.D. (n=2/group). One-way ANOVA followed by Tukey's multiple comparisons test. *****P*** **< 0.01, ******P*** **< 0.001 and *******P*** **< 0.0001 vs. Control; ##*P* < 0.01 and ####*P* < 0.0001 vs. DEHP.**

4. DISCUSSION

Early sAD pathological processes in the brain – neuroinflammation, imbalance in the action of neurotransmitter systems and mitochondrial dysfunction cause neuronal death, thereby leading to the disruption in cell-cell communication, as well as in transfer and retention of information. All these events manifest as progressive deterioration of cognitive functions, and result in memory loss and dementia, characteristics of AD. Latest promising pharmacotherapeutic strategies are directed at preventing neurodegenerative processes before the manifestation of protein pathologies in the pre-dementia stages (Villemagne et al., 2018).

Recent data have highlighted the importance of the GABAergic system in compensating the synaptic dysfunction in AD (Nava-Mesa et al., 2014). GABAergic system deficits and memory impairment precedes Aβ42 pathology in mouse models of AD and in human AD patients (Riese et al., 2015; Wang et al., 2014). Therefore, an approach that halts neurodegenerative processes in the early stages of AD by focusing therapy on the GABAergic system may be considered a novel, yet effective strategy (Calsolaro and Edison, 2016). Unfortunately, there is no available data on the use of GABAergic compounds in the treatment of AD and in animal models. The only data that have been found show anti-inflammatory and memory-enhancing effects of low dose (0.1 mg/kg) of muscimol in a rat exhaustion model (Ding et al., 2015) and the positive effects of diazepam at subsedative doses on animal memory, synaptic plasticity and decreasing Aß42 formation (Umeda et al., 2017).

However, several authors report the effects of GABA receptor agonists in AD in *in vitro* models. Muscimol at 1 μM inhibited Aß-induced cortical and hippocampal neuronal death (Paula-Lima et al., 2005). In another model, glial cell lines, muscimol reduced the lipopolysaccharide (LPS)-induced release of pro-inflammatory cytokines (Kim et al., 2012). Therefore, current doctoral thesis study was focused on the influence of GABAergic compounds in brain processes through modeling of sAD *in vivo*.

4.1. Memory-improving effects of the studied compounds

Up to now, memory-impairing effects of GABA receptor agonists' medium and high doses have been described: diazepam at 2 mg/kg in rats (Sevastre-Berghian et al., 2017), muscimol at 1 mg/kg impaired memory consolidation in mice (Castellano and McGaugh, 1990), baclofen at 10 and 30 mg/kg impaired memory retention in mice (Castellano et al., 1989).

Our concept is based on the notion that these compounds might show memory-enhancing effects when administered at 10-100 times lower (subsedative) doses. These paradoxical effects might be explained by the principles of allosteric modulation, when a compound binds to an allosteric modulatory receptor protein site instead of the usual specific site. Results obtained in this study confirm the idea expressed in the concept, because the studied compounds demonstrated memory-enhancing effects at very low and low doses. Thus, GABA-A receptor GABA site agonist muscimol (0.01 and 0.05 mg/kg) after 7-day administration completely reversed STZ-induced impairments in spatial learning (on training days 2-4) in the Morris water maze test by shortening rat escape latency. Muscimol also improved spatial memory in the probe trial to the control group values.

Diazepam, GABA-A receptor agonist that acts through the modulatory site of the receptor, at 0.05 and 1 mg/kg (administered for 16 days) had similar action on learning and memory. Diazepam did not cause sedation at these doses, as evidenced by the swimming speed during acquisition trials and, in the open field, did not influence neither time spent in the center zone, nor the total walked distance.

Interestingly, memory-enhancing effects of low dose diazepam were also reported in other model animals. For instance, in acutely stressed middle aged mice, at 0.25 and 0.5 mg/kg doses, diazepam improved memory performance (Béracochéa et al., 2011); while 0.1 mg/kg diazepam (administered for 5 days) increased GABAergic and glutamatergic activity and protected against autoimmune encephalomyelitis by inhibiting inflammation in the rat frontal cortex (Bibolini et al., 2011). Moreover, 1 mg/kg diazepam enhanced mitochondrial function and decreased lipid peroxidation in the striatum of acutely immobilized rats (Méndez-Cuesta et al., 2011). The only study of diazepam in an AD model *in vivo* was done in fAD model (6-month old Osaka knock-in mice), where long-term (2 month) diazepam administration was done at 2 μg/mouse (i.e., about 0.07 mg/kg) dose (Umeda et al., 2017). Memory improvement was observed at 8 months of age.

In our studies, memory enhancement in rats was seen also when GABA-B receptor agonist baclofen was administered at low doses – 0.025 and 0.05 mg/kg (7 days), as shown on training days 2-4. Therefore, despite of the difference in both GABA receptor structural functions (GABA-A is an ionotropic, whereas GABA-B – metabotropic receptor), agonists of both receptors at very low and low doses similarly improved spatial memory forming processes.

Even more interestingly, GABA elements-containing compound gammapyrone that did not exhibit affinity towards GABA receptors, at both 0.1 and 0.5 mg/kg doses (11-day administration) improved spatial learning and memory in STZ animals.

Obtained results allow us to suggest that all studied compounds may act on more or less similar allosteric receptor proteins or targets apart from specific binding to GABA receptors.

4.2. Anti-neuroinflammatory effects

One of the key mechanisms that initiate AD and cell death is neuroinflammation that occurs when there is an excessive activation of microglia (Calsolaro and Edison, 2016; McNaull et al., 2010; Southam et al., 2016) and macroglia (astrocytes) (Chen et al., 2012; Verkhratsky et al., 2016). Overactivated glial cells release free radicals, proinflammatory cytokines, fatty acid metabolites and prevent neuronal regulatory functioning, thereby inducing learning and memory deficits (Liu and Hong, 2003). Learning and memory processes are also influenced by GABA concentrations present in astrocytes, hence making GABA a gliotransmitter (Ding et al., 2007). However, in astrocytosis, GABA released from astrocytes might detrimentally affect the synaptic plasticity in the cortex (Ding et al., 2007) and hippocampus (Jourdain et al., 2007). Therefore, pharmacotherapeutic approaches that aim to protect against neuroinflammation are currently considered very promising for the treatment of the various neurodegenerative diseases (Balducci and Forloni, 2018; González-Reyes et al., 2017).

Results of the doctoral thesis study showed that STZ induced astrogliosis by a 3-fold increase GFAP density in both studied structures, while muscimol regulated this elevation to the control group levels. Other authors in an exhaustion model reported the ability of low dose muscimol (0.1 mg/kg) to reduce astrogliosis and diminished apoptosis processes in the hippocampus (Ding et al., 2015).

In our studies, GABA-A receptor modulatory site agonist diazepam similarly ameliorated astrogliosis. This compound also decreased microgliosis by maintaining control group values of Iba-1 density. Previously, anti-inflammatory effects of diazepam (0.5 mg/kg) have been observed in the model of autoimmune encephalomyelitis, where it decreased cell proliferation and the generation of pro-inflammatory cytokines (Fernández Hurst et al., 2017). Perhaps, diazepam can participate in the regulation of immune processes, since it was also found to stimulate neurosteroid synthesis in glial cells (Fernández Hurst et al., 2017).

We have observed in our studies that baclofen also prevented STZ-induced cortical and hippocampal astrogliosis. The anti-inflammatory action of baclofen (0.01 and 1 mg/kg) has been described in allergic dermatitis mice model (Duthey et al., 2010) and *in vitro*: in the immune cells of multiple sclerosis patients, it reduced inflammation by attenuating cytokine production

(Crowley et al., 2015), and in Wistar rat activated microglial cells baclofen at 10 μM, 100 μM and 1 mM concentrations attenuated the LPS-induced increase in cytokine release (Kuhn et al., 2004).

4.3. Neurotransmitter regulation

4.3.1. Normalization of acetylcholine cleavage

Acetylcholine plays an essential role in the maintenance of memory processes (Micheau and Marighetto, 2011), therefore, inhibition of its cleavage is still considered a treatment strategy to delay the development of AD (Haussmann and Donix, 2016). Increased AChE activity and a concomitant deficit in acetylcholine is observed in the early stages of AD.

In our study, STZ caused a 2-fold increase in AChE density in the nerve fibers of cortical and hippocampal neurons. All studied compounds normalized AChE expression, indicating their ability to prevent cholinergic deficits.

4.3.2. Normalization of GABA production

It has been proven that GABA can co-exist in the same cells with acetylcholine and dopamine (Tritsch et al., 2016) and participate in the development of the CNS and disease pathogenesis (Dulcis et al., 2013; Hnasko and Edwards, 2012). Although GABA production in the brains of AD patients is considered stable (Luchetti et al., 2011; Rissman et al., 2007; Warren et al., 2013), post-mortem studies of the brains from patients with AD showed substantial (20-47%) reductions in the GABA concentrations and GAD activity (Lanctôt et al., 2004).

We have found that in the STZ rats, cortical and hippocampal GAD67 density was decreased by approximately 25%. Both GABA-A receptor agonists muscimol and diazepam, as well as GABA-B receptor agonist baclofen prevented this reduction, indicating a normalization of the GABA synthesis. Similarly, gammapyrone also normalized STZ-induced decrease in GAD67 density in the cortex and hippocampus of STZ rats. This fact is in good agreement with previous data obtained in naïve rats that demonstrated the ability of gammapyrone to enhance naïve rat memory in the conditioned avoidance response test, as well as increase cortical and hypothalamic levels of GABA, noradrenaline and 5-hydroxyindoleacetic acid (Misane et al., 1993).

Since studied compounds normalized the actions of both activatory (cholinergic) and inhibitory (GABA) system, one can consider that the maintenance of the balance of their activity is a crucial mechanism involved in the ability of these compounds to maintain the functioning of normal cognitive processes.

4.4. Regulatory effects of diazepam on synaptic protein SYP1 expression

GABA, particularly produced in the hippocampal DG, is involved in providing synaptogenesis and neurogenesis (Liu and Song, 2016; Lledo et al., 2006). SYP1, a presynaptic membrane protein, is essential for synaptic plasticity and the formation of synaptic vesicles.

In our study, icv injection of STZ led to a significant decrease in the density of SYP1 in the hippocampal CA1 and a mild – in CA3. Diazepam at 0.05 mg/kg dose normalized SYP1 density in these regions, which points to its neurotrophic action that might be considered vital in the treatment of early sAD stages. An increase in synaptophysin density in the hippocampal CA3 was also observed in Osaka mice fAD model, where diazepam was administered at 0.07 mg/kg (Umeda et al., 2017).

4.5. Normalizing actions on the mitochondrial processes by gammapyrone *in vitro*

The dysfunction of mitochondrial processes has an essential impact on the development of sAD (Correia et al., 2013). Therefore, one of the important targets for early anti-AD strategies are mitochondrial bioenergetic processes (Wilkins and Swerdlow, 2016) and/or factors that regulate apoptosis (Shimohama, 2000). The exact relationship between mitochondrial impairments and neuroinflammation is still uncertain, but both of these phenomena influence each other (Wilkins and Swerdlow, 2016). Manifestation of these two processes in the cells results in increased ROS concentrations that induce overactivation of both astroglial and microglial nitric oxide synthases, thereby causing neuronal damage (Morgan and Liu, 2011; Verri et al., 2012). This means that mitochondria have a major role in protein synthesis and remodeling (Devine and Kittler, 2018).

In this study, we only assessed the protective effects of gammapyrone, since the regulating effects of muscimol (Kinjo et al., 2018), diazepam (Van Der Kooij et al., 2018) and baclofen (Liu et al., 2015) in models of mitochondrial dysfunction have been described previously.

In PC12 cells, gammapyrone protected cells against death, apoptosis and mitochondrial damage induced by toxic compound DEHP (Zeng et al., 2012; Rowdhwal and Chen, 2018). Although gammapyrone slightly decreased mitochondrial membrane potential, it prevented DEHP-induced sharp decrease in mitochondrial membrane potential, normalized ROS production and the functioning of all mitochondrial respiratory chain complexes (I-V). Moreover, gammapyrone acted as an anti-apoptotic substance by regulating the density of proteins involved in cell apoptosis (Bax, CASP 3 and p53).

These data show that the prevention of mitochondrial impairments is a crucial component of the neuroprotective repertoire of gammapyrone’s actions.

4.6. General considerations

The data obtained in the current study raise the following questions: which are the targets for the memory-enhancing effects of low dose GABA receptor agonists? Why, regardless of the GABA receptor type, different agonists at subsedative doses produce similar effects?

Obtained data lead one to suggest that these effects might be explained not by the binding of the studied compounds to the specific GABA receptors, but by the allosteric modulatory properties of these compounds. The basis of this consideration is, firstly, the complexity of GABA receptors and differential localization in the neurons – synaptic and extrasynaptic, as well as in glial cells – perisynaptic. Moreover, recently identified multiple subunits for each GABA receptor may create numerous conformations and may bind ligands that would change the sensitivity, ion selectivity and kinetic properties of receptor ultrastructures (Enna and McCarson, 2013; Owens and Kriegstein, 2002). For example, different ultrastructures of GABA synapses are currently recognized, such as type 1 (primarily identified in the synaptic cleft and considered excitatory) and type 2 (generally thought to be inhibitory), which may provide distinct pharmacological sensitivity, ionic selectivity and kinetic properties (Owens and Kriegstein, 2002). Secondly, considering the differential chemical structures of the studied compounds, one may suggest that the regulatory action of these small molecules is governed by the common pharmacophores (e.g., positively charged nitrogen atoms) that target the same receptor protein recognition sites.

Although gammapyrone did not demonstrate binding to either GABA-A or GABA-B receptors and it is known to have no Ca^{2+} antagonism, it produced effects similar to that of the studied GABA receptor agonists. Considering the structure of gammapyrone, we suggest that, additionally to allosteric binding, it may also have dipeptide-mimicking regulatory activity, since gammapyrone has a dipeptide-like structure (free GABA and “crypto” GABA that are bound by a peptide bond). It is known that one of the characteristics of peptides is their regulatory action. The allosterism of gammapyrone may also be explained by the DHP ring in its molecule, which might act as a molecular chameleon (Triggle, 2007) by exerting actions on different proteins (receptors, enzymes, ion channels, etc.).

5. CONCLUSIONS

1. For the first time, we have shown that GABA-A receptor agonists muscimol and diazepam, GABA-B receptor agonist baclofen and GABA element-containing gammapyrone at very low and moderate doses significantly enhance spatial learning/memory processes in sAD (icv STZ) model animals.
2. All studied compounds exhibited anti-neuroinflammatory properties in both cortical and hippocampal structures of the STZ rat brain, as well as normalized the expression of enzymes involved in the cleavage of acetylcholine (AChE) and GABA synthesis (GAD67). Diazepam regulated synaptic protein SYP1 expression in the hippocampus.
3. Gammapyrone did not bind to GABA-A or GABA-B receptors; *in vitro* it ameliorated DEHP-induced mitochondrial dysfunction and apoptosis.
4. Memory-enhancing actions of GABA receptor agonists' low doses in sAD model rats might be explained by the allosteric modulatory properties of these compounds, and early regulation of cell biochemical processes can be considered targets for stopping or halting cognitive deficits.
5. Structures of GABA receptor agonists and gammapyrone might serve as prototype molecules for the design of novel anti-dementia drugs.

ACKNOWLEDGEMENTS

I am expressing my gratitude to my colleagues: head of the Department of Pharmacology (UL MF): Professor Baiba Jansone, as well as Dr. med. Zane Dzirkale, Dr. med. Jolanta Pupure and Dr. med. Ulrika Beitnere for the assistance in the experimental work. I am also thankful to the chemists of the Latvian Institute of Organic Synthesis Prof. Ivars Poikāns, Prof. Egils Bisenieks for the synthesis of gammapyrone and to Prof. Gunārs Duburs for the preparation of the figure that depicts the structure of gammapyrone; I thank Dr. pharm. Edijs Vāvers for the analysis of gammapyrone binding to GABA-B receptors. I am grateful to our collaborators, the research group of the Department of Biomedical and Biotechnological Sciences at the University of Catania, Italy, led by Professor Vittorio Calabrese, for conducting *in vitro* experiments with gammapyrone in PC12 cells. For huge help with microphotograph analysis and selection I thank Associated Professors Inga Kadish and Thomas van Groen from the Department of Cell, Developmental and Integrative Biology at the University of Alabama at Birmingham, USA.

A big thank you goes to my colleague Karīna Narbute who has helped me both in experimental work, scientific article preparation and in the popularization of science.

I express the biggest gratitude towards my mentor and doctoral thesis supervisor – Professor Vija Zaiga Kluša. Not only did she spark in me the interest to work in science, but always has supported my scientific work, skill and competence development, as well as bringing exciting ideas to life.

SCIENTIFIC PUBLICATIONS AND CONFERENCE PRESENTATIONS

Scientific publications

- **V. Pilipenko**, K. Narbute, I. Amara, A. Trovato, M. Scuto, J. Pupure, B. Jansone, J. Poikans, E. Bisenieks, V. Klusa, V. Calabrese. GABA-containing compound gammapyrone protects against brain impairments in Alzheimer's disease model male rats and prevents mitochondrial dysfunction in cell culture. Journal of Neuroscience Research. 2019, 97(4):378-86.
- **V. Pilipenko**, K. Narbute, U. Beitnere, J. Rumaks, J. Pupure, B. Jansone, V. Klusa. Neuroprotective action of diazepam at very low and moderate doses in Alzheimer's disease model rats. Neuropharmacology. 2019, 144:319-326.
- **V. Pilipenko**, K. Narbute, J. Pupure, J. Rumaks, B. Jansone, V. Klusa. Very low doses of muscimol and baclofen ameliorate cognitive deficits and regulate protein expression in the brain of a rat model of streptozocin-induced Alzheimer's disease. European Journal of Pharmacology. 2018, 818:381-399.

Poster presentations at international conferences

- **V. Pilipenko**, U. Beitnere, K. Narbute, J. Pupure, R. Skumbins, Z. Dzirkale, J. Rumaks, B. Jansone, V. Klusa. Extremely low doses of muscimol induce memory-enhancing, anti-inflammatory and protein expression regulating effects in non-transgenic Alzheimer's disease model rats. **13th International Conference AD/PD^{TM}**. Vienna, Austria, March 29-April 2, 2017.
- **V. Pilipenko**, J. Pupure, J. Rumaks, U. Beitnere, Z. Dzirkale, B. Jansone, R. Skumbins, V. Klusa. Muscimol effectively reverses impaired spatial memory in Alzheimer's disease-type streptozocin icv rat model. **ECNP Workshop for Junior Scientists in Europe**. Nice, France, March 17-20, 2016.
- **V. Pilipenko**, J. Pupure, J. Rumaks, U. Beitnere, Z. Dzirkale, R. Skumbins, V. Klusa. GABAA agonist muscimol ameliorates learning/memory deficits in streptozocin-induced Alzheimer's disease non-transgenic rat model. **Molecular Mechanisms of Regulation in the Nervous System**. Tartu, Estonia, June 14-17, 2015.

Selected oral presentations

- "Memory-improving, GABA-regulating and anti-neuroinflammatory effects of diazepam at very low and moderate doses in a rat model of Alzheimer's disease". Oral presentation at the **Juvenes Pro Medicina Conference**, University of Lodz, Poland, May 26, 2018.
- "Low and moderate dose of diazepam improves learning, prevents neuroinflammation and normalizes cholinergic activity in Alzheimer's disease model-rats". Oral presentation at the **76th International Scientific Conference on Medicine of the University of Latvia**, University of Latvia, Riga, Latvia, February 23, 2018.
- "Neuroprotective action of gammapyrone, a GABA-containing peptide-mimicking compound." Oral presentation at the **2nd International Conference in Pharmacology: from Cellular Processes to Drug Targets**. University of Latvia, Riga, Latvia, October 19, 2017.
- "Baclofen, a GABA-B receptor agonist, shows memory improving and anti-inflammatory activity and increases cholinergic activity in Alzheimer's disease model-rats". Oral presentation at **the 75th Conference of the University of Latvia International Medical Section**, University of Latvia, Riga, Latvia, February 24, 2017**.**
- **"**Muscimol effectively reverses impaired spatial memory in Alzheimer's disease-type streptozocin icv rat model**"**. Oral presentation at the Drug Discovery Conference, Riga, Latvia, August 27, 2015.

REFERENCES

Agosta, F., Vossel, K.A., Miller, B.L., Migliaccio, R., Bonasera, S.J., Filippi, M., Boxer, A.L., Karydas, A., Possin, K.L., Gorno-Tempini, M.L., 2009. Apolipoprotein E ε4 is associated with disease-specific effects on brain atrophy in Alzheimer's disease and frontotemporal dementia. Proc. Natl. Acad. Sci. 106, 2018–2022. https://doi.org/10.1073/pnas.0812697106

Ahring, P.K., Bang, L.H., Jensen, M.L., Strøbæk, D., Hartiadi, L.Y., Chebib, M., Absalom, N., 2016. A pharmacological assessment of agonists and modulators at α4β2γ2 and α4β2δ GABAA receptors: The challenge in comparing apples with oranges. Pharmacol. Res. 111, 563–576. https://doi.org/10.1016/j.phrs.2016.05.014

Arnold, S.E., Arvanitaki, Z., S.L., M.-R., Koenig, A.M., Wang, H.Y., Ahima, R.S., Craft, S., Gandy, 2018. Brain insulin resistance in type 2 diabetes and Alzheimer disease: concepts and conundrums. Nat. Rev. Neurol. 14, 168–181. https://doi.org/10.1038/nrneurol.2017.185

Bachmann, M.F., Jennings, G.T., Vogel, M., 2018. A vaccine against Alzheimer`s disease: anything left but faith? Expert Opin. Biol. Ther. 19, 73–78. https://doi.org/10.1080/14712598.2019.1554646

Balducci, C., Forloni, G., 2018. Novel targets in Alzheimer's disease: A special focus on microglia. Pharmacol. Res. 130, 402–413. https://doi.org/10.1016/j.phrs.2018.01.017

Belinson, H., Lev, D., Masliah, E., Michaelson, D.M., 2008. Activation of the Amyloid Cascade in Apolipoprotein E4 Transgenic Mice Induces Lysosomal Activation and Neurodegeneration Resulting in Marked Cognitive Deficits. J. Neurosci. 28, 4690–4701. https://doi.org/10.1523/jneurosci.5633-07.2008

Béracochéa, D., Tronche, C., Coutan, M., Dorey, R., Chauveau, F., Piérard, C., 2011. Interaction between Diazepam and Hippocampal Corticosterone after Acute Stress: Impact on Memory in Middle-Aged Mice. Front. Behav. Neurosci. 5, 1–9. https://doi.org/10.3389/fnbeh.2011.00014

Bettler, B., Kaupmann, K., Mosbacher, J., Gassmann, M., 2004. Molecular Structure and Physiological Functions of GABA B Receptors . Physiol. Rev. 84, 835–867. https://doi.org/10.1152/physrev.00036.2003

Bhatti, J.S., Bhatti, G.K., Reddy, P.H., 2017. Mitochondrial dysfunction and oxidative stress in metabolic disorders — A step towards mitochondria based therapeutic strategies. Biochim.

Biophys. Acta - Mol. Basis Dis. 1863, 1066–1077. https://doi.org/10.1016/j.bbadis.2016.11.010

Bibolini, M.J., Chanaday, N.L., Báez, N.S., Degano, A.L., Monferran, C.G., Roth, G.A., 2011. Inhibitory role of diazepam on autoimmune inflammation in rats with experimental autoimmune encephalomyelitis. Neuroscience 199, 421–428. https://doi.org/10.1016/j.neuroscience.2011.08.076

Bischoff, S., Leonhard, S., Reymann, N., Schuler, V., Shigemoto, R., Kaupmann, K., Bettler, B., 1999. Spatial distribution of GABA(B)R1 receptor mRNA and binding sites in the rat brain. J. Comp. Neurol. 412, 1–16. https://doi.org/10.1002/(SICI)1096-9861(19990913)412:1<1::AID-CNE1>3.0.CO;2-D

Bradford, M.M., 1976. A rapid and sensitive method for the quantitation of microgram quantities of protein utilizing the principle of protein-dye binding. Anal. Biochem. 72, 248–254. https://doi.org/10.1016/0003-2697(76)90527-3

Butterfield, D.A., Boyd-Kimball, D., 2018. Redox proteomics and amyloid β-peptide: insights into Alzheimer disease, Journal of Neurochemistry. https://doi.org/10.1111/jnc.14589

Butterfield, D.A., Perluigi, M., 2016. Redox Proteomics: A Key Tool for New Insights into Protein Modification with Relevance to Disease. Antioxid. Redox Signal. 26, 277–279. https://doi.org/10.1089/ars.2016.6919

Calsolaro, V., Edison, P., 2016. Neuroinflammation in Alzheimer's disease: Current evidence and future directions. Alzheimers Dement. 12, 719–732. https://doi.org/10.1016/j.jalz.2016.02.010

Calvo-Flores Guzmán, B., Vinnakota, C., Govindpani, K., Waldvogel, H.J., Faull, R.L.M., Kwakowsky, A., 2018. The GABAergic system as a therapeutic target for Alzheimer's disease. J. Neurochem. 146, 649–669. https://doi.org/10.1111/jnc.14345

Cardoso, S., Carvalho, C., Correia, S.C., Seiça, R.M., Moreira, P.I., 2016. Alzheimer's Disease: From Mitochondrial Perturbations to Mitochondrial Medicine. Brain Pathol. 26, 632–647. https://doi.org/10.1111/bpa.12402

Carson, M.J., Cameron Thrash, J., Walter, B., 2006. The cellular response in neuroinflammation: The role of leukocytes, microglia and astrocytes in neuronal death and survival. Clin. Neurosci. Res. 6, 237–245. https://doi.org/10.1016/j.cnr.2006.09.004

Castellano, C., Brioni, J.D., Nagahara, A.H., McGaugh, J.L., 1989. Post-training systemic and

intra-amygdala administration of the GABA-B agonist baclofen impairs retention. Behav. Neural Biol. 52, 170–179. https://doi.org/10.1016/S0163-1047(89)90285-9

Castellano, C., McGaugh, J.L., 1990. Effects of post-training bicuculline and muscimol on retention: Lack of state dependency. Behav. Neural Biol. 54, 156–164. https://doi.org/10.1016/0163-1047(90)91352-C

Cheignon, C., Tomas, M., Bonnefont-Rousselot, D., Faller, P., Hureau, C., Collin, F., 2018. Oxidative stress and the amyloid beta peptide in Alzheimer's disease. Redox Biol. 14, 450–464. https://doi.org/10.1016/j.redox.2017.10.014

Chen, W.W., Zhang, X., Huang, W.J., 2016. Role of neuroinflammation in neurodegenerative diseases (Review). Mol. Med. Rep. 13, 3391–3396. https://doi.org/10.3892/mmr.2016.4948

Chen, X., Zhong, Z., Xu, Z., Chen, L., Wang, Y., 2010. 2′,7′-Dichlorodihydrofluorescein as a fluorescent probe for reactive oxygen species measurement: Forty years of application and controversy. Free Radic. Res. 44, 587–604. https://doi.org/10.3109/10715761003709802

Chen, Y., Liang, Z., Blanchard, J., Dai, C.L., Sun, S., Lee, M.H., Grundke-Iqbal, I., Iqbal, K., Liu, F., Gong, C.X., 2013. A non-transgenic mouse model (icv-STZ mouse) of Alzheimer's disease: similarities to and differences from the transgenic model (3xTg-AD mouse). Mol. Neurobiol. 47, 711–725. https://doi.org/10.1007/s12035-012-8375-5

Chen, Y., Zhao, C., Zhang, C., Luo, L., Yu, G., 2012. Influence of chronic intermittent hypoxia on growth associated protein 43 expression in the hippocampus of young rats * ★. Neural Regen. Res. 7, 1241–1246. https://doi.org/10.3969/j.issn.1673-5374.2012.16.006

Chin, J., 2005. Fyn Kinase Induces Synaptic and Cognitive Impairments in a Transgenic Mouse Model of Alzheimer's Disease. J. Neurosci. 25, 9694–9703. https://doi.org/10.1523/jneurosci.2980-05.2005

Cooperstein, S., Lazarow, A., 1951. A microspectrophotometric method for the determination of cytochrome oxidase. J Biol Chem 665–670.

Correia, S.C., Santos, R.X., Santos, M.S., Casadesus, G., LaManna, J.C., Perry, G., Smith, M.A., Moreira, P.I., 2013. Mitochondrial Abnormalities in a Streptozotocin-Induced Rat Model of Sporadic Alzheimer's Disease. Curr. Alzheimer Res. 10, 406–419. https://doi.org/10.2174/1567205011310040006

Croteau, E., Castellano, C.A., Fortier, M., Bocti, C., Fulop, T., Paquet, N., Cunnane, S.C., 2018. A cross-sectional comparison of brain glucose and ketone metabolism in cognitively

healthy older adults, mild cognitive impairment and early Alzheimer's disease. Exp. Gerontol. 107, 18–26. https://doi.org/10.1016/j.exger.2017.07.004

Crowley, T., Fitzpatrick, J.-M., Kuijper, T., Cryan, J.F., O'Toole, O., O'Leary, O.F., Downer, E.J., 2015. Modulation of TLR3/TLR4 inflammatory signaling by the GABAB receptor agonist baclofen in glia and immune cells: relevance to therapeutic effects in multiple sclerosis. Front. Cell. Neurosci. 9, 284. https://doi.org/10.3389/fncel.2015.00284

Dambrova, M., Zvejniece, L., Liepinsh, E., Cirule, H., Zharkova, O., Veinberg, G., Kalvinsh, I., 2008. Comparative pharmacological activity of optical isomers of phenibut. Eur. J. Pharmacol. 583, 128–134. https://doi.org/10.1016/j.ejphar.2008.01.015

Datta, M., Staszewski, O., Raschi, E., Frosch, M., Hagemeyer, N., Tay, T.L., Blank, T., Kreutzfeldt, M., Merkler, D., Ziegler-Waldkirch, S., Matthias, P., Meyer-Luehmann, M., Prinz, M., 2018. Histone Deacetylases 1 and 2 Regulate Microglia Function during Development, Homeostasis, and Neurodegeneration in a Context-Dependent Manner. Immunity 48, 514-529.e6. https://doi.org/10.1016/j.immuni.2018.02.016

Davies, P., Maloney, A.J., 1976. Selective Loss of Central Cholinergic Neurons in Alzheimer'S Disease. Lancet 2, 1403.

De Strooper, B., Karran, E., 2016. The Cellular Phase of Alzheimer's Disease. Cell 164, 603–615. https://doi.org/10.1016/j.cell.2015.12.056

Debbasch, C., Pisella, P.J., De Saint Jean, M., Rat, P., Warnet, J.M., Baudouin, C., 2001. Mitochondrial activity and glutathione injury in apoptosis induced by unpreserved and preserved β-blockers on chang conjunctival cells. Investig. Ophthalmol. Vis. Sci. 42, 2525–2533. https://doi.org/10.1117/12.626961

Deng, Y., Li, B., Liu, Y., Iqbal, K., Grundke-Iqbal, I., Gong, C.X., 2009. Dysregulation of insulin signaling, glucose transporters, O-GlcNAcylation, and phosphorylation of tau and neurofilaments in the brain: Implication for Alzheimer's disease. Am. J. Pathol. 175, 2089–2098. https://doi.org/10.2353/ajpath.2009.090157

Devine, M.J., Kittler, J.T., 2018. Mitochondria at the neuronal presynapse in health and disease. Nat. Rev. Neurosci. 19, 63–80. https://doi.org/10.1038/nrn.2017.170

Di Domenico, F., Barone, E., Perluigi, M., Butterfield, D.A., 2017. The Triangle of Death in Alzheimer's Disease Brain: The Aberrant Cross-Talk Among Energy Metabolism, Mammalian Target of Rapamycin Signaling, and Protein Homeostasis Revealed by Redox

Proteomics. Antioxid. Redox Signal. 26, 364–387. https://doi.org/10.1089/ars.2016.6759

Di Domenico, F., Tramutola, A., Foppoli, C., Head, E., Perluigi, M., Butterfield, D.A., 2018. mTOR in Down syndrome: Role in Aß and tau neuropathology and transition to Alzheimer disease-like dementia. Free Radic. Biol. Med. 114, 94–101. https://doi.org/10.1016/j.freeradbiomed.2017.08.009

Ding, S., Fellin, T., Zhu, Y., Lee, S., Auberson, Y.P., Meaney, D.F., Coulter, D.A., Carmignoto, G., Haydon, P.G., 2007. Enhanced Astrocytic Ca2+ Signals Contribute to Neuronal Excitotoxicity after Status Epilepticus. J. Neurosci. 27, 10674–10684. https://doi.org/10.1523/JNEUROSCI.2001-07.2007

Ding, Y., Xie, L., Chang, C.Q., Chen, Z.M., Ai, H., 2015. Activation of γ-aminobutyric acid (A) receptor protects hippocampus from intense exercise-induced synapses damage and apoptosis in rats. Chin. Med. J. (Engl). 128, 2330–2339. https://doi.org/10.4103/0366-6999.163392

Dorey, E., Chang, N., Liu, Q.Y., Yang, Z., Zhang, W., 2014. Apolipoprotein E, amyloid-beta, and neuroinflammation in Alzheimer's disease. Neurosci. Bull. 30, 317–330. https://doi.org/10.1007/s12264-013-1422-z

Drachman, D.A., Leavitt, J., 1974. Human Memory and the Cholinergic System: A Relationship to Aging? Arch. Neurol. 30, 113–121. https://doi.org/10.1001/archneur.1974.00490320001001

Dulcis, D., Jamshidi, P., Leutgeb, S., Spitzer, N.C., 2013. Neurotransmitter switching in the adult brain regulates behavior. Science 340, 449–53. https://doi.org/10.1126/science.1234152

Duthey, B., Hübner, A., Diehl, S., Boehncke, S., Pfeffer, J., Boehncke, W.H., 2010. Anti-inflammatory effects of the GABAB receptor agonist baclofen in allergic contact dermatitis. Exp. Dermatol. 19, 661–666. https://doi.org/10.1111/j.1600-0625.2010.01076.x

Eimer, W.A., Vassar, R., 2013. Neuron loss in the 5XFAD mouse model of Alzheimer's disease correlates with intraneuronal Aβ42 accumulation and Caspase-3 activation. Mol. Neurodegener. 8, 1. https://doi.org/10.1186/1750-1326-8-2

Ellender, T.J., Paulsen, O., 2010. The many tunes of perisomatic targeting interneurons in the hippocampal network. Front. Cell. Neurosci. 4, 1–11. https://doi.org/10.3389/fncel.2010.00026

Enna, S.J., McCarson, K.E., 2013. Characterization of GABA receptors. Curr. Protoc. Pharmacol. 1, 1–20. https://doi.org/10.1002/0471141755.ph0107s63

Fernández Hurst, N., Zanetti, S.R., Báez, N.S., Bibolini, M.J., Bouzat, C., Roth, G.A., 2017. Diazepam treatment reduces inflammatory cells and mediators in the central nervous system of rats with experimental autoimmune encephalomyelitis. J. Neuroimmunol. 313, 145–151. https://doi.org/10.1016/j.jneuroim.2017.09.012

Fritschy, J.M., Brünig, I., 2003. Formation and plasticity of GABAergic synapses: Physiological mechanisms and pathophysiological implications. Pharmacol. Ther. 98, 299–323. https://doi.org/10.1016/S0163-7258(03)00037-8

Froestl, W., 2010. Chemistry and pharmacology of GABAB receptor ligands. Adv. Pharmacol. 58, 19–62. https://doi.org/10.1016/S1054-3589(10)58002-5

Fuhrmann, M., Bittner, T., Jung, C.K.E., Burgold, S., Page, R.M., Mitteregger, G., Haass, C., Laferla, F.M., Kretzschmar, H., Herms, J., 2010. Microglial Cx3cr1 knockout prevents neuron loss in a mouse model of Alzheimer's disease. Nat. Neurosci. 13, 411–413. https://doi.org/10.1038/nn.2511

Gassmann, M., Bettler, B., 2012. Regulation of neuronal GABABreceptor functions by subunit composition. Nat. Rev. Neurosci. 13, 380–394. https://doi.org/10.1038/nrn3249

Giovannetti, E.A., Fuhrmann, M., 2019. Unsupervised excitation: GABAergic dysfunctions in Alzheimer's disease. Brain Res. 1707, 216–226. https://doi.org/10.1016/j.brainres.2018.11.042

González-Reyes, R.E., Nava-Mesa, M.O., Vargas-Sánchez, K., Ariza-Salamanca, D., Mora-Muñoz, L., 2017. Involvement of Astrocytes in Alzheimer's Disease from a Neuroinflammatory and Oxidative Stress Perspective. Front. Mol. Neurosci. 10, 1–20. https://doi.org/10.3389/fnmol.2017.00427

Govindpani, K., Guzmán, B.C.F., Vinnakota, C., Waldvogel, H.J., Faull, R.L., Kwakowsky, A., 2017. Towards a better understanding of GABAergic remodeling in alzheimer's disease. Int. J. Mol. Sci. 18. https://doi.org/10.3390/ijms18081813

Grieb, P., 2016. Intracerebroventricular Streptozotocin Injections as a Model of Alzheimer's Disease: in Search of a Relevant Mechanism. Mol. Neurobiol. 53, 1741–1752. https://doi.org/10.1007/s12035-015-9132-3

Guerreiro, R., Ph, D., Wojtas, A., Bras, J., Carrasquillo, M., Rogaeva, E., Majounie, E.,

Cruchaga, C., Kauwe, J.S.K., Younkin, S., Hazrati, L., Lambert, J., Amouyel, P., Goate, A., Singleton, A., Hardy, J., 2013. TREM2 variants in Alzheimer's Disease. N. Engl. J. Med. 368, 117–127. https://doi.org/10.1056/NEJMoa1211851.TREM2

Hampel, H., Mesulam, M.M., Cuello, A.C., Farlow, M.R., Giacobini, E., Grossberg, G.T., Khachaturian, A.S., Vergallo, A., Cavedo, E., Snyder, P.J., Khachaturian, Z.S., 2018. The cholinergic system in the pathophysiology and treatment of Alzheimer's disease. Brain 141, 1917–1933. https://doi.org/10.1093/brain/awy132

Hansen, R.A., Gartlehner, G., Webb, A.P., Morgan, L.C., Moore, C.G., Jonas, D.E., 2008. Efficacy and safety of donepezil, galantamine, and rivastigmine for the treatment of Alzheimer's disease: A systematic review and meta-analysis. Clin. Interv. Aging 3, 211–225.

Hardy, J., Cowburn, R., Barton, A., Reynolds, G., Lofdahl, E., O'Carroll, A.M., Wester, P., Winblad, B., 1987. Region-specific loss of glutamate innervation in Alzheimer's disease. Neurosci. Lett. 73, 77–80. https://doi.org/10.1016/0304-3940(87)90034-6

Haussmann, R., Donix, M., 2016. Memantin als Add-on-Medikation zur Acetylcholinesteraseinhibitor-Therapie bei Alzheimer-Demenz. Nervenarzt. https://doi.org/10.1007/s00115-016-0237-3

Heaney, C.F., Kinney, J.W., 2016. Neuroscience and Biobehavioral Reviews Role of GABA B receptors in learning and memory and neurological disorders. Neurosci. Biobehav. Rev. 63, 1–28. https://doi.org/10.1016/j.neubiorev.2016.01.007

Hnasko, T.S., Edwards, R.H., 2012. Neurotransmitter Co-release: Mechanism and Physiological Role. Annu Rev Physiol 225–243. https://doi.org/10.1146/annurev-physiol-020911-153315.Neurotransmitter

Howell, O., Atack, J.R., Dewar, D., McKernan, R.M., Sur, C., 2000. Density and pharmacology of α5 subunit-containing GABA(A) receptors are preserved in hippocampus of Alzheimer's disease patients. Neuroscience 98, 669–675. https://doi.org/10.1016/S0306-4522(00)00163-9

Itzhaki, R.F., 2018. Corroboration of a major role for herpes simplex virus type 1 in Alzheimer's disease. Front. Aging Neurosci. 10, 1–11. https://doi.org/10.3389/fnagi.2018.00324

Jo, S., Yarishkin, O., Hwang, Y.J., Chun, Y.E., Park, M., Woo, D.H., Bae, J.Y., Kim, T., Lee, J., Chun, H., Park, H.J., Lee, D.Y., Hong, J., Kim, H.Y., Oh, S.J., Park, S.J., Lee, H., Yoon,

B.E., Kim, Y., Jeong, Y., Shim, I., Bae, Y.C., Cho, J., Kowall, N.W., Ryu, H., Hwang, E., Kim, D., Lee, C.J., 2014. GABA from reactive astrocytes impairs memory in mouse models of Alzheimer's disease. Nat. Med. 20, 886–896. https://doi.org/10.1038/nm.3639

Jourdain, P., Bergersen, L.H., Bhaukaurally, K., Bezzi, P., Santello, M., Domercq, M., Matute, C., Tonello, F., Gundersen, V., Volterra, A., 2007. Glutamate exocytosis from astrocytes controls synaptic strength. Nat. Neurosci. 10, 331–339. https://doi.org/10.1038/nn1849

Kadish, I., Van Groen, T., 2002. Low levels of estrogen significantly diminish axonal sprouting after entorhinal cortex lesions in the mouse. J. Neurosci. 22, 4095–4102. https://doi.org/20026393

Kamat, P., 2015. Streptozotocin induced Alzheimer′s disease like changes and the underlying neural degeneration and regeneration mechanism. Neural Regen. Res. 10, 1050. https://doi.org/10.4103/1673-5374.160076

Kamat, P.K., Kalani, A., Rai, S., Swarnkar, S., Tota, S., Nath, C., Tyagi, N., 2016. Mechanism of Oxidative Stress and Synapse Dysfunction in the Pathogenesis of Alzheimer's Disease: Understanding the Therapeutics Strategies. Mol. Neurobiol. 53, 648–661. https://doi.org/10.1007/s12035-014-9053-6

Karnovsky, J.M., Roots, L., 1964. A "direct-coloring" thiocholine method for cholinesterases. J Histochem Cytochem 219–221. https://doi.org/10.1177/12.3.219

Karve, I.P., Taylor, J.M., Crack, P.J., 2016. The contribution of astrocytes and microglia to traumatic brain injury. Br. J. Pharmacol. 173, 692–702. https://doi.org/10.1111/bph.13125

Kaytor, M.D., Orr, H.T., 2002. The GSK3β signaling cascade and neurodegenerative disease. Curr. Opin. Neurobiol. 12, 275–278. https://doi.org/10.1016/S0959-4388(02)00320-3

Kim, D.H., Kim, J.M., Park, S.J., Cai, M., Liu, X., Lee, S., Shin, C.Y., Ryu, J.H., 2012. GABA(A) receptor blockade enhances memory consolidation by increasing hippocampal BDNF levels. Neuropsychopharmacology 37, 422–33. https://doi.org/10.1038/npp.2011.189

Kim, Y.S., Joh, T.H., 2006. Microglia, major player in the brain inflammation: Their roles in the pathogenesis of Parkinson's disease. Exp. Mol. Med. 38, 333–347. https://doi.org/10.1038/emm.2006.40

Kim, Y.S., Yoon, B.-E., 2017. Altered GABAergic Signaling in Brain Disease at Various Stages of Life. Exp. Neurobiol. 26, 122. https://doi.org/10.5607/en.2017.26.3.122

Kinjo, T., Ashida, Y., Higashi, H., Sugimura, S., Washida, M., Niihara, H., Ogita, K., Yoneda, Y., Kuramoto, N., 2018. Alleviation by GABAB Receptors of Neurotoxicity Mediated by Mitochondrial Permeability Transition Pore in Cultured Murine Cortical Neurons Exposed to N-Methyl-d-aspartate. Neurochem. Res. 43, 70–79. https://doi.org/10.1007/s11064-017-2311-z

Kinney, J.W., Bemiller, S.M., Murtishaw, A.S., Leisgang, A.M., Salazar, A.M., Lamb, B.T., 2018. Inflammation as a central mechanism in Alzheimer's disease. Alzheimer's Dement. Transl. Res. Clin. Interv. 4, 575–590. https://doi.org/10.1016/j.trci.2018.06.014

Klusa, V., 2016. Atypical 1,4-dihydropyridine derivatives, an approach to neuroprotection and memory enhancement. Pharmacol. Res. 113, 754–759. https://doi.org/10.1016/j.phrs.2016.05.017

Krishnan, K.J., Ratnaike, T.E., De Gruyter, H.L.M., Jaros, E., Turnbull, D.M., 2012. Mitochondrial DNA deletions cause the biochemical defect observed in Alzheimer's disease. Neurobiol. Aging 33, 2210–2214. https://doi.org/10.1016/j.neurobiolaging.2011.08.009

Kuhn, S.A., Van Landeghem, F.K.H., Zacharias, R., Färber, K., Rappert, A., Pavlovic, S., Hoffmann, A., Nolte, C., Kettenmann, H., 2004. Microglia express GABAB receptors to modulate interleukin release. Mol. Cell. Neurosci. 25, 312–322. https://doi.org/10.1016/j.mcn.2003.10.023

Kwakowsky, A., Calvo-Flores Guzmán, B., Pandya, M., Turner, C., Waldvogel, H.J., Faull, R.L., 2018. GABAAreceptor subunit expression changes in the human Alzheimer's disease hippocampus, subiculum, entorhinal cortex and superior temporal gyrus, Journal of Neurochemistry. https://doi.org/10.1111/jnc.14325

Lanctôt, K.L., Herrmaan, N., Mazzotta, P., Khan, L.R., Ingber, N., 2004. GABAergic function in Alzheimer's disease: Evidence for dysfunction and potential as a therapeutic target for the treatment of behavioral and psychological symptoms of dementia. Can. J. Psychiatry 49, 439–453. https://doi.org/10.1177/070674370404900705

Lawrence, J.J., 2008. Cholinergic control of GABA release: emerging parallels between neocortex and hippocampus. Trends Neurosci. 31, 317–327. https://doi.org/10.1016/j.tins.2008.03.008

Lee, M., Schwab, C., Mcgeer, P.L., 2011. Astrocytes are GABAergic cells that modulate microglial activity. Glia 59, 152–165. https://doi.org/10.1002/glia.21087

Leybaert, L., De Bock, M., Van Moorheim, M., Decrock, E., De Vuyst, E., 2007. Neurobarrier Coupling in the Brain: Adjusting Glucose Entry With Demand. J. Neurosci. Res. 85, 3213–3220. https://doi.org/10.1002/jnr.21189

Li, G., Bien-ly, N., Andrews-zwilling, Y., Xu, Q., Bernardo, A., Ring, K., Halabisky, B., Deng, C., Mahley, R.W., 2010. NIH Public Access 5, 634–645. https://doi.org/10.1016/j.stem.2009.10.015.GABAergic

Li, Y., Sun, H., Chen, Z., Xu, H., Bu, G., Zheng, H., 2016. Implications of GABAergic neurotransmission in Alzheimer's disease. Front. Aging Neurosci. 8, 1–12. https://doi.org/10.3389/fnagi.2016.00031

Liddelow, S.A., Guttenplan, K.A., Clarke, L.E., Bennett, F.C., C.J., B., 2017. Neurotoxic reactive astrocytes are induced by activated microglia. Nature 541, 481–487. https://doi.org/10.1038/nature21029

Lie, M.E.K., Al-khawaja, A., Damgaard, M., Haugaard, A.S., Schousboe, A., Clarkson, A.N., Wellendorph, P., 2017. Glial Amino Acid Transporters. https://doi.org/10.1007/978-3-319-55769-4

Lienhard, G.E., Secemski, I.I., 1973. P1,P5-Di(adenosine-5')pentaphosphate, a Potent Multisubstrate Inhibitor of Adenylate Kinase. J Biol Chem 248, 1121–1123.

Limon, A., Reyes-Ruiz, J.M., Miledi, R., 2012. Loss of functional GABAA receptors in the Alzheimer diseased brain. Proc. Natl. Acad. Sci. 109, 10071–10076. https://doi.org/10.1073/pnas.1204606109

Liu, B., Hong, J.-S., 2003. Role of Microglia in Inflammation-Mediated Neurodegenerative Diseases: Mechanisms and Strategies for Therapeutic Intervention. J. Pharmacol. Exp. Ther. 304, 1–7. https://doi.org/10.1124/jpet.102.035048

Liu, H., Song, N., 2016. Molecular Mechanism of Adult Neurogenesis and its Association with Human Brain Diseases. J. Cent. Nerv. Syst. Dis. 8, 5–11. https://doi.org/10.4137/JCNSD.S32204

Liu, L., Li, C.J., Lu, Y., Zong, X.G., Luo, C., Sun, J., Guo, L.J., 2015. Baclofen mediates neuroprotection on hippocampal CA1 pyramidal cells through the regulation of autophagy under chronic cerebral hypoperfusion. Sci. Rep. 5, 1–17. https://doi.org/10.1038/srep14474

Liu, Xiaonan, Chen, K., Wu, T., Weidman, D., Lure, F., Li, J., 2018. Use of multi-modality imaging and artificial intelligence for diagnosis and prognosis of early stages of

Alzheimer's disease. Transl. Res. 194, 56–67. https://doi.org/10.1016/j.trsl.2018.01.001

Liu, X., Jiao, B., Shen, L., 2018. The Epigenetics of Alzheimer's Disease: Factors and Therapeutic Implications. Front. Genet. 9, 1–10. https://doi.org/10.3389/fgene.2018.00579

Liu, Y., Liu, F., Iqbal, K., Grundke-Iqbal, I., Gong, C.-X., 2008. Decreased glucose transporters correlate to abnormal hyperphosphorylation of tau in Alzheimer disease. FEBS Lett. 582, 359–364. https://doi.org/https://dx.doi.org/10.1016%2Fj.febslet.2007.12.035

Lledo, P.M., Alonso, M., Grubb, M.S., 2006. Adult neurogenesis and functional plasticity in neuronal circuits. Nat. Rev. Neurosci. 7, 179–193. https://doi.org/10.1038/nrn1867

Luchetti, S., Huitinga, I., Swaab, D.F., 2011. Neurosteroid and GABA-A receptor alterations in Alzheimer's disease, Parkinson's disease and multiple sclerosis. Neuroscience 191, 6–21. https://doi.org/10.1016/j.neuroscience.2011.04.010

Magalingam, K.B., Radhakrishnan, A., Ping, N.S., Haleagrahara, N., 2018. Current Concepts of Neurodegenerative Mechanisms in Alzheimer's Disease. Biomed Res. Int. 2018, 1–12. https://doi.org/10.1155/2018/3740461

Marioni, R.E., Harris, S.E., Zhang, Q., McRae, A.F., Hagenaars, S.P., Hill, W.D., Davies, G., Ritchie, C.W., Gale, C.R., Starr, J.M., Goate, A.M., Porteous, D.J., Yang, J., Evans, K.L., Deary, I.J., Wray, N.R., Visscher, P.M., 2018. GWAS on family history of Alzheimer's disease. Transl. Psychiatry 8, 8–14. https://doi.org/10.1038/s41398-018-0150-6

Markesbery, W.R., 2010. Neuropathologic Alterations in Mild Cognitive Impairment: A Review. J. Alzheimer's Dis. 19, 221–228. https://doi.org/10.3233/JAD-2010-1220

Marshall, F.H., Jones, K.A., Kaupmann, K., Bettler, B., 1999. GABA(B) receptors - The first 7TM heterodimers. Trends Pharmacol. Sci. 20, 396–399. https://doi.org/10.1016/S0165-6147(99)01383-8

Massoud, F., Gauthier, S., 2010. Update on the Pharmacological Treatment of Alzheimers Disease. Curr. Neuropharmacol. 8, 69–80. https://doi.org/10.2174/157015910790909520

McCombe, P.A., Henderson, R.D., 2011. The Role of Immune and Inflammatory Mechanisms in ALS. Curr. Mol. Med. 11, 246–254. https://doi.org/10.2174/1566211213754895240

McDade, E., Bateman, R.J., 2017. Stop Alzheimer's before it starts. Nature 547, 153. https://doi.org/10.1038/547153a

McLennan, H.R., Esposti, M.D., 2000. The contribution of mitochondrial respiratory complexes to the production of reactive oxygen species. J. Bioenerg. Biomembr. 32, 153–162.

https://doi.org/10.1023/A:1005507913372

McNaull, B.B.A., Todd, S., McGuinness, B., Passmore, A.P., 2010. Inflammation and anti-inflammatory strategies for Alzheimer's disease - A mini-review. Gerontology 56, 3–14. https://doi.org/10.1159/000237873

McQuade, A., Blurton-Jones, M., 2019. Microglia in Alzheimer's Disease: Exploring How Genetics and Phenotype Influence Risk. J. Mol. Biol. 431, 1805–1817. https://doi.org/10.1016/j.jmb.2019.01.045

Mehler, M.F., 2008. Epigenetic principles and mechanisms underlying nervous system functions in health and disease. Prog. Neurobiol. 86, 305–341. https://doi.org/10.1016/j.pneurobio.2008.10.001

Méndez-Cuesta, L.A., Márquez-Valadez, B., Pérez-De La Cruz, V., Escobar-Briones, C., Galván-Arzate, S., Alvarez-Ruiz, Y., Maldonado, P.D., Santana, R.A., Santamaría, A., Carrillo-Mora, P., 2011. Diazepam Blocks Striatal Lipid Peroxidation and Improves Stereotyped Activity in a Rat Model of Acute Stress. Basic Clin. Pharmacol. Toxicol. 109, 350–356. https://doi.org/10.1111/j.1742-7843.2011.00738.x

Mendiola-Precoma, J., Berumen, L.C., Padilla, K., Garcia-Alcocer, G., 2016. Therapies for Prevention and Treatment of Alzheimer's Disease. Biomed Res. Int. 2016. https://doi.org/10.1155/2016/2589276

Mesulam, M.M., 2013. Cholinergic circuitry of the human nucleus basalis and its fate in Alzheimer's disease. J. Comp. Neurol. 521, 4124–4144. https://doi.org/10.1002/cne.23415

Micheau, J., Marighetto, A., 2011. Acetylcholine and memory: A long, complex and chaotic but still living relationship. Behav. Brain Res. 221, 424–429. https://doi.org/10.1016/j.bbr.2010.11.052

Minett, T., Classey, J., Matthews, F.E., Fahrenhold, M., Taga, M., Brayne, C., Ince, P.G., Nicoll, J.A.R., Boche, D., 2016. Microglial immunophenotype in dementia with Alzheimer's pathology. J. Neuroinflammation 13, 1–10. https://doi.org/10.1186/s12974-016-0601-z

Ming, G. li, Song, H., 2011. Adult Neurogenesis in the Mammalian Brain: Significant Answers and Significant Questions. Neuron 70, 687–702. https://doi.org/10.1016/j.neuron.2011.05.001

Misane, I., Cebers, G., Liepa, I., Dambrova, M., Germane, S., Klusa, V., Duburs, G., Bisenieks,

E., 1993. Cyclic nootropics: similarity and differences in their memory improving action.

Morales, I., GuzmÃ¡n-MartÃ-nez, L., Cerda-Troncoso, C., FarÃ-as, G.A., Maccioni, R.B., 2014. Neuroinflammation in the pathogenesis of Alzheimerâ€™s disease. A rational framework for the search of novel therapeutic approaches. Front. Cell. Neurosci. 8. https://doi.org/10.3389/fncel.2014.00112

Morgan, M.J., Liu, Z.G., 2011. Crosstalk of reactive oxygen species and NF-κB signaling. Cell Res. 21, 103–115. https://doi.org/10.1038/cr.2010.178

Mu, Y., Gage, F.H., 2011. A Century of Alzheimer's Disease. Science (80-.). 6, 1–9. https://doi.org/10.1126/science.1132814

Muñoz, S.S., Garner, B., Ooi, L., 2018. Understanding the Role of ApoE Fragments in Alzheimer's Disease. Neurochem. Res. 0, 0. https://doi.org/10.1007/s11064-018-2629-1

Nava-Mesa, M.O., Jiménez-Díaz, L., Yajeya, J., Navarro-Lopez, J.D., 2014. GABAergic neurotransmission and new strategies of neuromodulation to compensate synaptic dysfunction in early stages of Alzheimer's disease. Front. Cell. Neurosci. 8, 167. https://doi.org/10.3389/fncel.2014.00167

Nhan, H.S., Chiang, K., Koo, E.H., 2015. The multifaceted nature of amyloid precursor protein and its proteolytic fragments: friends and foes. Prax. Klin. Pneumol. 129, 1–19. https://doi.org/10.1007/s00401-014-1347-2

O'Leary, O.F., Felice, D., Galimberti, S., Savignac, H.M., Bravo, J.A., Crowley, T., El Yacoubi, M., Vaugeois, J.-M., Gassmann, M., Bettler, B., Dinan, T.G., Cryan, J.F., 2014. GABA $_{B(1)}$ receptor subunit isoforms differentially regulate stress resilience. Proc. Natl. Acad. Sci. 111, 15232–15237. https://doi.org/10.1073/pnas.1404090111

Ognjanovski, N., Schaeffer, S., Wu, J., Mofakham, S., Maruyama, D., Zochowski, M., Aton, S.J., 2017. Erratum: Parvalbumin-expressing interneurons coordinate hippocampal network dynamics required for memory consolidation. Nat. Commun. 8, 16120. https://doi.org/10.1038/ncomms16120

Olsen, R.W., Sieghart, W., 2008. International Union of Pharmacology. LXX. Subtypes of -Aminobutyric AcidA Receptors: Classification on the Basis of Subunit Composition, Pharmacology, and Function. Update. Pharmacol. Rev. 60, 243–260. https://doi.org/10.1124/pr.108.00505

Owens, D.F., Kriegstein, A.R., 2002. Is there more to GABA than synaptic inhibition? Nat. Rev.

Neurosci. 3, 715–727. https://doi.org/10.1038/nrn919

Padgett, C.L., Slesinger, P.A., 2010. GABAB receptor coupling to G-proteins and ion channels. Adv. Pharmacol. 58, 123–147. https://doi.org/10.1016/S1054-3589(10)58006-2

Palop, J.J., 2005. Vulnerability of Dentate Granule Cells to Disruption of Arc Expression in Human Amyloid Precursor Protein Transgenic Mice. J. Neurosci. 25, 9686–9693. https://doi.org/10.1523/jneurosci.2829-05.2005

Palop, J.J., Mucke, L., 2010. Synaptic depression and aberrant excitatory network activity in alzheimer's disease: Two faces of the same coin? NeuroMolecular Med. 12, 48–55. https://doi.org/10.1007/s12017-009-8097-7

Panzeri, S., Macke, J.H., Gross, J., Kayser, C., 2015. Neural population coding: Combining insights from microscopic and mass signals. Trends Cogn. Sci. 19, 162–172. https://doi.org/10.1016/j.tics.2015.01.002

Paula-Lima, A.C., De Felice, F.G., Brito-Moreira, J., Ferreira, S.T., 2005. Activation of GABAA receptors by taurine and muscimol blocks the neurotoxicity of β-amyloid in rat hippocampal and cortical neurons. Neuropharmacology 49, 1140–1148. https://doi.org/10.1016/j.neuropharm.2005.06.015

Paxinos, G., Watson, C., 2007. The Rat Brain. Academic Press.

Pilipenko, V., Narbute, K., Amara, I., Trovato, A., Scuto, M., Pupure, J., Jansone, B., Poikans, J., Bisenieks, E., Klusa, V., Calabrese, V., 2019. GABA-containing compound gammapyrone protects against brain impairments in Alzheimer's disease model male rats and prevents mitochondrial dysfunction in cell culture. J. Neurosci. Res. 1–19. https://doi.org/10.1002/jnr.24396

Rai, S., Kamat, P.K., Nath, C., Shukla, R., 2014. Glial activation and post-synaptic neurotoxicity: The key events in Streptozotocin (ICV) induced memory impairment in rats. Pharmacol. Biochem. Behav. 117, 104–117. https://doi.org/10.1016/j.pbb.2013.11.035

Readhead, B., Haure-Mirande, J.V., Funk, C.C., Richards, M.A., Shannon, P., Haroutunian, V., Sano, M., Liang, W.S., Beckmann, N.D., Price, N.D., Reiman, E.M., Schadt, E.E., Ehrlich, M.E., Gandy, S., Dudley, J.T., 2018. Multiscale Analysis of Independent Alzheimer's Cohorts Finds Disruption of Molecular, Genetic, and Clinical Networks by Human Herpesvirus. Neuron 99, 64-82.e7. https://doi.org/10.1016/j.neuron.2018.05.023

Riese, F., Gietl, A., Zölch, N., Henning, A., O'Gorman, R., Kälin, A.M., Leh, S.E., Buck, A.,

Warnock, G., Edden, R.A.E., Luechinger, R., Hock, C., Kollias, S., Michels, L., 2015. Posterior cingulate γ-aminobutyric acid and glutamate/glutamine are reduced in amnestic mild cognitive impairment and are unrelated to amyloid deposition and apolipoprotein E genotype. Neurobiol Aging 36, 53–59. https://doi.org/10.1016/j.neurobiolaging.2014.07.030

Rissman, R.A., De Blas, A.L., Armstrong, D.M., 2007. GABAA receptors in aging and Alzheimer's disease. J. Neurochem. 103, 1285–1292. https://doi.org/10.1111/j.1471-4159.2007.04832.x

Roux, L., Buzsáki, G., 2015. Tasks for inhibitory interneurons in intact brain circuits. Neuropharmacology 88, 10–23. https://doi.org/10.1016/j.neuropharm.2014.09.011

Rowdhwal, S.S.S., Chen, J., 2018. Toxic Effects of Di-2-ethylhexyl Phthalate: An Overview. Biomed Res. Int. 2018. https://doi.org/10.1155/2018/1750368

Santos, T. de O., Mazucanti, C.H.Y., Xavier, G.F., da Silva Torrão, A., 2012. Early and late neurodegeneration and memory disruption after intracerebroventricular streptozotocin. Physiol. Behav. 107, 401–413. https://doi.org/10.1016/j.physbeh.2012.06.019

Saxena, G., Patro, I.K., Nath, C., 2011. ICV STZ induced impairment in memory and neuronal mitochondrial function: A protective role of nicotinic receptor. Behav. Brain Res. 224, 50–57. https://doi.org/10.1016/j.bbr.2011.04.039

Scheltens, P., Blennow, K., Breteler, M.M.B., de Strooper, B., Frisoni, G.B., Salloway, S., Van der Flier, W.M., 2016. Alzheimer's disease. Lancet 388, 505–517. https://doi.org/10.1007/978-1-4939-7880-9_9

Sevastre-Berghian, A.C., Făgărăsan, V., Toma, V.A., Bâldea, I., Olteanu, D., Moldovan, R., Decea, N., Filip, G.A., Clichici, S. V., 2017. Curcumin reverses the diazepam-induced cognitive impairment by modulation of oxidative stress and erk 1/2/nf-κ b pathway in brain. Oxid. Med. Cell. Longev. 2017. https://doi.org/10.1155/2017/3037876

Shimohama, S., 2000. Apoptosis in Alzheimer ' s disease — an update 5, 9–16.

Sigel, E., Ernst, M., 2018. The Benzodiazepine Binding Sites of GABAA Receptors. Trends Pharmacol. Sci. 39, 659–671. https://doi.org/10.1016/j.tips.2018.03.006

Signorile, A., Micelli, L., De Rasmo, D., Santeramo, A., Papa, F., Ficarella, R., Gattoni, G., Scacco, S., Papa, S., 2014. Regulation of the biogenesis of OXPHOS complexes in cell transition from replicating to quiescent state. Involvement of PKA and effect of

hydroxytyrosol. Biochim. Biophys. Acta - Mol. Cell Res. 1843, 675–684. https://doi.org/10.1016/j.bbamcr.2013.12.017

Simpson, M.D.C., Cross, A.J., Slater, P., 1988. Neural Transmission 219–226.

Singh, S.K., Srivastav, S., Yadav, A.K., Srikrishna, S., Perry, G., 2016. Overview of Alzheimer's disease and some therapeutic approaches targeting A β by using several synthetic and herbal compounds. Oxid. Med. Cell. Longev. 2016. https://doi.org/10.1155/2016/7361613

Sosna, J., Philipp, S., Albay, R.I., Reyes-Ruiz, J.M., Baglietto-Vargas, D., LaFerla, F.M., Glabe, C.G., 2018. Early long-term administration of the CSF1R inhibitor PLX3397 ablates microglia and reduces accumulation of intraneuronal amyloid, neuritic plaque deposition and pre-fibrillar oligomers in 5XFAD mouse model of Alzheimer's disease. Mol. Neurodegener. 13, 1–11. https://doi.org/10.1186/s13024-018-0244-x

Sousa, J.S., D'Imprima, E., Vonck, J., 2018. Mitochondrial respiratory chain complexes, Subcellular Biochemistry. https://doi.org/10.1007/978-981-10-7757-9_7

Southam, K.A., Vincent, A.J., Small, D.H., 2016. Do Microglia Default on Network Maintenance in Alzheimer's Disease? J. Alzheimer's Dis. 51, 657–669. https://doi.org/10.3233/JAD-151075

Sultana, R., Perluigi, M., Butterfield, D.A., 2009. Oxidatively modified proteins in Alzheimer's disease (AD), mild cognitive impairment and animal models of AD: Role of Abeta in pathogenesis. Acta Neuropathol. 118, 131–150. https://doi.org/10.1007/s00401-009-0517-0

Sun, Q., Xie, N., Tang, B., Li, R., Shen, Y., 2017. Alzheimer's Disease: From Genetic Variants to the Distinct Pathological Mechanisms. Front. Mol. Neurosci. 10, 1–14. https://doi.org/10.3389/fnmol.2017.00319

Teich, A.F., Arancio, O., 2012. Is the Amyloid Hypothesis of Alzheimer's disease therapeutically relevant? Biochem. J. 446, 165–177. https://doi.org/10.1042/BJ20120653.Is

Terunuma, M., 2018. Diversity of structure and function of GABA B receptors : a complexity of GABA B -mediated signaling. Proc. Jpn. Acad. 94, 390–411.

Tiwari, V., Kuhad, A., Bishnoi, M., Chopra, K., 2009. Chronic treatment with tocotrienol, an isoform of vitamin E, prevents intracerebroventricular streptozotocin-induced cognitive impairment and oxidative-nitrosative stress in rats. Pharmacol. Biochem. Behav. 93, 183–189. https://doi.org/10.1016/j.pbb.2009.05.009

Tohgi, H., Utsugisawa, K., Nagane, Y., Yoshimura, M., Genda, Y., Ukitsu, M., 1999. Reduction with age in methylcytosine in the promoter region -224~-101 of the amyloid precursor protein gene in autopsy human cortex. Mol. Brain Res. 70, 288–292. https://doi.org/10.1016/S0169-328X(99)00163-1

Toni, N., Laplagne, D.A., Zhao, C., Lombardi, G., Ribak, C.E., Gage, F.H., Schinder, A.F., 2008. Neurons born in the adult dentate gyrus form functional synapses with target cells. Nat. Neurosci. 11, 901–907. https://doi.org/10.1038/nn.2156

Tramutola, A., Triplett, J.C., Di Domenico, F., Niedowicz, D.M., Murphy, M.P., Coccia, R., Perluigi, M., Allan Butterfield, D., 2015. Alteration of mTOR signaling occurs early in the progression of Alzheimer disease (AD): Analysis of brain from subjects with pre-clinical AD, amnestic mild cognitive impairment and late-stage AD. J. Neurochem. 133, 739–749. https://doi.org/10.1111/jnc.13037

Triggle, D.J., 2003. 1,4-Dihydropyridines as calcium channel ligands and privileged structures. Cell. Mol. Neurobiol. 23, 293–303. https://doi.org/10.1023/A:1023632419813

Tritsch, N.X., Granger, A.J., Sabatini, B.L., 2016. Mechanisms and functions of GABA co-release. Nat. Rev. Neurosci. 17, 139–145. https://doi.org/10.1038/nrn.2015.21

Umeda, T., Kimura, T., Yoshida, K., Takao, K., Fujita, Y., Matsuyama, S., Sakai, A., Yamashita, M., Yamashita, Y., Ohnishi, K., Suzuki, M., Takuma, H., Miyakawa, T., Takashima, A., Morita, T., Mori, H., Tomiyama, T., 2017. Mutation-induced loss of APP function causes GABAergic depletion in recessive familial Alzheimer's disease: analysis of Osaka mutation-knockin mice. Acta Neuropathol. Commun. 5, 59. https://doi.org/10.1186/s40478-017-0461-5

Urwyler, S., Gjoni, T., Koljatić, J., Dupuis, D.S., 2005. Mechanisms of allosteric modulation at GABAB receptors by CGP7930 and GS39783: Effects on affinities and efficacies of orthosteric ligands with distinct intrinsic properties. Neuropharmacology 48, 343–353. https://doi.org/10.1016/j.neuropharm.2004.10.013

Valenti, D., De Rasmo, D., Signorile, A., Rossi, L., de Bari, L., Scala, I., Granese, B., Papa, S., Vacca, R.A., 2013. Epigallocatechin-3-gallate prevents oxidative phosphorylation deficit and promotes mitochondrial biogenesis in human cells from subjects with Down's syndrome. Biochim. Biophys. Acta - Mol. Basis Dis. 1832, 542–552. https://doi.org/10.1016/j.bbadis.2012.12.011

Van Der Kooij, M.A., Hollis, F., Lozano, L., Zalachoras, I., Abad, S., Zanoletti, O., Grosse, J.,

Guillot De Suduiraut, I., Canto, C., Sandi, C., 2018. Diazepam actions in the VTA enhance social dominance and mitochondrial function in the nucleus accumbens by activation of dopamine D1 receptors. Mol. Psychiatry 23, 569–578. https://doi.org/10.1038/mp.2017.135

Verkhratsky, A., Zorec, R., Rodríguez, J.J., Parpura, V., 2016. Astroglia dynamics in ageing and Alzheimer's disease. Curr. Opin. Pharmacol. 26, 74–79. https://doi.org/10.1016/j.coph.2015.09.011

Verri, M., Pastoris, O., Dossena, M., Aquilani, R., Guerriero, F., Cuzzoni, G., Venturini, L., Ricevuti, G., Bongiorno, A.I., 2012. Mitochondrial alterations, oxidative stress and neuroinflammation in Alzheimer's disease. Int. J. Immunopathol. Pharmacol. 25, 345–353. https://doi.org/10.1177/039463201202500204

Villemagne, V.L., Doré, V., Burnham, S.C., Masters, C.L., Rowe, C.C., 2018. Imaging tau and amyloid-β proteinopathies in Alzheimer disease and other conditions. Nat. Rev. Neurol. 14, 225–236. https://doi.org/10.1038/nrneurol.2018.9

Wang, B., Wang, Z., Sun, L., Yang, L., Li, H., Cole, A.L., Rodriguez-Rivera, J., Lu, H.-C., Zheng, H., 2014. The Amyloid Precursor Protein Controls Adult Hippocampal Neurogenesis through GABAergic Interneurons. J. Neurosci. 34, 13314–13325. https://doi.org/10.1523/JNEUROSCI.2848-14.2014

Wang, Q., Liu, Y., Zhou, J., 2015. Neuroinflammation in Parkinson's disease and its potential as therapeutic target. Transl. Neurodegener. 4, 1–9. https://doi.org/10.1186/s40035-015-0042-0

Wang, R., Reddy, P.H., 2017. Role of Glutamate and NMDA Receptors in Alzheimer's Disease. J. Alzheimer's Dis. 57, 1041–1048. https://doi.org/10.3233/JAD-160763

Wang, X.-K., 2001. Pharmacological study on recombinant human GABA-A receptor complex containing alpha5 (leucine155 to valine) combined with beta3gamma2s subunits. Acta Pharmacol Sin 22, 521–523.

Wang, Z., Xu, P., Chen, B., Zhang, Z., Zhang, C., Zhan, Q., Huang, S., Xia, Z.A., Peng, W., 2018. Identifying circRNA-associated-ceRNA networks in the hippocampus of Aß1-42-induced Alzheimer's disease-like rats using microarray analysis. Aging (Albany. NY). 10, 775–788. https://doi.org/10.18632/aging.101427

Warren, J.D., Rohrer, J.D., Schott, J.M., Fox, N.C., Hardy, J., Rossor, M.N., 2013. Molecular nexopathies: A new paradigm of neurodegenerative disease. Trends Neurosci. 36, 561–569.

https://doi.org/10.1016/j.tins.2013.06.007

Wilkins, H.M., Koppel, S.J., Bothwell, R., Mahnken, J., Burns, J.M., Swerdlow, R.H., 2017. Platelet cytochrome oxidase and citrate synthase activities in APOE ε4 carrier and non-carrier Alzheimer's disease patients. Redox Biol. 12, 828–832. https://doi.org/10.1016/j.redox.2017.04.010

Wilkins, H.M., Swerdlow, R.H., 2016. Relationships Between Mitochondria and Neuroinflammation: Implications for Alzheimer's Disease. Curr Top Med Chem 16, 849–857. https://doi.org/10.1097/OGX.0000000000000256.Prenatal

Wisniewski, H.M., Moretz, R.C., Lossinsky, A.S., 1981. Evidence for induction of localized amyloid deposits and neuritic plaques by an infectious agent. Ann. Neurol. 10, 517–522. https://doi.org/10.1002/ana.410100605

Wu, Z., Guo, Z., Gearing, M., Chen, G., 2014. Tonic inhibition in dentate gyrus impairs long-term potentiation and memory in an Alzhiemer' s disease model. Nat. Commun. 5, 1–10. https://doi.org/10.1038/ncomms5159

Xu, C., Zhang, W., Rondard, P., Pin, J.P., Liu, J., 2014. Complex GABAB receptor complexes: How to generate multiple functionally distinct units from a single receptor. Front. Pharmacol. 5 FEB. https://doi.org/10.3389/fphar.2014.00012

Xu, Q., 2006. Profile and Regulation of Apolipoprotein E (ApoE) Expression in the CNS in Mice with Targeting of Green Fluorescent Protein Gene to the ApoE Locus. J. Neurosci. 26, 4985–4994. https://doi.org/10.1523/jneurosci.5476-05.2006